UNIVERSIDADE DE LISBOA
FACULDADE DE CIÊNCIAS
DEPARTAMENTO DE FÍSICA

Electroweak Loop Corrections to High Energy Processes

Sancho Moura Oliveira

DOUTORAMENTO EM FÍSICA

2008

Electroweak Loop Corrections to High Energy Processes

Sancho Moura Oliveira

Tese orientada pelo Professor Doutor Augusto Barroso

DOUTORAMENTO EM FÍSICA

2008

Abstract

This work is organized in two distinct parts. In the first part we present limits on a sequential down-type quark, b', based on the most recent experimental data from DELPHI[1], CDF and D0. We use all available experimental data to constrain the b' quark mass as a function of the Cabibbo-Kobayashi-Maskawa elements in a sequential four generations model. We conclude that a sequential four generations model is far from being experimentally excluded.

In the second part we study the non-radiative scattering amplitudes for electron-positron annihilation into quark and lepton pairs in the TeV energy range. These amplitudes are calculated in the double-logarithmic approximation. The expressions for the amplitudes are obtained using infrared evolution equations with different cut-offs for virtual photons and for W and Z bosons, and compared with previous results obtained with an universal cut-off. We also study the production of electroweak bosons in e^+e^- annihilation into quarks and into leptons at energies much greater than 100 Gev. We account for double-logarithmic contributions to all orders in electroweak couplings. It is assumed that the bosons are emitted in the multi-Regge kinematics. The explicit expressions for the scattering amplitudes of the process are obtained. It is shown that the cross sections of the photon and Z production have the identical energy dependence and asymptotically their ratio depends only on the Weinberg angle whereas the energy dependence of the cross section of the W production is suppressed by a factor $s^{-0.4}$ compared to them.

The original work done in this thesis was published in the following papers:

- J. Abdallah *et al.* [DELPHI Collaboration], Eur. Phys. J. C **50** (2007) 507 [arXiv:0704.0594 [hep-ex]].

- S. M. Oliveira and R. Santos, Acta Phys. Polon. B **34** (2003) 5523 [arXiv:hep-ph/0311047].

- S. M. Oliveira and R. Santos, Phys. Rev. D **68** (2003) 093012 [arXiv:hep-ph/0307318].

- A. Barroso, B. I. Ermolaev, M. Greco, S. M. Oliveira and S. I. Troyan, Phys. Rev. D **69** (2004) 034012 [arXiv:hep-ph/0309230].

- B. I. Ermolaev, S. M. Oliveira and S. I. Troyan, Phys. Rev. D **66** (2002) 114018 [arXiv:hep-ph/0207159].

KEY WORDS:
STANDARD MODEL; CKM; FOURTH GENERATION QUARKS;
DOUBLE LOGARITHMIC APPROXIMATION; INFRARED EVOLUTION EQUATIONS;
SUDAKOV PARAMETRIZATION; ELECTRON-POSITRON ANNIHILATION.

Resumo

Este trabalho está organizado em duas partes distintas. Na primeira parte, foram utilizados os últimos dados experimentais de DELPHI[1], CDF e D0, com o objectivo de impor limites à existência de um quarto *quark down*, b'. Com base nos dados disponíveis para $m_{b'} > 96$ GeV procurámos restringir a massa do b' em função dos elementos da matriz Cabibbo-Kobayashi-Maskawa para um modelo de quatro gerações sequenciais. A análise dos resultados a que chegámos permite-nos concluir que num modelo deste tipo, a existência de um *quark b'* está longe de poder ser excluída.

Na segunda parte, foram calculadas as amplitudes de dispersão da aniquilação de electrão positrão para pares de *quarks* ou de leptões em processos não radiactivos na gama de energia dos TeV. Estas amplitudes foram calculadas com base na aproximação de duplos-logaritmos (DLA) e usando as equações de evolução dos infra-vermelhos com cortes diferentes para os fotões virtuais e para os bosões W e Z. Os resultados obtidos foram comparados com os resultados calculados anteriormente noutros trabalhos com um corte universal. Estudámos, ainda, a produção de bosões electrofracos na aniquilação e^+e^- para *quarks* ou leptões com energias muito superiores a 100 GeV. Foram calculadas as expressões explícitas destas amplitudes, considerando-se que todas as contribuições são do tipo duplos-logaritmos a todas as ordens no acoplamento electrofraco e assumindo-se que os bosões produzidos são emitidos na cinemática multi-Regge. Finalmente, verificámos que as secções eficazes da produção de fotões e de Z têm a mesma dependência na energia e que, no limite, o seu rácio depende apenas do ângulo de Weinberg. Em comparação com estas secções eficazes, a produção de W decresce de um factor de $s^{-0.4}$.

iv

Agradecimentos

Em primeiro lugar, quero agradecer ao meu orientador, Professor Doutor Augusto Barroso, por me ter apoiado e estimulado neste longo processo de aprendizagem com o seu saber, interesse e disponibilidade.

Quero agradecer, também, de uma forma muito especial, ao Doutor Rui Santos que foi um segundo orientador e um amigo. Durante estes últimos anos ensinou-me muito, tendo sido essencial o seu entusiasmo e motivação para que esta tese fosse concluída.

Agradeço, ainda, ao Doutor Boris Ermolaev a oportunidade que me deu de trabalhar com ele e a disponibilidade que sempre demonstrou durante este processo.

Aos meus colegas do DCTI-ISCTE, agradeço o óptimo ambiente de trabalho e, em especial, ao Professor Doutor Luís Nunes, o facto de me ter dado condições que me permitiram ter mais tempo para terminar esta tese.

Agradeço, ainda, ao Centro de Física Teórica e Computacional da Universidade de Lisboa, as excelentes condições de trabalho proporcionadas e à Fundação para a Ciência e a Tecnologia, o apoio financeiro concedido através da bolsa SFRH/BD/6455/2001.

Finalmente, agradeço a todos os familiares e amigos, em particular, à Ana, ao Duarte e aos meus pais.

Resumo alargado

Pretende-se neste resumo alargado evidenciar os aspectos mais importantes desta tese. Esta encontra-se organizada em duas partes distintas. Na primeira parte foram utilizados os últimos dados experimentais de DELPHI[1], CDF e D0 para impor limites à existência de um quarto *quark down*, b'. Na segunda parte são calculadas as amplitudes de dispersão da aniquilação de um electrão e um positrão para um par de *quarks* ou de leptões em processos não radiactivos na gama de energia dos TeV. São ainda calculadas as amplitudes de dispersão da produção de bosões electrofracos na aniquilação e^+e^- para *quarks* ou leptões com energias muito superiores a 100 GeV.

Primeira parte - Limites para a massa do *quark* b'

Apesar dos constrangimentos e restrições existentes para que uma nova família seja adicionada ao modelo padrão (MP) parece-nos fazer sentido tentar excluir experimentalmente a existência de um *quark* de quarta geração. Existem actualmente quatro limites para a massa do *quark* b', mas em todos se assume que a taxa de decaimento é 100% para um canal de decaimento específico. No primeiro e no segundo ([2],[3]), impõe-se que $m_{b'} > 268$ GeV mas assume-se que o $Br(b' \rightarrow b\,Z) = 100\%$. No terceiro [4] impõe-se que $m_{b'} > 128$ GeV assumindo que o $Br(b' \rightarrow c\,W) = 100\%$. O quarto limite vem de CDF [5] e depende muito do tempo de vida do b'. Neste caso também se assume que o $Br(b' \rightarrow b\,Z) = 100\%$.

Exitem diversas formas de estender o modelo padrão para este incluir uma quarta família de *quarks* e/ou leptões. Para uma revisão sobre as diferentes possibilidades podem ser consultados os trabalhos [6, 7]. O principal problema está na definição da estrutura da nova família. Esta pode ser quiral ou não-quiral (tipo-vectoriais), o que permite um conjunto de modelos diferentes. A forma mais natural de adicionar uma nova família de *quarks* ao modelo padrão é incluir um novo par de *quarks* (t', b') com os mesmos números quânticos e acoplamentos similares aos *quarks* conhecidos. O mesmo terá de ser feito no sector leptónico. A este novo modelo dá-se o nome de modelo sequencial de quatro gerações (SM4). A matriz CKM resultante tem uma estrutura idêntica à da do MP. Para além das quatro novas massas, a nova matriz CKM_{SM4} necessita de 9 parâmetros ao contrário dos 4 necessários à matriz CKM_{SM}. São necessários 6 ângulos de mistura em vez de 3 e 3 fases complexas em vez de 1. Como não estamos preocupados com as violações de CP considerámos que todos os elementos da matriz CKM são reais. É de

notar que existe uma maior liberdade nos valores dos elementos da matriz CKM que não foram testados experimentalmente devido aos novos parâmetros inseridos. Este modelo tem sido sujeito a diversos estudos publicados na literatura.

A produção do *quark* b' sequencial foi feita no Large Electron-Positron (LEP) em pares pelo seguinte processo: $e^+ e^- \rightarrow b' \bar{b}'$. No Tevatron a sua produção segue um processo equivalente que é $p \bar{p} \rightarrow b' \bar{b}' + X$. Os processos de decaimento do *quark* b' foram intensivamente estudados por Hou e Stuart [8, 9, 10, 11] e por Haeri, Eilam e Soni [12]. Os decaimentos para duas partículas, ilustrados na Fig. 2.1, podem ocorrer por correntes carregadas (CC) ou neutras (NC). Apesar dos decaimentos neutros ocorrerem através de *loops*, foi demonstrado que, para alguns valores da matriz CKM e das massas dos *quarks*, estes dacaimentos podem ser comparáveis com os das CC. A razão é simples: se os canais $b' \rightarrow W\,t$ e $b' \rightarrow W\,t'$ não forem permitidos, o decaimento CC dominante é $b' \rightarrow W\,c$ que é duplamente suprimido. Enquanto o canal do Higgs estiver fechado, o canal NC dominante é o $b' \rightarrow b\,Z$. Quando o canal do Higgs abre pode ter valores comparáveis com os do Z.

A matriz CKM deste modelo é uma matriz 4×4 unitária o que nos permite escrever:

$$V_{tb}V_{tb'} + V_{tb'}V_{t'b'} + V_{cb'}V_{ts} + V_{td}V_{ub'} = 0. \tag{1}$$

Se assumirmos que é aproximadamente simétrica, que $V_{ub'}\,V_{td} \approx 0$ e que $V_{ts} \approx 10^{-2}$, verifica-se que $V_{cb'}V_{ts}$ tem de ser muito pequeno e portanto $V_{t'b'}V_{t'b} \approx -V_{tb}V_{tb'}$. Isto permite-nos escrever todos os resultados em função de apenas três variáveis: R_{CKM}, $m_{t'}$ e $m_{b'}$, sendo R_{CKM} definido como:

$$R_{CKM} = \left| \frac{V_{cb'}}{V_{tb'}\,V_{tb}} \right|. \tag{2}$$

Os dados experimentais existentes permitem variar a massa do b' entre 96 GeV e 180 GeV. Os valores possíveis de $m_{t'}$ estão restringidos pelas medidas de precisão. Assim foram estudados os dois limites extremos dentro do intervalo possível, $m_{t'} = m_{b'} + 50$ GeV e $m_{t'} = m_{b'} + 1$ GeV. O R_{CKM} foi considerado como um parâmetro livre não tendo sido feitas quaisquer restrições aos seus valores. Na Fig. 2.2 apresentam-se as taxas de decaimento em função da massa do b', assumindo $R_{CKM} = 0.001$ para ambos os limites de $m_{t'}$. Na Fig. 2.3 apresentam-se as taxas de decaimento em função de R_{CKM} com $m_{b'} = 110$ GeV e também para ambos os limites de $m_{t'}$. Com base nos dados experimentais existentes foram calculadas as zonas de exclusão nos planos $(R_{CKM}, m_{b'})$ e $(m_{t'}, m_{b'})$ assumindo-se como parâmetros, no primeiro caso, $m_{t'}$ e, no segundo, R_{CKM}. Para os dados de DELPHI foram produzidos três gráficos de exclusão. Na Fig. 2.8 está representado o plano $(m_{t'}, m_{b'})$ e nas Figs. 2.9 e 2.10 o plano $(R_{CKM}, m_{b'})$. O limite de $Br_{b' \rightarrow cW}$ impõe as zonas de exclusão representadas por uma faixa centrada em m_t na Fig. 2.8 e a parte superior nas Figs. 2.9 e 2.10. As restantes zonas de exclusão são devidas ao limite $Br_{b' \rightarrow bZ}$. Quando $(m_{t'} - m_t) \rightarrow 0$, o $Br_{b' \rightarrow bZ}$ decresce como consequência do mecanismo de Glashow-Iliopoulos-Maiani (GIM) e por esta razão o $Br_{b' \rightarrow cW}$ torna-se o decaimento dominante, chegando mesmo a $Br_{b' \rightarrow cW} \approx 100\%$ no ponto $m_{t'} - m_t = 0$. Este mecanismo leva a que exista sempre uma faixa de exclusão à volta do valor de m_t. Na Fig. 2.8 pode verificar-se que quando os

valores de R_{CKM} crescem, as CC começam a ser dominantes o que leva a que a faixa de exclusão alargue e as outras duas regiões diminuam. Este fenómeno também é visível na Fig. 2.9 onde o espaço de $m_{b'}$ está totalmente excluído quando $R_{CKM} > 0.0015$. Quando a diferença $m_{t'} - m_{b'}$ diminui, como se pode ver na Fig. 2.10, a região permitida aumenta. Na Fig. 2.9 devido à competição existente entre as NC não existe um limite inferior perto de 96 GeV. No limiar do $Z\,b$ (≈ 96 GeV), o canal $b' \to b\,g$ é superior a ao $b' \to b\,Z$, tornando o limite do $Br_{b' \to b\,Z}$ inútil. Ao afastarmo-nos deste limiar o canal $b' \to b\,Z$ passa a dominar as correntes neutras. A existência de um limite inferior para $m_{b'} = 100$ GeV na Fig. 2.9, mas não na Fig. 2.10, é explicada pelo facto de $Br_{b' \to b\,Z}$ cair menos abruptamente do que as outras correntes neutras com a $m_{t'}$. Finalmente, verifica-se que para valores superiores a 102 GeV não existem grandes zonas de exclusão, dado que os limites experimentais não o permitem.

Nas Figs. 2.11 a 2.13 estão representadas as regiões de exclusão para os dados de CDF e D0. Os dados de D0 permitem testar as correntes carregadas e os de CDF as neutras. As 3 curvas, representadas como *upper*, *central* e *lower* nas Figs. 2.12 e 2.13, estão relacionadas com as barras de erro teórico associadas à produção do b'. Pelas mesmas razões que vimos para o caso das Figs. de DELPHI, existe na Fig. 2.11 uma faixa em torno do valor de m_t. Esta faixa termina perto de $m_{b'} = 130$ GeV, que é o valor aproximado do limite de D0 para $m_{b'}$. É interessante verificar que quer com os dados de DELPHI, quer com os de D0/CDF as zonas de exclusão aumentam com $m_{t'} - m_{b'}$. Este facto está em sintonia com as medidas de precisão que também desfavorecem e existência de uma quarta família caracterizada por uma grande diferença de massas entre os seus dois *quarks*. No entanto, não podemos deixar de verificar que para qualquer valor de $m_{b'}$ existe sempre um valor de $m_{t'}$ que não está excluído, desde que o valor de R_{CKM} não seja muito grande. No limite em que $R_{CKM} \to 0$ o valor de $Br_{b' \to b\,Z} \approx 100\%$ e obtemos, como não podia deixar de ser, o limite de CDF[2].

Em alguns casos, a sobreposição dos resultados de CDF/DO e DELPHI permite aumentar a área excluída. Por exemplo, quando $m_{b'} = 100$ GeV e $m_{t'} - m_{b'} = 50$ GeV, os dados de DELPHI implicam que $4.5 \times 10^{-4} < R_{CKM} < 8.4 \times 10^{-4}$ e os dados de CDF/D0 (*lower*) implicam que $6.7 \times 10^{-4} < R_{CKM} < 1.1 \times 10^{-3}$. Assim a área de exclusão combinada é: $6.7 \times 10^{-4} < R_{CKM} < 8.4 \times 10^{-4}$.

Com o limite $|V_{tb}|^2 + 0.75|V_{t'b}|^2 \leq 1.14$ [13] e assumindo que $|V_{tb}| \approx 1$, é possível impor um limite ao valor do elemento $V_{cb'}$ da matriz CKM. Por exemplo, fixando $m_{b'} = 100$ GeV e $m_{t'} = m_{b'} + 50 = 150$ GeV sabemos que $R_{CKM} < 8.4 \times 10^{-4}$ e por isso

$$V_{cb'} < 8.4 \times 10^{-4} \sqrt{0.14/0.75} \approx 3.6 \times 10^{-4}$$

Este limite enfraquece para valores de $m_{t'}$ menores [13].

Foram ainda estudadas as implicações da abertura do canal do Higgs, assumindo $m_H = 115$ GeV. Como era de esperar a inclusão deste novo canal vai diminuir as zonas excluídas. O canal $b' \to b\,H$ cresce da mesma forma que $b' \to b\,Z$ para valores pequenos de R_{CKM} e grandes de $m_{b'}$. Assim, dada a competição nesta região, a zona excluída reduz-se.

Foram calculados os valores permitidos para $m_{b'}$ em função dos valores da matriz CKM de um *quark* sequencial de quarta geração. Concluímos que existe ainda espaço nos parâmetros do

modelo para contemplar a existência de um *quark b'* com massa superior a 96 GeV. Mostrámos também que o espaço diminui quando o valor de m'_t aumenta. Todos os gráficos mostram que o valor de R_{CKM} é menor que $\approx 10^{-2}$, sendo mesmo possível ter valores inferiores a $\approx 10^{-4}$, o que está de acordo com os valores da matriz CKM conhecidos.

Quanto ao futuro, é necessário esperar pelas analises do RunII do Tevatron e pelo arranque do Large Hadron Collider (LHC). No LHC a produção de pares $b'\bar{b}'$ aumentará em duas ordens de grandeza comparativamente à do Tevatron. Isto permitirá estudar um grande espectro da massa do b'. Acreditamos que existe ainda bastante trabalho teórico e experimental a ser feito para encontrar ou excluir definitivamente um *quark* sequencial de quarta geração.

Segunda parte - Aniquilação de electrão-positrão a altas energias

Amplitudes electrofracas para aniquilação de electrão-positrão a altas energias

A aproximação por duplos-logaritmos (DLA) foi introduzida na Física de partículas por V.V. Sudakov que verificou que as maiores contribuições radiactivas para o factor de forma $f(q^2)$ do electrão, quando q^2 é muito grande, são do tipo duplos-logaritmos (DL) isto é aproximadamente $(\alpha \ln^2(q^2/m^2))^n$ para $n = 1, 2, ..$ onde m é a escala de massa. Tendo em conta todas as ordens em α, no limite em que $q^2 \gg m^2$, Sudakov chegou ao seguinte resultado [14]:

$$f(q^2) \sim e^{-(\alpha/4\pi)\ln^2(q^2/m)} \tag{3}$$

O passo seguinte [15] foi estudar os limites de DL na teoria Eletrodinâmica Quântica (QED). Posteriormente, em estudos feitos para amplitudes de dispersão na teoria Quantum Chromo-dynamics (QCD) verificou-se não existirem grandes diferenças técnicas para processos elásticos em relação à QED ([16]). No entanto, para processos não elásticos (radiactivos) o cálculo das amplitudes em QCD revelou-se bastante mais complexo ([17, 18]). Esta técnica pode ser aplicada em processos electrofracos (EW), desde que a energia total seja elevada de modo a que as massas dos bosões electrofracos possam ser desprezadas. A estas energias ($\gg 100$ GeV), muitos dos detalhes técnicos utilizados quer em QED, quer em QCD, podem ser aplicados [19].

O estudo tradicional da aniquilação de $e^+e^- \to q\bar{q}$ pode ser feito em dois passos: o primeiro consiste em assumir que o processo é mediado por apenas um fotão virtual: $e^+e^- \to \gamma^* \to q\bar{q}$ e o segundo passo é calcular as correcções radiactivas de QCD. No entanto, em algumas regiões cinemáticas, torna-se necessário incluir as correcções radiactivas electrofracas, pois estas podem ser importantes. Estas regiões são denominadas como região de cinemática *forward* e cinemática *backward*. A cinemática diz-se *forward* quando o ângulo no centro de massa entre o electrão inicial e a partícula de carga negativa final é $\ll 1$. A cinemática diz-se *backward* quando este ângulo é $\sim \pi$. A amplitude de dispersão da aniquilação $e^+e^- \to q\bar{q}$ pode ser definida do seguinte

modo:

$$A = q^{k'}(p_1')\,\bar{q}_{i'}(-p_2')\,\widetilde{A}_{kk'}^{ii'}\,l^k(p_1)\,\bar{l}_i(-p_2) \tag{4}$$

Assim podemos escrever as cinemáticas de Regge:

(i) cinemática *forward* ou t quando:

$$-t = -(p_1' - p_1)^2 << s = (p_1 + p_2)^2 \approx -u = -(p_2' - p_1)^2 \ , \tag{5}$$

(ii) cinemática *backward* ou u quando:

$$-u = -(p_2' - p_1)^2 << s = (p_1 + p_2)^2 \approx -t = -(p_1' - p_1)^2 \ . \tag{6}$$

Para se simplificar a estrutura do isospin é conveniente expandir a matriz $\widetilde{A}_{kk'}^{ii'}$ numa soma de termos que correspondam a uma representação irredutível de $SU(2)$:

$$A_{kk'}^{ii'} = \frac{\bar{u}(-p_2')\gamma_\mu u(p_1')\bar{u}(-p_2)\gamma^\mu u(p_1)}{s}\Big[(P_j)_{kk'}^{ii'}A_j + (P_{j+1})_{kk'}^{ii'}A_{j+1}\Big] \ , \tag{7}$$

com $j = 1$ para a cinemática t e $j = 3$ para a cinemática u. Os operadores de projecção P_j são definidos da seguinte forma:

$$\begin{aligned}
(P_1)_{kk'}^{ii'} &= \frac{1}{2}\delta_k^{k'}\delta_{i'}^i, \\
(P_2)_{kk'}^{ii'} &= 2(t_c)_k^{k'}(t_c)_{i'}^i \ , \\
(P_3)_{kk'}^{ii'} &= \frac{1}{2}\left[\delta_k^i\delta_{i'}^{k'} - \delta_k^{k'}\delta_{i'}^i\right] \ , \\
(P_4)_{kk'}^{ii'} &= \frac{1}{2}\left[\delta_k^i\delta_{i'}^{k'} + \delta_k^{k'}\delta_{i'}^i\right] \ .
\end{aligned} \tag{8}$$

Tendo sido calculadas as amplitudes A_j podemos usá-las para escrever as amplitudes da aniquilação de e^+e^- para *quarks* em ambas as cinemáticas:

$$\begin{aligned}
A_F(e^+e^- \to u\bar{u}) &= R\,A_2(s,t), \\
A_F(e^+e^- \to d\bar{d}) &= R\,[A_1(s,t) + A_2(s,t)]/2 \ , \\
A_B(e^+e^- \to u\bar{u}) &= R\,[A_3(s,t) + A_4(s,t)]/2 \ , \\
A_B(e^+e^- \to d\bar{d}) &= R\,A_4(s,t) \ .
\end{aligned} \tag{9}$$

As amplitudes da aniquilação de e^+e^- para leptões podem ser escritas de uma forma idêntica:

$$\begin{aligned}
A_F(e^+e^- \to \mu^+\mu^-) &= R\,[A_1(s,t) + A_2(s,t)]/2, \\
A_F(e^+e^- \to \nu_\mu\bar{\nu}_\mu) &= R\,[A_3(s,t) + A_4(s,t)]/2, \\
A_B(e^+e^- \to \mu^+\mu^-) &= R\,A_2(s,t) \ , \\
A_B(e^+e^- \to \nu_\mu\bar{\nu}_\mu) &= R\,A_4(s,t) \ .
\end{aligned} \tag{10}$$

Para calcularmos as amplitudes A_j a todas as ordens no acoplamento electrofraco na DLA constrói-se e resolve-se uma equação de evolução do infravermelho (*infrared evolution equations* (IREE)). Esta equação descreve a evolução de A_j ($j = 1, 2, 3, 4$) em relação a um corte no infravermelho. Consideramos neste trabalho dois cortes no infravermelho, μ e M. Assumimos que $M \approx M_Z \approx M_W$ e usamos este corte para regularizar as contribuições DL que envolvem bosões virtuais W, Z de muito baixa energia (quase na camada de massa). As divergências no infravermelho provenientes de fotões de baixa energia são reguladas com o corte μ, assumindo que $\mu \approx m_q \ll M$ onde m_q é a massa do *quark* mais pesado. Começamos por calcular A_j na cinemática colinear, onde as partículas produzidas seguem uma direcção muito próxima à do eixo inicial de e^+e^-. Esta cinemática implica as seguintes restrições para o t:

$$s \sim -u \gg M^2 \gg \mu^2 \geq -t \tag{11}$$

e para o u:

$$s \sim -t \gg M^2 \gg \mu^2 \geq -u . \tag{12}$$

Na cinemática colinear, A_j depende apenas dos logaritmos de s, M^2 e μ^2 sendo conveniente representá-la da seguinte forma:

$$A_j(s, \mu^2, M^2) = A_j^{(QED)}(s, \mu^2) + A'_j(s, \mu^2, M^2) , \tag{13}$$

onde $A_j^{(QED)}(s, \mu^2)$ representa apenas as contribuições DL para QED, isto é, contém apenas os diagramas de Feynman onde não existem bosões virtuais W ou Z. No cálculo de $A_j^{(QED)}(s, \mu^2)$ é apenas usado o corte μ. A amplitude $A'_j(s, \mu^2, M^2)$ depende dos dois cortes sendo consideradas as contribuições DL dos diagramas de Feynman que contêm como propagadores um ou mais bosões virtuais W ou Z. No entanto, por questões técnicas, é interessante introduzir duas amplitudes auxiliares. A primeira $\tilde{A}_j^{(QED)}(s, M^2)$ é idêntica à amplitude $A_j^{(QED)}(s, \mu^2)$ mas usa M como corte. A segunda $\tilde{A}_j(s, M^2)$ contém todas as contribuições DL electrofracas, tendo sido usado o corte M para regularizar as divergências no infravermelho das contribuições dos fotões virtuais e dos bosões W e Z. O objectivo deste trabalho foi calcular a amplitude A'_j, pois as amplitudes $A_j^{(QED)}$, $\tilde{A}_j^{(QED)}$ e $\tilde{A}_j(s/M^2)$ já tinham sido calculadas por Ermolarv et. al.[20].

Para simplificar a resolução da IREE usa-se a transformação de Sommerfeld-Watson. No entanto, esta transformação coincide com a transformação de Mellin se apenas forem consideradas as amplitudes de assinatura positiva. Neste caso é conveniente definir as seguintes transformações:

$$A_j^{(QED)}(s/\mu^2) = \int_{-\imath\infty}^{\imath\infty} \frac{d\omega}{2\pi\imath} \left(\frac{s}{\mu^2}\right)^\omega f_j^{(0)}(\omega) , \tag{14}$$

$$\tilde{A}_j^{(QED)}(s/M^2) = \int_{-\imath\infty}^{\imath\infty} \frac{d\omega}{2\pi\imath} \left(\frac{s}{M^2}\right)^\omega f_j^{(0)}(\omega) , \tag{15}$$

$$\tilde{A}_j(s/M^2) \;\; = \;\; \int_{-\imath\infty}^{\imath\infty} \frac{d\omega}{2\pi\imath} \Big(\frac{s}{M^2}\Big)^\omega f_j(\omega) \,, \tag{16}$$

$$A'_j(s/M^2, \varphi) \;\; = \;\; \int_{-\imath\infty}^{\imath\infty} \frac{d\omega}{2\pi\imath} \Big(\frac{s}{M^2}\Big)^\omega F_j(\omega, \varphi) \,. \tag{17}$$

A IREE pode ser escrita em função das transformações de Mellin $F_j(\omega, \varphi)$ da seguinte forma:

$$
\begin{aligned}
\int_{-\imath\infty}^{\imath\infty} \frac{d\omega}{2\pi\imath} \Big(\frac{s}{M^2}\Big)^\omega F_j(\omega, \varphi) \;\; = \;\; & \int_{-\imath\infty}^{\imath\infty} \frac{d\omega}{2\pi\imath} \Big(\frac{s}{M^2}\Big)^\omega [f_j(\omega) - f_j^{(0)}(\omega)] \\
& - \int_{-\imath\infty}^{\imath\infty} \frac{d\omega}{2\pi\imath} \Big(\frac{s}{M^2}\Big)^\omega \frac{1}{8\pi^2} b_j^{(\gamma)} \int_{\mu^2}^{M^2} \frac{dk_\perp^2}{k_\perp^2} \ln(s/k_\perp^2) F_j(\omega, \varphi') \\
& + \int_{-\imath\infty}^{\imath\infty} \frac{d\omega}{2\pi\imath} \Big(\frac{s}{M^2}\Big)^\omega c_j \int_{\mu^2}^{M^2} \frac{dk_\perp^2}{k_\perp^2} \Big(2f_j^{(0)}(\omega) F_j(\omega, \varphi') + F_j^2(\omega, \varphi') \Big) \Big] \,,
\end{aligned}
\tag{18}
$$

onde $\varphi \equiv \ln(M^2/\mu^2)$ e $\varphi' = \ln(M^2/k_\perp^2)$. Os factores b_j^γ são definidos por:

$$
\begin{aligned}
b_1^{(\gamma)} \;\; &= \;\; g^2 \sin^2 \theta_W \frac{(Y_2 - Y_1)^2}{4}, \\
b_2^{(\gamma)} \;\; &= \;\; g^2 \sin^2 \theta_W \Big[\frac{1}{6} + \frac{(Y_2 - Y_1)^2}{4} \Big] \,, \\
b_3^{(\gamma)} \;\; &= \;\; g^2 \sin^2 \theta_W \frac{(Y_2 + Y_1)^2}{4}, \\
b_4^{(\gamma)} \;\; &= \;\; g^2 \sin^2 \theta_W \Big[\frac{1}{6} + \frac{(Y_2 + Y_1)^2}{4} \Big]
\end{aligned}
\tag{19}
$$

e os factores $c_1 = c_2 = -c_3 = -c_4 = \frac{1}{8\pi^2}$.

A diferenciação da IREE na camada de massa em ordem a μ^2 resulta na seguinte equação para $F_j(\omega, \varphi)$:

$$\frac{\partial F_j}{\partial \varphi} = -\frac{1}{8\pi^2} b_j^{(\gamma)} \Big(-\frac{\partial F_j}{\partial \omega} + \varphi F_j \Big) + c_j \Big(2f_j^{(0)}(\omega) F_j + F_j^2 \Big) \,, \tag{20}$$

em que usamos o facto de $\ln(s/\mu^2)$ ser igual a $\ln(s/M^2) + \varphi$ e de $\ln(s/M^2)$ corresponder a $-\partial/\partial\omega$.

Para resolver a eq. 20 começamos por considerar o caso particular em que $b_1^{(\gamma)} = 0$. Este caso contribui para o processo $e^+e^- \to \mu^+\mu^-$ na cinemática *forward*. Na notação usada corresponde a:

$$Y_1 = Y_2 = -1. \tag{21}$$

Deve notar-se que a amplitude A_j com $j = 1$ contribui também para a aniquilação $e^+e^- \to d\bar{d}$. No entanto, neste caso $Y_1 = -1$ e $Y_2 = 1/3$ e por isso $b_1^{(\gamma)} \neq 0$. Para evitar confusões entre estes dois casos introduz-se uma nova notação onde $\Phi_1 \equiv F_1$, $\phi_1 \equiv f_1$ e $\phi_1^{(0)} \equiv f_1^{(0)}$ quando

$Y_1 = Y_2 = -1$. Assim a solução para $L_1 \equiv A_1$ quando $Y_1 = Y_2 = -1$ é:

$$L_1 = \int_{-\iota\infty}^{\iota\infty} \frac{d\omega}{2\pi\iota} \left(\frac{s}{\mu^2}\right)^\omega \phi_1^{(0)}(\omega) + \int_{-\iota\infty}^{\iota\infty} \frac{d\omega}{2\pi\iota} \left(\frac{s}{M^2}\right)^\omega \frac{2\phi_1^{(0)}(\phi_1 - \phi_1^{(0)})e^{2c\phi_1^{(0)}\varphi}}{\phi_1^{(0)} + \phi_1 - (\phi_1 - \phi_1^{(0)})e^{2c\phi_1^{(0)}\varphi}} \tag{22}$$

em que

$$\begin{aligned}
\phi_1^{(0)} &= 8\pi^2(\omega - \sqrt{\omega^2 - \chi_0^2}), \\
\chi_0^2 &= 2\alpha/\pi, \\
\phi_1 &= 4\pi^2(\omega - \sqrt{\omega^2 - \chi^2}), \\
\chi^2 &= [3g^2 + g'^2]/(8\pi^2).
\end{aligned} \tag{23}$$

Como seria de esperar quando $\mu \to M$, L_1 converge para a amplitude calculada usando apenas um corte.

Considera-se em seguida o caso geral em que o factor $b_j^{(\gamma)}$ é diferente de zero. Neste caso, esta equação descreve a aniquilação e^+e^- para um par de leptões $(\mu^+\mu^-)$ na cinemática *backward* ou para um par de *quarks* na cinemática *forward*, sendo a amplitude neste caso dada por:

$$\begin{aligned}
A_j(s/M^2, \varphi) &= \int_{-\iota\infty}^{\iota\infty} \frac{d\omega}{2\pi\iota} \left(\frac{s}{\mu^2}\right)^\omega f_j^{(0)}(\omega) + \tag{24} \\
&\quad \int_{-\iota\infty}^{\iota\infty} \frac{d\omega}{2\pi\iota} \left(\frac{s}{M^2}\right)^\omega \frac{(f_j(x+y) - f_j^{(0)}(x+y))P_j(\sigma,\tau)}{P_j(\sigma,\sigma) - (f_j(x+y) - f_j^{(0)}(x+y))(Q_j(\sigma,\sigma) - Q_j(\sigma,\tau))}.
\end{aligned}$$

com

$$\begin{aligned}
P_j(\sigma,\tau) &= \exp\left(\sigma\tau - \tau^2/2 - 2q_j \int_\sigma^{\sigma+\tau} d\zeta f_j^{(0)}(\zeta)\right), \\
Q_j(\sigma,\tau) &= \int_\sigma^{\sigma+\tau} d\zeta P_j(\sigma,\zeta) \tag{25}
\end{aligned}$$

e

$$\begin{aligned}
\sigma &= (x+y)/2, \tag{26} \\
\tau &= (x-y)/2, \\
q_j &= c_j/\lambda_j, \\
x &= \omega/\lambda_j, \\
y &= \lambda_j\varphi, \\
\lambda_j &= \sqrt{b_j^{(\gamma)}/(8\pi^2)}.
\end{aligned}$$

As amplitudes $f_j^{(0)}$ podem ser obtidas a partir das expressões da amplitude de dispersão de QED $f_B^{(0)}$ na cinemática *forward* e $f_F^{(0)}$ cinemática *backward*. A amplitude *backward* é a seguinte:

$$f_B^{(0)}(x) = (4\pi\alpha e_q/p_B^{(0)})d\ln(e^{x^2/4} D_{p_B^{(0)}}(x))/dx, \tag{27}$$

em que D_p são as conhecidas funções parabólicas cilíndricas com $p_B^{(0)} = -2e_q/(1 + e_q)^2$. Na aniquilação para muões temos $e_q = 1$ e na aniquilação para os *quarks d (u)* temos $e_q = 1/3 \, (2/3)$. A amplitude *forward* é dada por:

$$f_F^{(0)}(x) = (4\pi\alpha e_q/p_F^{(0)}) d\ln(e^{x^2/4}D_{p_F^{(0)}}(x))/dx \; , \tag{28}$$

com $p_B^{(0)} = 2e_q/(1 - e_q)^2$. As amplitudes $f_{F,B}^{(0)}$ foram calculadas em [15]. As amplitudes f_j, calculadas em [20], são definidas como:

$$f_j(x) = \frac{a_j}{p_j}\frac{d\ln(e^{x^2/4}D_{p_j}(x))}{dx} = a_j\frac{D_{p_j-1}(x)}{D_{p_j}(x)} \; . \tag{29}$$

em que os factores a_j são dados por:

$$
\begin{aligned}
a_1 &= \frac{3g^2 + g'^2 Y_l Y_q}{4}, \\
a_2 &= \frac{-g^2 + g'^2 Y_l Y_q}{4}, \\
a_3 &= \frac{-3g^2 + g'^2 Y_l Y_q}{4}, \\
a_4 &= \frac{g^2 + g'^2 Y_l Y_q}{4} \; .
\end{aligned}
\tag{30}
$$

Estas equações são as expressões explícitas da amplitude de dispersão para a aniquilação de e^+e^- para *quarks* e leptões na cinemática colinear. Nelas estão incluídas todas as contribuições DL a todas as ordens no acoplamento electrofraco com dois cortes. Para se estimar o impacto do uso de dois cortes comparámos estes resultados com as amplitudes obtidas com apenas um corte. Estudámos o caso particular da amplitude de dispersão para a aniquilação de e^+e^- para leptões na cinemática colinear. Assim a amplitude $L_F^{(\mu)}$ de e^+e^- para $\mu^-\mu^+$ na cinemática *forward* é:

$$
\begin{aligned}
L_F^{(\mu)} =\; & \int_{-\imath\infty}^{\imath\infty}\frac{d\omega}{2\pi\imath}\left(\frac{s}{\mu^2}\right)^\omega \phi_F^{(0)}(\omega) \\
& +\frac{1}{2}\int_{-\imath\infty}^{\imath\infty}\frac{d\omega}{2\pi\imath}\left(\frac{s}{M^2}\right)^\omega \frac{4\phi_F^{(0)}(\phi_1 - 2\phi_F^{(0)})e^{4c\phi_F^{(0)}\varphi}}{2\phi_F^{(0)} + \phi_1 - (\phi_1 - 2\phi_F^{(0)})e^{4c\phi_F^{(0)}\varphi}} \\
& +\frac{1}{2}\int_{-\imath\infty}^{\imath\infty}\frac{d\omega}{2\pi\imath}\left(\frac{s}{M^2}\right)^\omega \frac{\phi_2(x + y)P_2(\sigma, \tau)}{P_2(\sigma, \sigma) - \phi_2(x + y)[Q_2(\sigma, \sigma) - Q_2(\sigma, \tau)]} \; .
\end{aligned}
\tag{31}
$$

No primeiro termo deste integral são incluídas as contribuições DL puramente QED que dependem apenas de um corte μ. Nos restantes termos são incluídas as contribuições DL dos termos que misturam QED e fracas dependendo assim dos dois cortes μ e M. Os valores do primeiro

e do segundo integral aumentam com s, enquanto que o valor do terceiro diminui substancialmente quando s aumenta. Assim, apenas consideramos as contribuições provenientes dos dois primeiros termos. Numa primeira fase comparámos as contribuições provenientes de um-loop e de dois-loops. A um-loop a contribuição para $L_F^{(\mu)}$ é:

$$L^{(1)} = \gamma_1^{(1)} \ln^2(s/\mu^2) + \gamma_2^{(1)} \ln(s/\mu^2) \ln(s/M^2) + \gamma_3^{(1)} \ln^2(s/M^2) \tag{32}$$

e para dois-loops:

$$\begin{aligned} L^{(2)} &= \gamma_1^{(2)} \ln^4(s/\mu^2) + \gamma_2^{(2)} \ln^3(s/\mu^2) \ln(s/M^2) + \\ &\quad \gamma_3^{(2)} \ln^2(s/\mu^2) \ln^2(s/M^2) + \gamma_4^{(2)} \ln(s/\mu^2) \ln^3(s/M^2) + \gamma_5^{(2)} \ln^4(s/M^2) \end{aligned} \tag{33}$$

em que os coeficientes $\gamma_i^{(k)}$ são dados por:

$$\begin{aligned} \gamma_1^{(1)} &= \frac{\pi^2 {\chi_0}^4}{4}, \\ \gamma_2^{(1)} &= \frac{\pi^2 \left(\chi^4 - 4\,{\chi_0}^4\right)}{4}, \\ \gamma_3^{(1)} &= -\frac{\pi^2 \left(\chi^4 - 6\,{\chi_0}^4\right)}{8}, \\ \gamma_1^{(2)} &= \frac{\pi^2 {\chi_0}^6}{96}, \\ \gamma_2^{(2)} &= 0, \\ \gamma_3^{(2)} &= \frac{\pi^2 \chi^2 \left(\chi^4 - 4\,{\chi_0}^4\right)}{32}, \\ \gamma_4^{(2)} &= -\frac{\pi^2 \left(\chi^6 - 6\,\chi^2\,{\chi_0}^4 + 2\,{\chi_0}^6\right)}{24}, \\ \gamma_5^{(2)} &= \frac{\pi^2 \left(3\,\chi^6 - 24\,\chi^2\,{\chi_0}^4 + 14\,{\chi_0}^6\right)}{192}. \end{aligned} \tag{34}$$

A comparação destes resultados para um-loop com os resultados obtidos com apenas um corte universal M, representado por $\tilde{L}(s/M^2)$, pode ser definido como $R^1 = L^1(s, \mu, M)/\tilde{L}^{(1)}(s, M)$ e é dado por:

$$R^{(1)} = \frac{L^{(1)}}{\tilde{\gamma}^1 \ln^2(s/M^2)} \tag{35}$$

onde $\tilde{\gamma}^1 = \pi^2 \chi^4 / 8$. Identicamente podemos definir o rácio $R^{(2)}$ para as contribuições a dois-loops:

$$R^{(2)} = \frac{L^{(2)}}{\tilde{\gamma}^2 \ln^4(s/M^2)}, \tag{36}$$

onde $\tilde{\gamma}^2 = \pi^2 \chi^6 / 64$. Como se pode ver nas Figs. 3.6 e 3.7 as diferenças entre as amplitudes calculadas com um corte $\tilde{L}$ e dois cortes $L_F^{(\mu)}$ aumentam com a ordem da expansão perturbativa,

mas diminuem rapidamente com s. Por esta razão será de esperar que quando forem somadas todas as ordens da série as diferenças entre $L_F^{(\mu)}$ e $\tilde{L}$ sejam significativas.

Estimámos o efeito das contribuições de ordem elevada entre o uso de um ou dois cortes comparando-os no limite assimptótico de alta energia. A amplitude *forward* L_F^μ da aniquilação de e^+e^- para $\mu^+\mu^-$ na cinemática colinear é dada por:

$$L_F^\mu \sim 4\pi^2\Big(\frac{s}{\mu^2}\Big)^{\chi_0}\chi_0 + 4\pi^2\Big(\frac{s}{M^2}\Big)^{\chi}\frac{2(\chi-\chi')(2\chi'-\chi)e^{2\varphi(\chi-\chi')}}{3\chi-2\chi'-(2\chi'-\chi)e^{2\varphi(\chi-\chi')}}. \tag{37}$$

onde para simplificar definimos $\chi' = \sqrt{\chi^2 - \chi_0^2}$. O primeiro termo desta equação representa as contribuições do limite assimptótico DL dos diagramas de Feynman de QED e o segundo, as contribuições dos termos de mistura de QED e fracas. No caso de ser usado apenas um corte no limite assimptótico, a amplitude $\tilde{L}_F^\mu$ tem o seguinte comportamento:

$$\tilde{L}_F^\mu \sim 4\pi^2\frac{\chi}{2}\Big(\frac{s}{M^2}\Big)^{\chi}. \tag{38}$$

Podemos então definir $Z(s,\varphi)$ como:

$$L_F^\mu = \tilde{L}_F^\mu(1 + Z(s,\varphi)), \tag{39}$$

Quando $\chi_0 < \chi$ e s aumenta, o valor de $Z(s)$ diminui levando a que no limite assimptótico de altas-energias as duas aproximações sejam equivalentes. Na Fig. 3.8 está representado o valor de $Z(s,\mu)$ para $\mu = 1$ GeV e $\mu = 0.5$ GeV.

Estimámos também qual a diferença entre as contribuições de QED (L_F^μ) e as contribuições electrofracas completas no limite assimptótico. Para isso definimos Δ_{EW}:

$$L_F^{(\mu)} = (L_F^{(\mu)})^{(QED)}(1 + \Delta_{EW}). \tag{40}$$

Neste caso, quando $\chi > \chi_0$ e s aumenta, o valor de Δ_{EW} também aumenta como se pode ver na Fig. 3.9. As contribuições da interacção fraca são aproximadamente da mesma ordem que as contribuições de QED e o seu rácio cresce rapidamente quando μ decresce.

Os novos aceleradores lineares de e^+e^- vão funcionar num domínio energético muito superior à massa dos bosões electrofracos. Assim, torna-se fundamental ter um conhecimento completo das amplitudes de dispersão para a aniquilação e^+e^- para um par de fermiões. Neste trabalho foram calculadas estas amplitudes na cinemática de Regge usando a DLA com dois cortes M e μ. Foram obtidas expressões explícitas para a cinemática colinear e para a cinemática em que todas as variáveis de Mandelstam são grandes.

Produção de bosões electrofracos na aniquilação de e^+e^- a altas energias

Após o estudo dos processos elásticos de $2 \to 2$ é interessante alargar o estudo para os processos $2 \to 2 + n$ em que a aniquilação é acompanhada da emissão de n bosões. A emissão de bosões

energéticos pode ser estudada usando a DLA a todas as ordens no acoplamento, desde que estes bosões sejam emitidos dentro de um cone com ângulos $\ll 1$ em relação ao eixo inicial de e^+e^-, isto é na cinemática de Regge. Neste caso, a parte mais importante das amplitudes de dispersão consiste num factor cinemático $\sim (1/k_{1\perp})\dots(1/k_{n\perp})$ multiplicado por uma função M a que se dá o nome de amplitude multi-Regge do processo. A dependência na energia de M é controlada pelos $n+1$ Reggeons electrofracos que propagam no canal cruzado. A amplitude para a produção de fotões multi-Regge na aniquilação *backward* de $e^+e^- \to \mu^+\mu^-$ foi descrita em [21] e [22]. A amplitude para produção de gluões multi-Regge na aniquilação *backward* de pares *quark-antiquark* foi considerada em [23].

Seguindo a metodologia aplicada na secção anterior para os processos de $2 \to 2$, em vez de calcularmos directamente a amplitude $A^{(\gamma,Z,W)}$, que descreve a emissão de qualquer γ, Z, W, é possível calcular as amplitudes $A^{(0)}$ e $A^{(r)}$ $(r=1,2,3)$ que descrevem respectivamente a emissão do bosão isoescalar e do bosão isovector. A partir destas expressões e das relações entre os campos γ, Z, W e os campos de $SU(2) \otimes U(1)$ (antes da quebra de simetria) é possível escrevermos $A^{(\gamma,Z,W)}$ em função de A_0 e A_r. Desta forma, o cálculo de $A^{(\gamma,Z,W)}$ é tecnicamente mais simples pois quando as correcções radiactivas forem incluídas na DLA os termos proporcionais às massas de todos os propagadores virtuais electrofracos podem ser desprezados e os campos isoescalar e isovector podem ser considerados independentes. Por esta razão é mais conveniente trabalhar com os bosões virtuais isoescalar e isovector do que com os bosões γ, Z, W.

Consideremos então o processo da aniquilação do leptão $l^i(p_1)$ e da sua antipartícula $\bar{l}_{i'}(p_2)$ para o par *quark-antiquark* $q^j(p'_1)\,\bar{q}_{j'}(p'_2)$ e um bosão. O bosão emitido A_c pode ser um isoescalar quando $c=0$ ou um isovector quando $c=1,2,3$.

Existem duas cinemáticas onde este processo produz correcções radiactivas do tipo DL. A primeira é a cinemática-t onde $p'_1 \sim p_1$, $p'_2 \sim p_2$. Esta cinemática define:

$$s = (p_1+p_2)^2 \gg t_{1,2} \,, \qquad t_1 = q_1^2 = (p'_1-p_1)^2 \,, \qquad t_2 = q_2^2 = (p_2-p'_2)^2 \,, \qquad (41)$$

e representa o caso em que as partículas finais estão no cone com ângulo de abertura $\theta \ll 1$ à volta do feixe e^+e^-. A segunda é a cinemática-u onde $p'_1 \sim p_2$, $p'_2 \sim p_1$ e

$$s = (p_1+p_2)^2 \gg u_{1,2} \,, \qquad u_1 = q'^2_1 = (p'_2-p_1)^2 \,, \qquad u_2 = q'^2_2 = (p_2-p'_1)^2. \qquad (42)$$

Neste caso, as partículas finais estão no cone com ângulo de abertura $\pi - \theta \ll 1$ à volta do feixe e^+e^-. Ambas as cinemáticas são do tipo Regge.

Podemos escrever a amplitude de dispersão deste processo como $q_j\bar{q}^{j'}(M^c)^{i'j}_{ij'}\bar{l}_{i'}l^i$ onde $(M^c)^{i'j}_{ij'}$ representa o objecto a ser calculado. De modo a simplificar a estrutura da matriz do isospin $(M^c)^{i'j}_{ij'}$ é conveniente trabalhar no canal t para a cinemática *forward* e no canal u para a cinemática *backward*. No canal t a amplitude do processo $l^i\bar{l}_{i'} \to q^j\bar{q}_{j'}A_c$ pode ser expressa pela mesma matriz $(M^c)^{i'j}_{ij'}$ mas com os estados iniciais (finais) $q_jl^i(A_c\bar{q}^{j'}\bar{l}_{i'})$:

$$M = \frac{2}{k_\perp^2}\, A_c\bar{q}^{j'}\bar{l}_{i'}(M^c)^{i'j}_{ij'}q_jl^i \,. \qquad (43)$$

Assim podemos representar $(M^c)^{i'j}_{ij'}$ como a soma:

$$(M^c)^{i'j}_{ij'} = \sum_{k=0}^{4} (P^c_k)^{i'j}_{ij'} M_k \ , \tag{44}$$

das amplitudes M_k ($k = 0, 1, 2, 3, 4$) multiplicadas pelos operadores de projecção $(P^c_k)^{i'j}_{ij'}$ que correspondem a formas irredutíveis $SU(2)$. As amplitudes M_k com $k = 0, 1$ correspondem à emissão do campo isoescalar e com $k = 2, 3, 4$ à emissão de um campo isovector. Os operadores de projecção são definidos como:

$$
\begin{aligned}
(P^c_0)^{i'j}_{ij'} &= \frac{1}{2} \delta^c_0 \delta^{i'}_{j'} \delta^j_i, \\
(P^c_1)^{i'j}_{ij'} &= 2 \, \delta^c_0 (t_m)^j_i (t_m)^{i'}_{j'}, \\
(P^c_2)^{i'j}_{ij'} &= (t_b)^j_i (T^c)_{ba} (t_a)^{i'}_{j'}, \\
(P^c_3)^{i'j}_{ij'} &= (t_c)^j_i \delta^{i'}_{j'} \ , \\
(P^c_4)^{i'j}_{ij'} &= \delta^j_i (t_c)^{i'}_{j'} \ .
\end{aligned}
\tag{45}
$$

As amplitudes M_3, M_4 não têm contribuições DL por esta razão apenas é necessário calcular as amplitudes $M_{0,1,2}$.

Nestas amplitudes estão incluídas as correcções radiactivas DLA para todas as ordens no acoplamento electrofraco. Os argumentos de M_k são:

$$
\begin{aligned}
s_1 &= (p'_1 + k)^2 \approx 2p_1 k \ , & t_1 &= q_1^2 = (p_1 - p'_1)^2, \\
s_2 &= (p'_2 + k)^2 \approx 2p_2 k \ , & t_2 &= q_2^2 = (p'_2 - p_2)^2 \ ,
\end{aligned}
\tag{46}
$$

de modo a que

$$s_1 \, s_2 = s \, k_\perp^2 \tag{47}$$

A cinemática deste processo é uma cinemática multi-Regge do canal t quando

$$s_{1,2} \gg t_{1,2} \geq M_Z^2 \ . \tag{48}$$

Assumimos ainda:

$$t_1 \gg t_2 \ . \tag{49}$$

Estas amplitudes dependem igualmente do corte do infravermelho μ inserido para evitar as singularidades no infravermelho da integração no momento das partículas virtuais. O corte infravermelho é inserido no espaço transverso seguindo o que foi feito em [24]. Se denotarmos $k'^{ab}_{l\perp}$ como sendo a componente do momento da partícula virtual transverso ao plano formado pelos momentos de a and b, com $a \neq b$ então o corte infravermelho μ obedece a:

$$\mu < k'^{ab}_{l\perp} \tag{50}$$

para todos os $l = 1, \ldots$ com $a, b = p_1, p_2, p'_1, p'_2, k$. Neste trabalho assumimos que $\mu \approx M_Z$.

A IREE para M_r é dada por:

$$\frac{\partial M_r}{\partial \rho_1} + \frac{\partial M_r}{\partial \rho_2} + \frac{\partial M_r}{\partial y_1} + \frac{\partial M_r}{\partial y_2} = -\frac{1}{8\pi^2}[b_r \ln(s/\mu^2) + h_r(y_1 + y_2) + m_k y_1]M_r \ . \tag{51}$$

Nesta equação foram introduzidas as seguintes variáveis:

$$\rho_{1,2} = \ln(s_{1,2}/\mu^2) \ , \qquad y_{1,2} = \ln(t_{1,2}/\mu^2) \ . \tag{52}$$

Os factores numéricos b_r, h_r e m_r são definidos como:

$$\begin{aligned}
b_0 &= \frac{g'^2(Y - Y')^2}{4} \ , \\
b_1 = b_2 &= 2g^2 + \frac{g'^2(Y - Y')^2}{4} \ , \\
h_0 &= \frac{3g^2}{4} + \frac{g'^2 Y Y'}{4} \ , \\
h_1 = h_2 &= -\frac{g^2}{4} + \frac{g'^2 Y Y'}{4} \ , \\
m_0 = m_1 &= 0 \ , \\
m_2 &= g^2 \ .
\end{aligned} \tag{53}$$

Como fizemos no caso anterior é conveniente usar-se a amplitude de Mellin F_r, que se relaciona com M_r através da transformação de Mellin definida por:

$$M_r = \int_{-\imath\infty}^{\imath\infty} \frac{d\omega_1}{2\imath\pi} \frac{d\omega_2}{2\imath\pi} e^{\omega_1\rho_1 + \omega_2\rho_2} F_r(\omega_1, \omega_2, y_1, y_2) \ . \tag{54}$$

Assim a solução da IREE é dada por:

$$M_r = G_r R_r \tag{55}$$

onde

$$\begin{aligned}
R_r &= \int_{-\imath\infty}^{\imath\infty} \frac{d\omega_1}{2\imath\pi} \frac{d\omega_2}{2\imath\pi} \left(\frac{s_1}{q_1^2}\right)^{\omega_1} \left(\frac{s_2}{\sqrt{q_1^2 q_2^2}}\right)^{\omega_2} \frac{1}{\omega_2 - \omega_1} \frac{D_{p_r - 1}(x_1 - z_1)}{D_{p_r}(x_1 - z_1)} \cdot \\
&\quad \frac{D_{p_r}(x_2 - z_1)}{D_{p_r}(x_2 - z_2)} \exp\left[-\frac{(1 - 2\beta_r)}{4}z_1^2 - \frac{(1 - 2\gamma_r)}{4}z_2^2\right] \ .
\end{aligned} \tag{56}$$

As funções $D_{p_r}(x)$ são as conhecidas funções parabólicas cilíndricas, que devem ser avaliadas com diferentes valores de p_r. Por conveniência, foram introduzidas as seguintes variáveis:

$$x_{1,2} = \omega_{1,2}/\lambda_r \ , \qquad z_{1,2} = -\lambda_r y_{1,2} \tag{57}$$

onde $\lambda_r = \sqrt{b_r/8\pi^2}$, $\beta_r = -(h_r + m_r)/b_r$ e $\gamma_r = -h_r/b_r$.

As amplitudes $M^{(\gamma)}, M^{(Z)}, M^{(W^{\pm})}$ da produção de bosões electrofracos podem ser expressos por R_r da seguinte forma:

$$
\begin{aligned}
M^{(\gamma)} &= \cos\theta_W M^{(0)} + \sin\theta_W M^{(3)} = g\cos\theta_W(R_0 + R_1) + g\sin\theta_W R_2 \ , \\
M^{(Z)} &= -\sin\theta_W M^{(0)} + \cos\theta_W M^{(3)} = -g\sin\theta_W(R_0 + R_1) + g\cos\theta_W R_2 \ , \\
M^{(W^{\pm})} &= (1/\sqrt{2})[M^{(1)} \pm \imath M^{(2)}] = (g/\sqrt{2})R_2.
\end{aligned}
\tag{58}
$$

Em que [20]:

$$
\begin{aligned}
p_0 &= \frac{3 + YY'\tan^2\theta_W}{(Y - Y')^2 \tan^2\theta_W}, \\
p_1 = p_2 &= -\frac{1 - YY'\tan^2\theta_W}{8 + (Y - Y')^2 \tan^2\theta_W}.
\end{aligned}
\tag{59}
$$

Como as intercepções dos Reggeons isoescalar são maiores do que Reggeons isovector (0.11 e 0.08) o limite assimptótico das secções eficazes $\sigma^{(\gamma)}$ e $\sigma^{(Z)}$ para a produção de fotões e Z é dado pelas contribuições dos Reggeons isoescalar. Por esta razão a única diferença entre estas secções eficazes está no acoplamento destes campos aos Reggeons isoscalar. Assim no limite assimptótico temos a seguinte relação:

$$
\frac{\sigma^{(Z)}}{\sigma^{(\gamma)}} \approx \tan^2\theta_W \ .
\tag{60}
$$

A contribuição de outros zeros altera o valor de $\sigma^{(\gamma)}$ e $\sigma^{(Z)}$, no entanto, não produz alterações na relação anterior. Ao contrário desta relação no limite assimptótico, a relação $\sigma^{(\gamma)}/\sigma^{(W)}$ depende do valor de s. Isto deve-se ao facto da secção eficaz da produção de W, depender do Reggeons isovector com intercepção menor (-0.08 e -0.27). No limite assimptótico as secções eficazes obedecem à seguinte relação:

$$
\frac{\sigma^{(\gamma)}}{\sigma^{(W)}} \sim s^{2(\Delta_S - \Delta_V)} = s^{-0.36} \ .
\tag{61}
$$

Esta relação sofre alterações se outros zeros da função D_p forem incluídos.

É interessante calcular também a aniquilação de e^+e^- para *quarks* acompanhados pela emissão de n bosões isoescalar ou isovector com momentos $k_1, ..., k_n$ na cinemática multi-Regge. Podem definir-se diferentes relações entre os diferentes processos radiactivos. Por exemplo:

$$
\begin{aligned}
\frac{\sigma^{(nZ)}}{\sigma^{(n\gamma)}} &\approx \tan^{2n}\theta_W \ , \\
\frac{\sigma^{(n\gamma)}}{\sigma^{(nW)}} &\sim s^{-0.36}.
\end{aligned}
\tag{62}
$$

Nas Figs. 4.6 e 4.7 apresenta-se o resultado numérico para as relações anteriores das secções eficazes da aniquilação e^+e^- para *quarks* acompanhados pela emissão de apenas um bosão.

Neste trabalho obtivemos expressões explícitas para as amplitudes de dispersão da aniquilação de e^+e^- para *quarks* ou leptões acompanhados por n bosões electrofracos na cinemática de multi-Regge para $\sqrt{s} \gg 100$ GeV. Os resultados obtidos mostram que a produção de um bosão Z é sempre acompanhada pela produção de um fotão com a mesma energia ($\gg 100$ GeV). Mostram ainda que, no limite assimptóptico, a dependência da energia na secção eficaz da produção de W é inferior à da produção de fotões ou de Z por um factor $s^{-0.36}$.

Contents

List of Figures

xxvi

List of Tables

xxx

Chapter 1

Introduction

One of the greatest developments in particle physics is the so called Standard Model (SM). Its main goal is to combine in a single theory the electroweak Glashow-Weinberg-Salam (GWS) model and the quantum chromodinamics (QCD) model, a quark-gluon theory of the strong interaction. During the last two decades this theory has been subject to intensive experimental testing with remarkable results. The extraordinary accuracy of the theoretical predictions compared with experimental measurements has strengthened the predictive power of this model. The theory accounts for all the detected particles and predicts the existence of an extra, not yet detected, scalar particle called the Higgs. The lack of experimental evidence for the existence of this particle is the main missing piece for the model, rising questions about its validity.

The GWS model is a non-Abelian gauge theory in which the local gauge invariance is 'hidden'. The vector-axialvector (V-A) structure of the leptons currents requires that the weak quanta must be vector particles. Since this is a short-range force it implies that these particles should be massive and charged. The only renormalizable theories involving charged massive vector bosons are those in which the bosons are the quanta associated with a gauge symmetry, which must be of the hidden variety in order for the bosons to acquire mass. The relevant weak gauge group was originally proposed by Glashow in 1961 and subsequently treated as a hidden gauge symmetry by Weinberg in 1967 and by Salam in 1968. This theory was later extended by several authors and the result is a solid theory that is in agreement with all known data. It is based on $SU(2) \times U(1)$ groups. However, as was already stated, this symmetry would predict massless bosons that would have been detected long ago. These bosons would correspond to long range forces. To deal with this problem it is possible to break this $SU(2) \times U(1)$ symmetry to a $U(1)_{EM}$ where only one boson remains massless. This is in agreement with experiment, and results in three massive bosons $W^{\pm}$, Z and a massless photon.

The QCD model is also a gauge field theory based on the $SU(3)$ color symmetry. In this case the symmetry will not be broken and there is one massless bosons for each symmetry generator. These bosons are the well known gluons. The QCD coupling is only small at high energies so QCD can only be treated as a perturbation theory in this domain.

The renormalizability of the SM was proved in 1972 by G. 't Hooft e M. Veltman [26]. Since

this proof was obtained, a great effort has been put into performing higher order calculations with the purpose of producing precise results. As the energies in the accelerators grow, theoretical results are needed and new techniques must be used to calculate all order corrections in these high energies regimes.

This work is organized in two distinct parts. In the first part, limits on the existence of a fourth generation b' quark are obtained using recent experimental data. In the second part some electroweak processes are calculated using double-logarithmic (DL) approximation (DLA).

1.1 Limits on b' quark

Since the number of fermion generations and their masses are not explained by the model, we could ask questions like "Is there space for a fourth family of fermions?" or "is a fourth family experimentally ruled out?". With this in mind we think it is worthwhile to reexamine the limits on the b' mass. We will use all data available to date for $m_{b'} > 96$ GeV from CDF, D0 and DELPHI. We will draw exclusion plots in the planes $(R_{CKM}, m_{b'})$ and $(m_{t'}, m_{b'})$, where $R_{CKM} = |\frac{V_{cb'}}{V_{tb'} V_{tb}}|$, without assuming a definite value for the branching ratios of specific channels. Notice that the use of the R_{CKM} variable provides a new way to look at the experimental results. This variable enable us to actually use and combine all the available data. Moreover, the new form in which the results are presented will serve as a guide to future experiments since it is possible to know how far one has to go to exclude the regions that are still allowed. Traditional one loop calculations are preformed to produce the allowed regions in parameter space for a b' quark. This theoretical predictions are then crossed with new experimental data from Delphi, CDF and D0 to establish new allowed regions in parameter space.

1.2 Amplitudes for electron positron annihilation at TeV energies

In the calculation of a perturbative process, like electron positron annihilation, infrared (IR) divergences arise from the regions of integrations where the momentum is small compared with the typical scale of the process. This is well known in QED where this divergence problem is solved by giving the photon a fictitious mass which acts as a cut-off for the IR integrals. The final result will be independent of this fictitious mass and the result will be finite when the real bremsstrahlung and virtual corrections are summed. But the double logarithms that are introduced by these corrections are significant and grow with the scale. They need to be re-summed. The technique used to re-sum these logarithms is called the double-logarithmic approximation (DLA) and was introduced in particle physics in the fifties by V.V. Sudakov. He found that the most important radiative corrections to the form factor $f(q^2)$ of electron-positron annihilation's at large q^2 are the double-logarithmic (DL) , i.e. $\sim (\alpha \ln^2(q^2/m^2))^n$ $(n = 1, 2, ..)$ with m being a mass scale. After accounting for these logarithms to all orders in α, $f(q^2)$

asymptotically reduces to[14]

$$f(q^2) \sim e^{-(\alpha/4\pi)\ln^2(q^2/m)} \tag{1.1}$$

when $q^2 \gg m^2$.

The next important step towards studying DL asymptotics in QED was done in Refs. [15]. Since then, calculating in DLA has become more technology than art. Studying the QCD scattering amplitudes showed that there is no big technical difference between QED and QCD for calculating amplitudes of elastic processes (see e.g. Ref. [27, 28, 29, 16]) whereas inelastic (radiative) QCD -amplitudes are much harder to calculate (see e.g. Refs. [30, 18]). The methods of calculating the DL asymptotics can be applied also to electroweak (EW) processes providing the total energy is high enough to neglect masses of the electroweak bosons. At such huge energies ($\gg 100$ GeV) many important technical details from QED and QCD can be used for calculating EW amplitudes[19].

In the near future, accelerators will operate in a very high energy domain, much higher than the electroweak boson masses. Linear e^+e^- colliders will need a full knowledge of the scattering amplitudes for the e^+e^- annihilation process. A well-known and successful prediction of the Standard Model, for e^+e^- annihilation, is the forward-backward asymmetry, which has been studied for many years both theoretically and experimentally, particularly around the Z boson [31, 32, 33]. This forward-backward asymmetry persists at asymptotically high energies due to the multiphoton contributions in higher orders in α. Such multiphoton contribution in $e^+e^- \to \mu^+\mu^-$ was studied in Refs. [34] in the double-logarithmic approximation (DLA). This forward-backward asymmetry for e^+e^- annihilation into leptons or hadrons produced at energies much greater than the W and Z boson masses has been recently considered in Ref. [20], where the electroweak radiative corrections were calculated to all orders in the double-logarithmic approximation (DLA). It was shown that the effect of the electroweak DL radiative corrections on the value of the forward-backward asymmetry is quite sizable and grows rapidly with the energy. As usual, the asymmetry is defined as the difference between the forward and the backward scattering amplitudes over their sum.

In the second part of this work a DLA approach is used to calculate some electroweak processes. First we calculate electroweak $2 \to 2$ amplitudes for the process of electron positron annihilation at TeV energies. This is done in special Regge kinematics with two different cut-offs for the electroweak bosons. Then we extend the approach to include hard electroweak boson production in electron positron annihilation. Emission of such hard electroweak boson can be studied in the DLA approach provided they are emitted in the cone with opening angle $<< 1$ around the initial e^+e^- beam.

The reader should pay special attention to the fact that the graphical representation of the Feynman diagrams used in the the second part will be different from the usual representation. This is due to the fact that in the literature of this specific area the diagram time line is represented from bottom to the top and not from left to right. This means that the process $e_{p_1}^+ e_{p_2}^- \to q_{p_1'} \bar{q}_{p_2'}$ will be represented as in Fig 1.1.
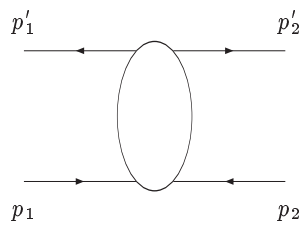
Figure 1.1: Scattering amplitude of the annihilation of $e^+_{p_1} e^-_{p_2} \to q_{p'_1} \bar{q}_{p'_2}$.

Chapter 2

New bounds on the mass of a b' quark

The Standard Model (SM) of particle physics describes elementary processes with great accuracy. It describes electroweak and strong interactions between the elementary particles. The replication of generations is a very interesting and intriguing feature in particle physics. Experimental data has proved the existence of three families but has not ruled out the possibility for the existence of more families.

In this chapter we analyse actual experimental data to impose new bounds on a fourth generation b' quark mass. A very brief and compact introduction to the SM is presented in section 2.1 pointing out the main elements necessary for this work. The problems we have to consider for the inclusion of an extra family of fermions is discussed in sections 2.2 and 2.3. Production and decay of the b' quark is the subject of section 2.4. The discussion of the obtained results and the conclusions are the subject of sections 2.5 and 2.6.

2.1 The Electroweak Lagrangian

The SM Electroweak Lagrangian can be written in the following form:

$$\mathcal{L} = \mathcal{L}_G + \mathcal{L}_Y + \mathcal{L}_S, \tag{2.1}$$

where $\mathcal{L}_G$ is the gauge Lagrangian, $\mathcal{L}_Y$ is the Yukawa Lagrangian and $\mathcal{L}_S$ is the scalar Lagrangian. The construction of this Lagrangian is done in a way that it is gauge invariant. This invariance will constrain the terms that we are allowed to include. The inclusion of mass terms that violate this invariance is not allowed. To solve this problem we need to use the "Higgs Mechanism" that will generate a new set of terms including mass terms for the gauge bosons and fermionic fields. This mechanism will also produce a new massive particle called the Higgs.

2.1.1 Gauge Lagrangian

The gauge sector Lagrangian can be written in the following form:

$$\mathcal{L}_G = -\frac{1}{4}\bar{A}_{\mu\nu}\bar{A}^{\mu\nu} - \frac{1}{4}B_{\mu\nu}B^{\mu\nu} \tag{2.2}$$

where $\bar{A}_{\mu\nu}$ is a $SU(2)$ tensor and $B_{\mu\nu}$ a $U(1)$ tensor. These tensors can be defined in terms of A_μ^a with $a = 1, 2, 3$ as $SU(2)$ fields and B_μ a $U(1)$ field by the following relations:

$$\begin{aligned}
\bar{A}_{\mu\nu} &= \partial_\mu\bar{A}_\nu - \partial_\nu\bar{A}_\mu + g\bar{A}_\mu \times \bar{A}_\nu \\
B_{\mu\nu} &= \partial_\mu B_\nu - \partial_\nu B_\mu,
\end{aligned} \tag{2.3}$$

where g is the gauge coupling constant of $SU(2)$.

2.1.2 Scalar Lagrangian

The scalar Lagrangian can be written as:

$$\mathcal{L}_S = (D_\mu\Phi)^\dagger(D^\mu\Phi) - V, \tag{2.4}$$

where D_μ is the covariant derivative, V is the potential, and Φ is an $SU(2)$ complex doublet scalar field with hyper-charge $Y = 1/2$. We need to work with a covariant derivative in the Lagrangian because we want it to be invariant under local gauge transformations. The covariant derivative is defined by:

$$D_\mu = \partial_\mu - igT_aA_\mu^a - ig'YB_\mu, \tag{2.5}$$

where T_a and Y are the generators for the groups $SU(2)$ and $U(1)$ and g' is the $U(1)$ coupling. T_a is defined as:

$$T_a = \frac{1}{2}\sigma^a, \tag{2.6}$$

where σ^a are the known Pauli matrices and

$$[T_a, T_b] = i\varepsilon_{abc}T_c, \tag{2.7}$$

and

$$Tr(T_aT_b) = \frac{1}{2}\delta_{ab}. \tag{2.8}$$

The Φ doublet can be written as:

$$\Phi(x) = \begin{pmatrix} \Phi^+(x) \\ \Phi^0(x) \end{pmatrix}, \tag{2.9}$$

and the most general form of a renormalizable potential is:

$$V(\Phi) = \frac{\lambda}{4}(\Phi^\dagger\Phi)^2 - \mu^2\Phi^\dagger\Phi, \tag{2.10}$$

6

where λ and μ^2 are arbitrary positive parameters. A potential with higher order terms of $\Phi^\dagger\Phi$ leads to a non renormalizable theory. As we are looking for a theory where the weak interaction is mediated by massive gauge bosons and the electromagnetic interaction is mediated by massless photons, we need to break spontaneously the $SU(2) \times U(1)$ symmetry, maintaining the electromagnetic gauge invariance $U(1)_{EM}$. To obtain this spontaneous symmetry breaking one needs to choose a vacuum expectation value (vev) for the Φ field that in the unitary gauge can be written as:

$$\Phi(x) = \begin{pmatrix} 0 \\ \frac{1}{\sqrt{2}}(v + H) \end{pmatrix}. \tag{2.11}$$

We can write at three level the potential as:

$$V = \frac{H^4 \lambda}{16} + \frac{H^3 v \lambda}{4} + \frac{v^4 \lambda}{16} - \frac{v^2 \mu^2}{2} + H^2 \left(\frac{3 v^2 \lambda}{8} - \frac{\mu^2}{2} \right) + H \left(\frac{v^3 \lambda}{4} - v \mu^2 \right) \tag{2.12}$$

where $H(x)$ describes a neutral particle, the Higgs, with mass given by $M_H = \sqrt{2}\mu$.

We define the transformation of the gauge group states into the mass states by a rotation such as:

$$\begin{bmatrix} Z_\mu \\ A_\mu \end{bmatrix} = \begin{bmatrix} -\cos\theta_W & \sin\theta_W \\ \sin\theta_W & \cos\theta_W \end{bmatrix} \begin{bmatrix} B_\mu \\ A_\mu^3 \end{bmatrix}, \tag{2.13}$$

$$W_\mu^\pm = \frac{1}{\sqrt{2}}(A_\mu^1 \mp i A_\mu^2), \tag{2.14}$$

where θ_W is the Weinberg angle and is determined by requiring that A_μ is the eigenvector with 0 mass. From this requirement it is possible to derive an important relation between the coupling constants:

$$\tan\theta_W = \frac{g'}{g}. \tag{2.15}$$

Inserting into eq.(2.2) the mass states $\bar{A}_{\mu\nu}$ and $B_{\mu\nu}$ we get:

$$\mathcal{L}_G = W_\mu^+(g^{\mu\nu}\partial^2 - \partial^\mu\partial_\nu)W_\nu^- + \frac{1}{2}Z_\mu(g^{\mu\nu}\partial^2 - \partial^\mu\partial_\nu)Z_\nu + \frac{1}{2}A_\mu(g^{\mu\nu}\partial^2 - \partial^\mu\partial_\nu)A_\nu +$$
$$+ cubic\ and\ quartic\ terms. \tag{2.16}$$

We can now write the covariante derivative in terms of the mass eigenstates:

$$D_\mu = \partial_\mu - \frac{ig}{\sqrt{2}} \begin{bmatrix} 0 & W_\mu^+ \\ W_\mu^- & 0 \end{bmatrix} - ig T_3 (Z_\mu \cos\theta - A_\mu \sin\theta) - ig' Y (Z_\mu \sin\theta + A_\mu \cos\theta). \tag{2.17}$$

The gauge boson mass matrix is generated by spontaneous symmetry break applied to the rest of the $\mathcal{L}_S$. By replacing Φ by its vev on the first term of $\mathcal{L}_S$ new terms will be generated and in particular quadratic terms with the following structure appear:

$$\mathcal{L}_{G,mass} = \frac{1}{4}g^2 v^2 W_\mu^+ W^{-\mu} + \frac{1}{8}(g^2 + g'^2)v^2 Z_\mu Z^\mu. \tag{2.18}$$

These new terms define masses for two complex vectorial fields $W_\mu^\pm$ and a vectorial field Z_μ. As expected there is no mass term to the vectorial field A_μ and so we identify it with the photon. We get the following masses for the gauge bosons:

$$
\begin{aligned}
M_W &= \frac{1}{2}gv \\
M_Z &= \frac{1}{2}\left(\sqrt{g^2 + g'^2}\right)v \\
M_A &= 0.
\end{aligned}
\tag{2.19}
$$

The gauge boson masses are related by the Weinberg relation:

$$
M_W = M_Z \cos\theta_W.
\tag{2.20}
$$

2.1.3 Fermionic Lagrangian for three families

The known fermions are distributed in 3 families with identical properties but different masses. This is an experimental observation that we need to account for when building the theory. In the GWS model there is no constraint in the number of families, only on the structure of each family. The weak charged currents mediated by the W boson are of $V - A$ type. This means that this interaction will only involve the left helicity component of the charged fermions. So the left fermions can be grouped in $SU(2)$ doublets in the following way:

$$
L_j = \begin{pmatrix} \nu_j^L \\ l_j^L \end{pmatrix}, \begin{pmatrix} u_j^L \\ d_j^L \end{pmatrix};
\tag{2.21}
$$

while the right fermions are $SU(2)$ singlets:

$$
R_j = l_j^R, u_j^R, d_j^R,
\tag{2.22}
$$

where ν, l, u and d stand for the neutrinos, charge leptons, up-quarks and the down-quarks respectively.

Since the rank of $SU(2) \times U(1)$ is 2 each particle in the theory will need two quantum numbers. These can be chosen as the pair Y and T_3 where Y is the weak hipercharge and T_3 represents the third component of the weak isospin. The values of Y are chosen so that the Lagrangian is Y invariant and to make the electromagnetic charge Q satisfy:

$$
Q = T_3 + Y.
\tag{2.23}
$$

The leptons quantum numbers are the following :

	U_L	D_L	U_R	D_R	e_L^-	e_R^-	ν_e
T_3	$\frac{1}{2}$	$-\frac{1}{2}$	0	0	$-\frac{1}{2}$	0	$\frac{1}{2}$
Y	$\frac{1}{6}$	$\frac{1}{6}$	$\frac{2}{3}$	$-\frac{1}{3}$	$-\frac{1}{2}$	-1	$-\frac{1}{2}$
$Q = T_3 + Y$	$\frac{2}{3}$	$-\frac{1}{3}$	$\frac{2}{3}$	$-\frac{1}{3}$	-1	-1	0

As stated before, mass terms added to the Lagrangian would violate local gauge invariance. But the mechanism of spontaneous symmetry break produces the necessary mass terms to various gauge and scalar fields. The same will happen in the fermion sector. We can separate the fermionic Lagrangian into its kinetic and Yukawa parts. The kinetic Lagrangian can be written as:

$$\mathcal{L}_{F,\mathcal{KIN}} = \sum_j \bar{L}_j i\gamma^\mu D_\mu^L L_j + \sum_j \bar{R}_j i\gamma^\mu D_\mu^R R_j, \tag{2.24}$$

with $j = 1, 2, 3$ representing each fermion family. The covariant derivative is defined by:

$$\begin{aligned} D_\mu^L &= \partial_\mu - igT_a A_\mu^a - ig'Y B_\mu \\ D_\mu^R &= \partial_\mu - ig'Y B_\mu. \end{aligned} \tag{2.25}$$

The Yukawa Lagrangian can be written as:

$$\mathcal{L}_{F,Y} = -\sum_{ij} \left(G_{ij}^l \bar{L}_i^l \Phi l_j^R + G_{ij}^d \bar{L}_i^q \Phi d_j^R + G_{ij}^u \bar{L}_i^q (i\sigma_2 \Phi^*) u_j^R \right) + h.c., \tag{2.26}$$

where $\sigma_2 = \begin{pmatrix} 0 & -i \\ i & 0 \end{pmatrix}$ and $h.c.$ stands for hermitian conjugate. Fermions mass terms are generated from this Lagrangian. After spontaneous symmetry break we can write the terms proportional to v as:

$$\mathcal{L}_{F,mass} = -\frac{v}{\sqrt{2}} \sum_{ij} \left(\bar{l}_i^{'L} G_{ij}^l l_j^{'R} + \bar{d}_i^{'L} G_{ij}^d d_j^{'R} + \bar{u}_i^{'L} G_{ij}^u u_j^{'R} \right) + h.c., \tag{2.27}$$

where $\frac{v}{\sqrt{2}} G_{ij}^{(l,u,d)}$ are the fermions mass matrices. It is possible to diagonalize each of these matrices with 2 unitary matrices like:

$$\begin{aligned} \frac{v}{\sqrt{2}} G_{ij}^l &= \sum_k M_{L,ik}^{L\dagger} m_k^l M_{L,kj}^R, \\ \frac{v}{\sqrt{2}} G_{ij}^d &= \sum_k M_{D,ik}^{L\dagger} m_k^d M_{D,kj}^R, \\ \frac{v}{\sqrt{2}} G_{ij}^u &= \sum_k M_{U,ik}^{L\dagger} m_k^u M_{U,kj}^R, \end{aligned} \tag{2.28}$$

where m^l, m^d e m^u are diagonal matrices. The following transformations lead to mass eigenstates of the fields:

$$
\begin{aligned}
l_i^{L,R} &= \sum_k M_{L,ik}^{L,R} l_k'^{L,R}, \\
\nu_i^L &= \sum_k M_{L,ik}^L \nu_k'^L, \\
d_i^{L,R} &= \sum_k M_{D,ik}^{L,R} d_k'^{L,R}, \\
u_i^{L,R} &= \sum_k M_{U,ik}^{L,R} u_k'^{L,R}.
\end{aligned}
\tag{2.29}
$$

From this transformations it is easy to see that the quark's charged currents are not diagonal in the mass eigenstates. This means that the interactions of quarks with the W or with the Goldstone bosons produces a mixture of different generations of quarks,

$$
\begin{aligned}
\mathcal{L}_{F,C} &= \frac{e}{\sqrt{2}s_W} \sum_{i,j,k} \left(\bar{l}_i^L \gamma_\mu \nu_i^L W^{-\mu} + \bar{\nu}_i^L \gamma_\mu l_i^L W^{+\mu} + \right. \\
&\quad \bar{u}_i^L \gamma_\mu M_{U,ik}^L M_{D,kj}^{L\dagger} d_j^L W^{+\mu} + \bar{d}_i^L \gamma_\mu M_{D,ik}^L M_{U,kj}^{L\dagger} U_j^L W^{-\mu} \Big) \\
&\quad - \frac{\sqrt{2}}{v} \sum_{i,j,k} \left[\left(\bar{\nu}_i^L m_{l,i} l_i^R G^+ + \bar{l}_i^L m_{l,i} l_i^R G^0 \right. \right. \\
&\quad \left. \left. + \bar{u}_i^L M_{U,ik}^L M_{D,kj}^{L\dagger} m_{d,j} d_j^R G^+ - \bar{d}_i^L M_{D,ik}^L M_{U,kj}^{L\dagger} m_{u,j} u_j^R G^- \right) + h.c. \right].
\end{aligned}
\tag{2.30}
$$

These mixtures are reflected in the Cabibbo-kobayashi-Maskawa (CKM) matrix:

$$
V_{CKM} = \begin{bmatrix} V_{ud} & V_{us} & V_{ub} \\ V_{cd} & V_{cs} & V_{cb} \\ V_{td} & V_{ts} & V_{tb} \end{bmatrix},
\tag{2.31}
$$

where

$$
V_{ij} = \sum_k M_{U,ik}^L M_{D,kj}^{L\dagger}.
\tag{2.32}
$$

In this theory the neutrinos are considered to be massless so any superimposition of neutrinos is still massless. This makes it always possible to absorb any necessary transformations in the neutrino mass state. If the neutrinos were considered with masses, as it is now know, it would be necessary to modify the theory to accommodate massive neutrinos.

As a result of this mass generation mechanism, the Yukawa interaction constant between the fermions and the Higgs boson is proportional to the fermions masses.

Finally we show the most recent values of the experimental magnitudes of CKM elements obtained from the PDG[35] are:

$$
|V_{ud}| = 0.97377 \pm 0.00027
$$

10

$$
\begin{aligned}
|V_{us}| &= 0.2257 \pm 0.0021 \\
|V_{ub}| &= (4.31 \pm 0.30) \times 10^3 \\
|V_{cd}| &= 0.230 \pm 0.011 \\
|V_{cs}| &= 0.957 \pm 0.017 \pm 0.093 \\
|V_{cb}| &= (41.6 \pm 0.6) \times 10^3 \\
|V_{td}| &= (7.4 \pm 0.8) \times 10^3 \\
|V_{ts}| &= (40.6 \pm 2.7) \times 10^3 \\
|V_{tb}| &> 0.78
\end{aligned}
$$

Using the unitary constraints together the experimental values the allowed ranges of the magnitudes of all nine CKM elements are:

$$
V_{CKM} = \begin{bmatrix}
0.97383^{+0.00024}_{-0.00023} & 0.2272^{\pm 0.0010} & (3.96^{\pm 0.09}) \times 10^{-3} \\
0.2271^{\pm 0.0010} & 0.97296^{\pm 0.00024} & (42.21^{+0.10}_{-0.80}) \times 10^{-3} \\
(8.14^{+0.32}_{-0.64}) \times 10^{-3} & (41.61^{+0.12}_{-0.78}) \times 10^{-3} & 0.999100^{+0.000034}_{-0.000004}
\end{bmatrix} , \tag{2.33}
$$

2.2 Is there space for a fourth family?

Since the number of fermion generations is not constrained by the theory, why should we fix it at 3? Is there space for a fourth family of fermions? Or is it experimentally ruled out? The introduction of a new generations in the SM has to be done with caution. Cancellation of gauge anomalies requires the addition of a family of leptons for each family of quarks added to the SM. In 1989 measurements of the Z decay width at LEP([36], [37], [38], [39]) has precisely fixed the number of light neutrinos ($m_\nu < M_Z/2$) to three [40].

Recent results from LEP Electroweak Working Group[1] compare the partial width of the Z leptonic decay ($\Gamma_{Z \to l_i l_i}$) with the partial width corresponding to the invisible decay of Z ($\Gamma_{Z \to inv}$) obtaining the following result:

$$
\frac{\Gamma_{Z \to inv}}{\Gamma_{Z \to l_i l_i}} = 5.942 \pm 0.016 . \tag{2.34}
$$

The SM prediction for the ratio of the neutrino decay and the charged leptons is[1]:

$$
\left(\frac{\Gamma_{Z \to \nu_i \nu_i}}{\Gamma_{Z \to l_i l_i}} \right)_{SM} = 1.9912 \pm 0.0012 . \tag{2.35}
$$

Now the number of neutrinos (N_ν) is given by the ratio of these two results:

$$
N_\nu = 2.9841 \pm 0.0083 . \tag{2.36}
$$

This result imposes that the number of light neutrinos is three with an error bellow 1%. Then a new lepton family has to accommodate a neutrino with a mass larger than around 45 GeV.

Hence, if a sequential fourth family exists it certainly has to show a much different structure in the leptonic sector.

Despite the strength of the previous argument one should try to experimentally exclude the existence of a fourth generation. In fact such evidence does not yet exist. The most recent precision electroweak results [41, 42] allow a sequential fourth generation if the quark masses are not too far apart. This result is a strong bound on the mass difference of a possible fourth generation. The same results also disfavor a degenerate fourth family if both the leptonic and hadronic sector are degenerate. This is in agreement with the conclusions of Erler and Langacker [40]. However, it was shown in [6] that even if one takes a degenerate fourth family of quarks with 150 GeV masses, it is enough to choose a non-degenerate family of leptons with masses of 100 GeV and 200 GeV and a Higgs mass of 180 GeV for the discrepancy with experimental data to fall from roughly three to two standard deviations. [1] Moreover, it is clear that any new physics will also influence these results.

It was shown in refs. [6, 43] that the mass range $|m_{t'} - m_{b'}| \leq 60$ GeV, where t' and b' are the fourth generation quarks, is consistent with the precision electroweak data on the ρ parameter. This range enable us to say that even if $m_{b'} > m_{t'}$, the decay $b' \to t' W$ is forbidden. The decay $b' \to t' W^*$ although allowed, is phase space suppressed and consequently extremely small in the mass range under study (from now on we consider $m_{b'} < m_{t'}$). Experimental data allow us to go only up to $m_{b'}$ close to 190 GeV. Hence, the b' can not decay to a top quark. Furthermore, while some recent studies (see [44]) have constrained the Cabibbo-Kobayashi-Maskawa (CKM) elements of the fourth generation, they do not influence our results. Nevertheless we will take into account the 2σ bound $|V_{tb}|^2 + 0.75|V_{t'b}|^2 \leq 1.14$ [13] coming from $Z \to b\bar{b}$ to constrain the CKM element $V_{cb'}$.

There are presently four bounds on the b' mass for $m_{b'} > 96$ GeV [2] and all of them suffer from the drawback of assuming a 100 % branching ratio for a specific decay channel. The first and the second one ([2],[3]), $m_{b'} > 268$ GeV, assumes that $Br(b' \to bZ) = 100\%$. As will see later, for these values of $m_{b'}$, this assumption is wrong. So we will drop this condition and use instead their plot of $\sigma(p\bar{p} \to b'\bar{b}' + X) \times Br^2(b' \to bZ)$ as a function of the b' mass. The third one [4] $m_{b'} > 128$ GeV, is based on the data collected in the top quark search. Because the D0 collaboration looked for $t \to bW$, the analysis can be used to set a limit on $\sigma(p\bar{p} \to b'\bar{b}' + X) \times Br^2(b' \to cW)$. By doing so we assume that the b and c quark masses are negligible and that $\sigma(p\bar{p} \to b'\bar{b}') \approx \sigma(p\bar{p} \to t\bar{t})$. The obtained limit $m_{b'} > 128$ GeV assumes $Br(b' \to cW) = 100\%$. The forth bound is from CDF [5] and is based on the decay $b' \to bZ$ followed by the search for $Z \to e^+ e^-$ with displaced vertices. They also assume $Br(b' \to bZ) = 100\%$ and their excluded region depends heavily on the b' lifetime. But, contrary to the top quark which has a lifetime of around $10^{-24} s$, the lifetime of a sequential b' quark is expected to be extremely large, especially knowing that we are considering a heavy

---

[1]Notice that we make no assumptions on the values of the masses and couplings of the leptonic sector of the model.

[2]This is the approximate value for which the $b' \to bZ$ channel opens. We will come back to this point later.

b'. In fact, depending on the CKM values and on the b' and t' masses, the decay length can be as large as 10^{-4} cm or even 10^{-3} cm in extreme cases. Nevertheless, in this model, it is very hard to go beyond that value. It is worth mentioning that even with this huge lifetime, the b' always decays inside the detector and hadronization occurs before it decays. Thus, the limit obtained in [5] which, on top of what was said assumes $Br(b' \to b\,Z) = 100\%$, can not be used in our analysis.

2.3 Models with extra generations

There are several ways of extending the SM to accommodate a fourth family of quarks and/or leptons. A review of the different models in the literature is available in [6, 7]. When a fourth family is added to the SM we need to decide the structure of the new family. Quarks and leptons can be chiral or non-chiral(vector-like). This allows a few diferent possible models. Obviously, the most natural and straightforward way to introduce a fourth family in the SM is just to add a (t', b') family with the same quantum numbers and similar couplings to all other known quarks

$$\begin{pmatrix} t' \\ b' \end{pmatrix}_L t'_R, b'_R, \tag{2.37}$$

The same can be done for the lepton sector[3]. [3] This is called a sequential fourth generation model and is sometimes referred to as SM4. Another possibility is to add mirror chiral doublets [45, 46]

$$t'_L, b'_L, \begin{pmatrix} t' \\ b' \end{pmatrix}_R. \tag{2.38}$$

These have opposite chiral properties to the sequential fermions. It is also possible to add a vector-like or non-chiral fermions family, where left and right components transform identically under electroweak $SU(2) \times U(1)$ group [47, 48, 49, 50]

$$\begin{pmatrix} t' \\ b' \end{pmatrix}_L, \begin{pmatrix} t' \\ b' \end{pmatrix}_R. \tag{2.39}$$

In this work we will use the sequential fourth generation model. We assume that the resulting CKM matrix has a very similar structure to the SM one. It is a 4×4 unitary matrix and it is assumed to be approximately symmetric

$$CKM_{SM4} = \begin{bmatrix} V_{ud} & V_{us} & V_{ub} & V_{ub'} \\ V_{cd} & V_{cs} & V_{cb} & V_{cb'} \\ V_{td} & V_{ts} & V_{tb} & V_{tb'} \\ V_{t'd} & V_{t's} & V_{t'b} & V_{t'b'} \end{bmatrix}. \tag{2.40}$$

---

[3]Now that it is finally accepted that neutrinos have mass, the SM has to be changed to accommodate this new feature. We do not restrict ourselves to any specific mechanism that generates the very high neutrino mass needed in SM4.

Besides the four new masses, the new CKM_{SM4} matrix will have 9 parameters compared with the 4 needed by the CKM_{SM}. There are 6 mixing angles instead of 3 and 3 complex phases instead of 1. Because we are not concerned with CP-violation we take all CKM values to be real. In the SM4, the CKM elements that are not determined experimentally have more freedom due to the extra parameters introduced. This model has been the subject of wide study in the literature. Production cross sections for lepton and hadron colliders and b' branching fractions were calculated long ago.

2.4 b' production and decay

At LEP, a pair of $b' \bar{b}'$ quarks is produced via $e^+ e^- \rightarrow b' \bar{b}'$. The corresponding cross section was calculated using PYTHIA [51] with initial state radiation (ISR), final state radiation and QCD corrections turned on. We have cross checked the results using a simple program with the formulas of refs. [52] and [53], which also include QCD corrections and ISR. Since the larger contribution to the cross section comes from ISR we have double checked by making use of the formulas presented in [17]. The results agree very well with the PYTHIA results. It should be noticed that near the threshold bound states would surely be formed. Without a detailed analysis of such bound states it is impossible to evaluate whether their contribution to the cross section would be relevant or not. So, if bound states do exist above the threshold, we are assuming that they give a negligible contribution to the cross section. Far away from the threshold the problem ceases to exist and the results we will show for hadron colliders are not affected by this approximation.

The equivalent process at the Tevatron is $p \bar{p} \rightarrow b' \bar{b}' + X$ with the relevant processes being $g g \, (q \bar{q}) \rightarrow b' \bar{b}'$. Due to its hadronic nature, this cross section is equal to the top quark production one and it is known to order α_s^3 [25] see table 2.1.

This approximation is used both by the CDF and the D0 collaborations in their studies on b' production and decay.

All b' decays were exhaustively studied by Hou and Stuart in [8, 9, 10, 11] and by Haeri, Eilam and Soni [12]. Two body b' decays occur either through neutral currents (NC) or through charged currents (CC) as shown in Fig. 2.1. Although NC proceed only via loops, it was shown in [8] that depending on the values of the CKM matrix elements and on the values of the quark masses, they can be comparable to CC decays. The reason is simple: if $b' \rightarrow W t$ and $b' \rightarrow W t'$ are not allowed, the dominant CC decay is $b' \rightarrow W c$ which is doubly Cabibbo suppressed. As long as the Higgs channel is closed the dominant neutral decay is $b' \rightarrow b Z$. Other neutral decays like $b' \rightarrow b g$ and $b' \rightarrow b \gamma$ give smaller contributions but can sometimes be relevant. As soon as the Higgs channel opens the decay $b' \rightarrow b H$ can be as large as $b' \rightarrow b Z$. The three body decays $b' \rightarrow b e^+ e^-$, $b' \rightarrow b \nu \bar{\nu}$ and $b' \rightarrow b q \bar{q}$, including box diagrams were calculated in [10]. At that time, the top mass was still unknown and the t' was taken to be much larger than the top mass. Under these conditions and for the range of the b' mass in study, the sum of all three body decays could be as large as $b' \rightarrow b g$. It could be even larger for a "small"

Table 2.1: *"The first and fifth column contain the top quark mass in* GeV/c^2*. The columns denoted by 'Lower' show our lower limit estimate of the top quark cross section in picobarns, the columns denoted by 'Central' show our central value estimate, and the columns denoted by 'Upper' show our upper limit estimate"*[25].

m_{top}	σ (pb) Lower	σ (pb) Central	σ (pb) Upper	m_{top}	σ (pb) Lower	σ (pb) Central	σ (pb) Upper
90	148	180	259	146	12.1	13.6	16.2
92	132	160	227	148	11.3	12.6	15.0
94	118	143	204	150	10.5	11.7	13.8
96	106	127	180	152	9.79	10.9	12.8
98	95.2	114	158	154	9.14	10.1	11.9
100	86.3	102	141	156	8.52	9.40	11.0
102	77.8	92.4	127	158	7.94	8.77	10.3
104	70.6	83.2	113	160	7.41	8.16	9.53
106	64.0	75.4	102	162	6.92	7.62	8.82
108	58.1	68.0	90.9	164	6.48	7.11	8.25
110	52.7	61.6	81.4	166	6.07	6.67	7.70
112	48.2	55.9	73.6	168	5.68	6.23	7.18
114	43.9	51.2	66.6	170	5.32	5.83	6.68
116	40.2	46.6	60.6	172	4.98	5.45	6.25
118	36.8	42.4	54.7	174	4.67	5.10	5.83
120	33.7	38.9	49.7	176	4.38	4.79	5.46
122	31.1	35.6	45.4	178	4.11	4.49	5.09
124	28.4	32.6	41.1	180	3.86	4.21	4.78
126	26.2	29.9	37.5	182	3.63	3.94	4.47
128	24.2	27.5	34.5	184	3.40	3.70	4.16
130	22.3	25.4	31.6	186	3.20	3.48	3.92
132	20.6	23.3	29.0	188	3.00	3.27	3.67
134	19.1	21.5	26.5	190	2.83	3.06	3.44
136	17.6	19.9	24.3	192	2.67	2.88	3.22
138	16.3	18.3	22.4	194	2.50	2.70	3.02
140	15.1	16.9	20.5	196	2.36	2.55	2.85
142	14.0	15.7	19.0	198	2.22	2.40	2.68
144	13.0	14.5	17.4	200	2.09	2.26	2.52
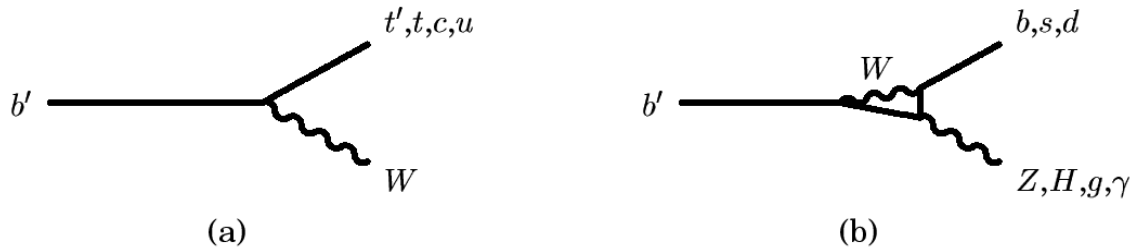
Figure 2.1: Diagrams for b' decay. In fig (a) CC decays and in b) NC decays.

t mass and a very large t' mass [10]. But it turned out that the top mass is ≈ 175 GeV and electroweak precision measurements force $m_{t'}$ to be close to $m_{b'}$ for the range of b' mass under consideration. In our case we estimate all three body decays plus the decay $b' \to b\gamma$ to be smaller than $b' \to b\,g$. Nevertheless, because we want to make a conservative estimate we will take it to be as large as $b' \to b\,g$. When $m_{b'}$ is greater than 200 Gev, the decay mode $b' \to tW^*$ increses and starts to be comparable to $b' \to bZ$. As soon as $m_{b'} \geq 250$ GeV this process becomes the dominant process [54] and when $m_{b'} \geq 255$ GeV the process $b' \to tW$ will be to real particles and always dominate[55].

Assuming that the CKM matrix is unitary, we can write:

$$V_{tb}V_{tb'} + V_{tb'}V_{t'b'} + V_{cb'}V_{ts} + V_{td}V_{ub'} = 0 \tag{2.41}$$

assuming that it is approximatly symmetric and taking $V_{ub'}V_{td} \approx 0$ and $V_{ts} \approx 10^{-2}$ which implies that $V_{cb'}V_{ts}$ is very small then $V_{t'b'}V_{t'b} \approx -V_{tb}V_{tb'}$. This allows us to write all branching fractions as a function of three quantities alone: R_{CKM}, $m_{t'}$ and $m_{b'}$. Where R_{CKM} is defined as:

$$R_{CKM} = \left| \frac{V_{cb'}}{V_{tb'}\,V_{tb}} \right|. \tag{2.42}$$

Notice that the two last conditions do not play a significant role in the final result. Using a very large value like for instance $V_{ub'}V_{ub} \approx 10^{-4}$ gives a contribution much less than 1 % to the $b' \to b\,Z$ decay width. The same is true when we relax the condition $V_{t'b'}V_{t'b} \approx -V_{tb}V_{tb'}$ near to a GIM cancellation region. Relaxing this condition leads to an increase by several orders of magnitude of the values of the NC decay widths but they are always much smaller than the CC decays in that region.

The experimental setup used by both experiments can only produce b' with masses between 96 GeV and 180 GeV. This retricts the possible values used for $m_{b'}$ parameter. So, we just have to decide on what values of R_{CKM} and $m_{t'}$ to use. The values of $m_{t'}$ are limited by precision data. It is interesting to study the two most extreme cases in the allowed region. We have considered $m_{t'} = m_{b'} + 50$ GeV and the almost degenerate case $m_{t'} = m_{b'} + 1$ GeV. In the exclusion plots R_{CKM} is a free parameter and so no assumptions on its variation range were

made. However, there is a hint on its most significant values coming from the fact that the competing NC and CC cross at $10^{-3} \leq R_{CKM} \leq 10^{-2}$.

One-loop calculations of the NC b' decays were performed using the FeynArts and FeynCalc [56, 57, 58] packages for generating and computing the complete set of diagrams and the Loop-Tools/FF [59, 60, 61] packages for the numerical analysis. We have carried out several checks in the four generations model following [43, 8, 9, 10, 11] and in the SM against [62, 63]. We have found full agreement in both cases.

In Fig. 2.2 we present the branching ratios as a function of the b' mass with $R_{CKM} = 0.001$ for both limits of $m_{t'}$, $m_{t'} - m_{b'} = 1$ GeV and $m_{t'} - m_{b'} = 50$ GeV. The closer to $m_{b'} = 96$ GeV we are the larger $b' \rightarrow b\,g$ gets due to phase space suppression of the competing NC $b' \rightarrow b\,Z$. In fact, for an almost degenerate fourth family and small values of R_{CKM}, $b' \rightarrow b\,g$ can be the dominant NC for $m_{b'} = 96$ GeV. As soon as one moves away from this value, $b' \rightarrow b\,Z$ becomes the dominant NC. If the Higgs channel is closed , for $m_{b'} \geq 97$ GeV, the competition is always between $b' \rightarrow c\,W$ and $b' \rightarrow b\,Z$. As $m_{b'}$ rises so does the NC except if the GIM mechanism gets in the way. It can be clearly seen in the figure the GIM mechanism acting for $m_{b'} \approx 125$ GeV, that is, $m_{t'} - m_t = 0$. Then the NC rises again and the CC falls crossing at 140 GeV. When R_{CKM} grows so does $b' \rightarrow c\,W$ and the crossing point is shifted to the left. As the mass difference tends to zero the GIM effect is shifted to $m_{b'} \approx m_t$.

In Fig. 2.3 we show the branching ratios as a function of R_{CKM} with $m_{b'} = 110$ GeV for both limits of $m_{t'}$, $m_{t'} - m_{b'} = 1$ GeV and $m_{t'} - m_{b'} = 50$ GeV. As we already knew, the NC are favoured by small values of R_{CKM} because R_{CKM} is a direct measure of the charged currents. Again, when $m_{b'}$ grows so does $b' \rightarrow b\,Z$ and the crossing point is shifted to the left. The same happens when $m_{t'} - m_{b'}$ decreases as explained above.

The average length traveled by the b' quark strongly depends on the values of its mass and of R_{CKM}. In Fig. 2.4 and Fig. 2.5 we can see different average distance in cm as function of R_{CKM} or $m_{b'}$ both with $m_{t'} = m_{b'} + 50$. The three lines represented in Fig. 2.4 represent diferent values of $m_{b'}$ (upper $m_{b'} = 100$, central $m_{b'} = 150$ and lower $m_{b'} = 200$). As can be seen in this figure, very small value of R_{CKM} leads to higher distances. This is due to the fact that small values of R_{CKM} reduce the influence of $b' \rightarrow cW$ chanel.

In Fig. 2.5 the three lines corresponds to diferent values of R_{CKM} (upper $R_{CKM} = 0.00002$, central $R_{CKM} = 0.0002$ and lower $R_{CKM} = 0.002$. As the $m_{t'} \approx m_t$ the GIM mechanism cancels the influence of the neutral processes, so when R_{CKM} is small traveled distances can be several meters. For distances greater than 3 meters, b' will appear to a stable particle. This is ruled out (above some mass) by stable quark searches (see discussion in [55]).

2.5   Results and discussion

Using the latest experimental data from the DELPHI collaboration Fig. 2.6 and the data from the CDF and D0 collaborations Fig. 2.7 we have drawn exclusion plots on the plane $(R_{CKM}, m_{b'})$ with $m_{t'}$ as a parameter and on the plane $(m_{t'}, m_{b'})$ with R_{CKM} as a parameter. The results
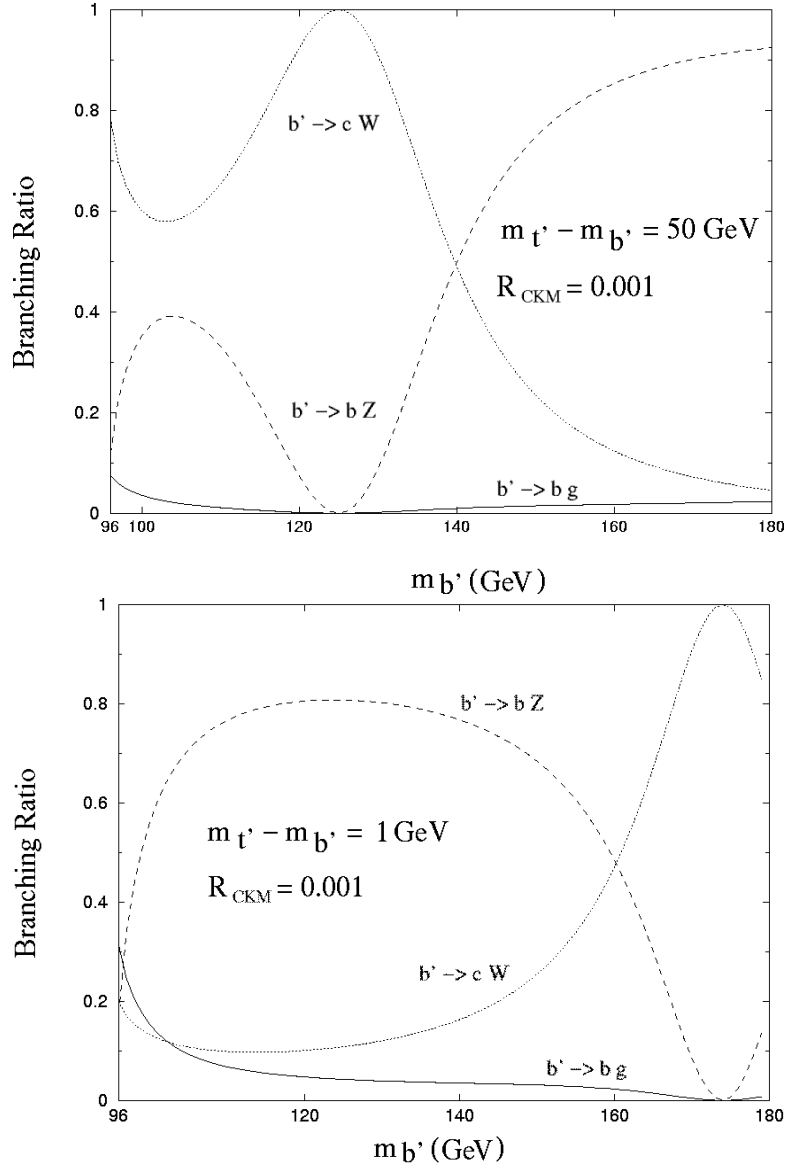
Figure 2.2: Branching ratios as a function of the b' mass. The Higgs channel is closed. The dashed line is $b' \to b\, Z$; the full line is $b' \to b\, g$ and the dotted line is $b' \to c\, W$.
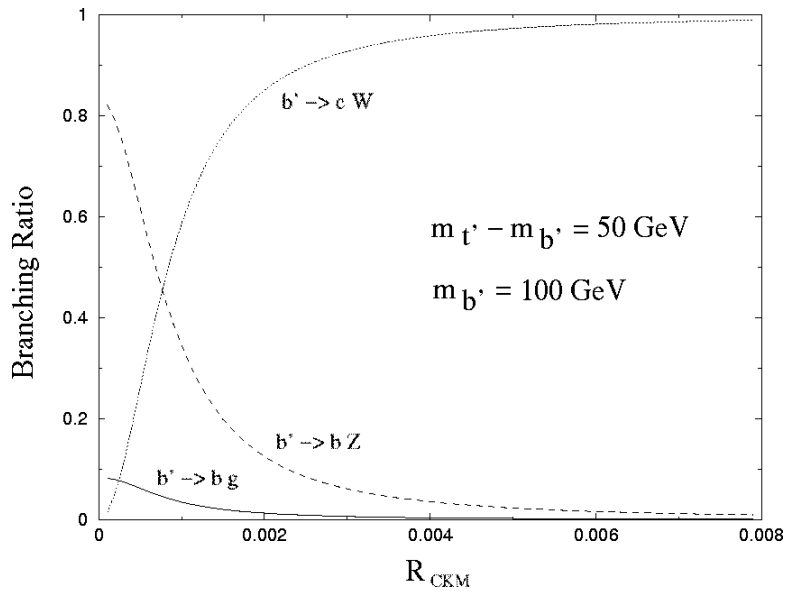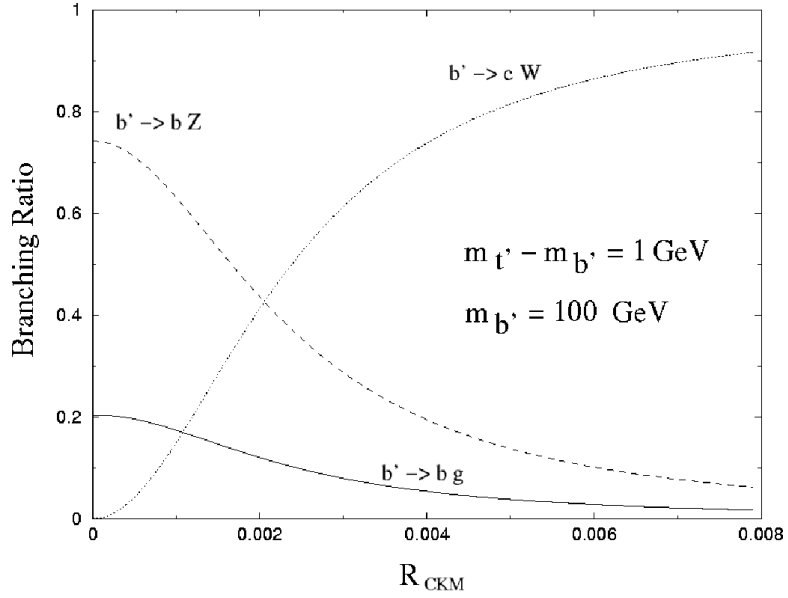
Figure 2.3: Branching ratios as a function of the R_{CKM} with $m_{b'} = 110$ GeV and $m_{t'} = m_{b'} + 1$ GeV. The dashed line is $b' \rightarrow b\,Z$; the full line is $b' \rightarrow b\,g$ and the dotted line is $b' \rightarrow c\,W$. Higgs channel is closed.
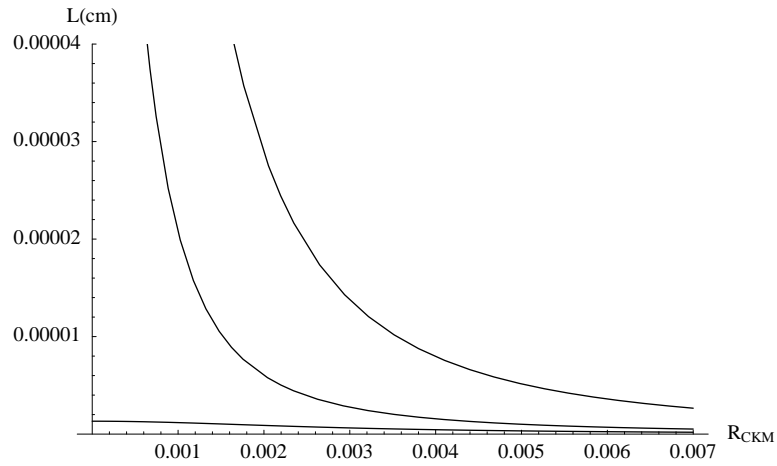
Figure 2.4: b' traveled distance as function of R_{CKM}. Upper line $m_{b'} = 100$, central line $m_{b'} = 150$ and bottom line $m_{b'} = 200$.
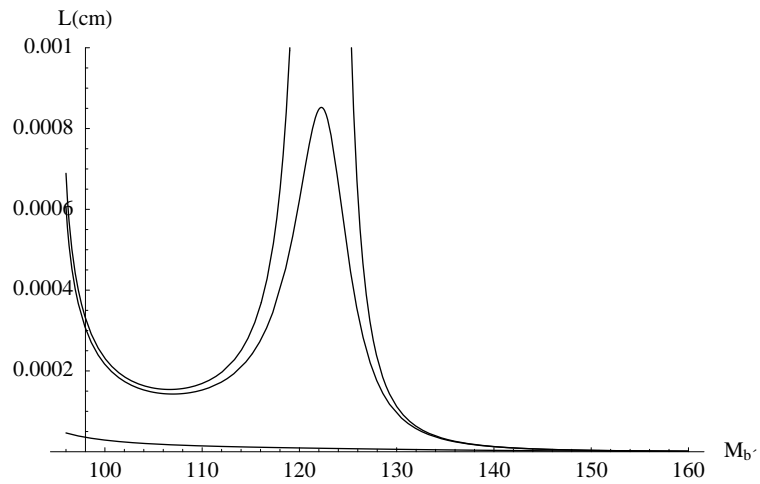
Figure 2.5: Traveled distance as function of $m_{b'}$. Upper line $R_{CKM} = 0.00002$, central line $R_{CKM} = 0.0002$ and bottom line $R_{CKM} = 0.002$.
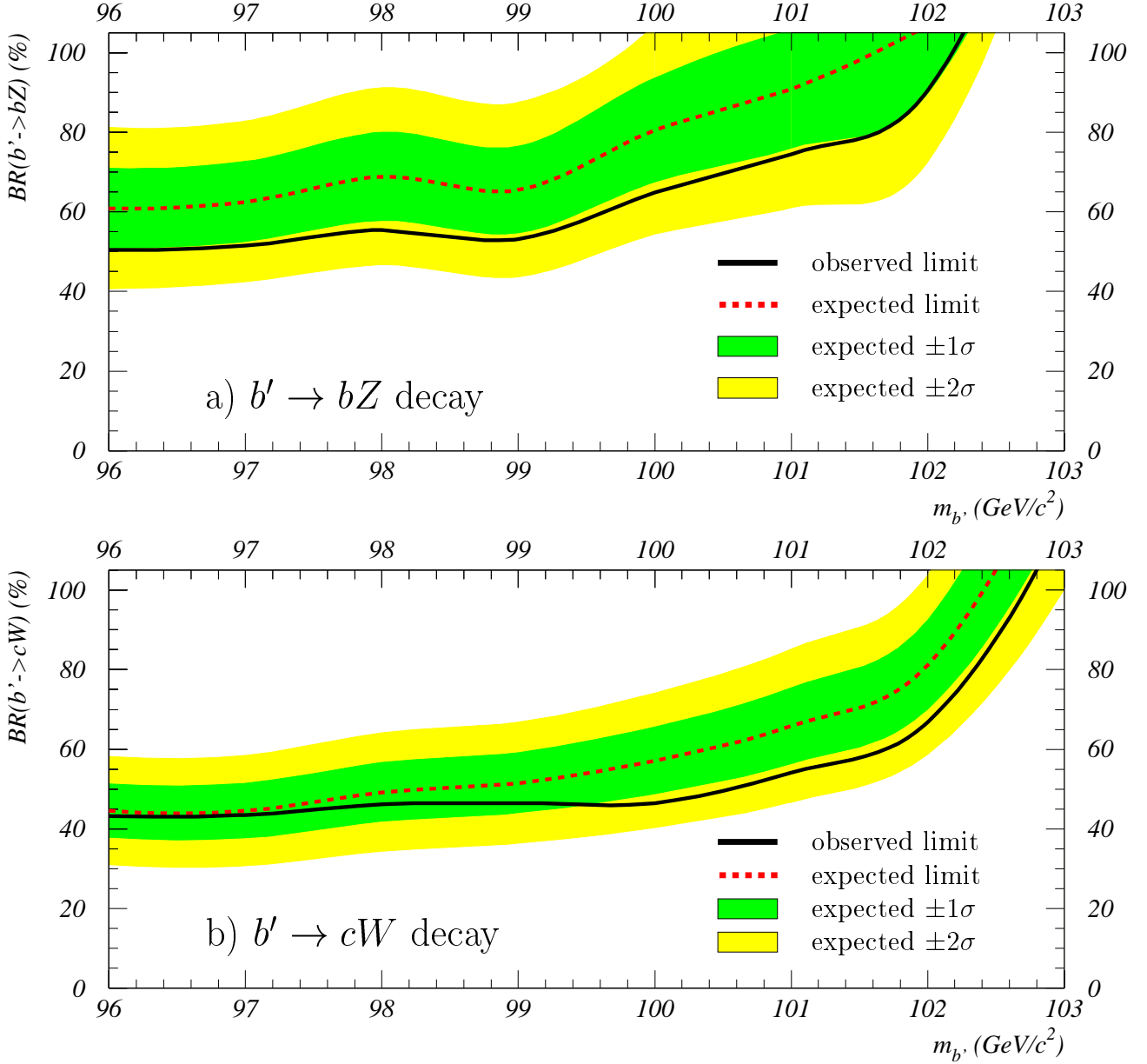
Figure 2.6: DELPHI experimental data. Observed and expected (median) upper limits at 95 % confidence level on a) $BR_{b' \to cZ}$ and b) $BR_{b' \to cW}$. The 1σ and 2σ bands around the expected median limit are also shown.
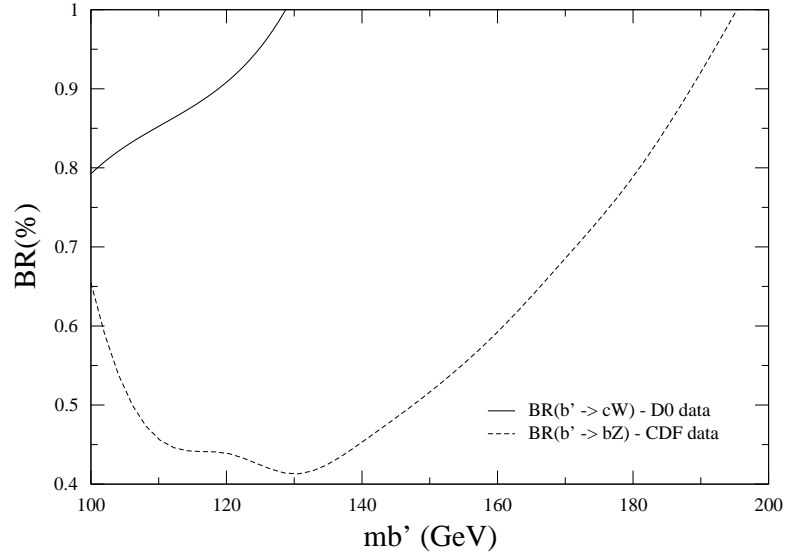
Figure 2.7: CDF and D0 Branching Ratio limmits.
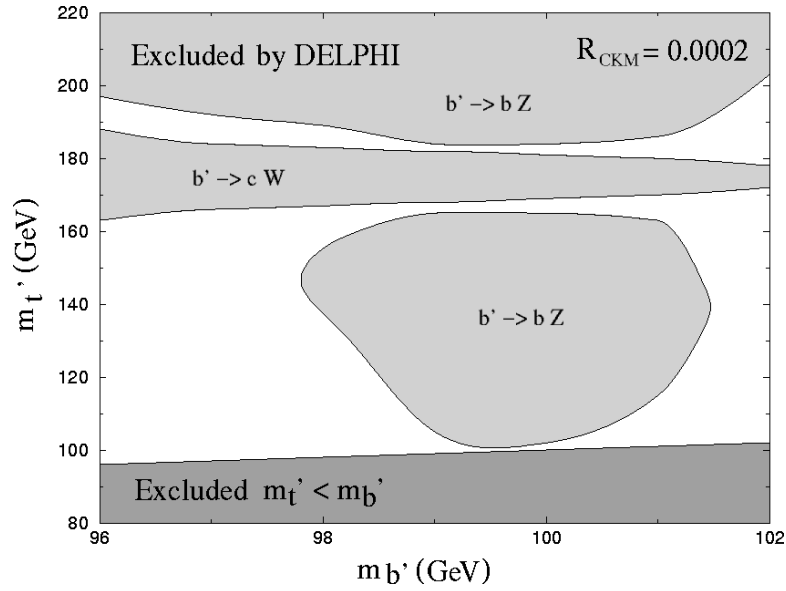
Figure 2.8: 95 % confidence level (CL) excluded region in the plane $(m_{t'}, m_{b'})$ with $R_{CKM} = 0.0002$, obtained from limits on $Br_{b' \to bZ}$ and $Br_{b' \to cW}$.

Figure 2.9: 95 % CL excluded region in the plane $(R_{CKM},\ m_{b'})$ with $m_{t'} - m_{b'} = 50$ GeV, obtained from limits on $Br_{b'\to bZ}$ (bottom) and $Br_{b'\to cW}$ (top).

Figure 2.10: 95 % CL excluded region in the plane $(R_{CKM},\ m_{b'})$ with $m_{t'} - m_{b'} = 1\,GeV$, obtained from limits on $Br_{b'\to bZ}$ and $Br_{b'\to cW}$ (top).

based on the DELPHI data, are shown in Figs. 2.8 for the $(m_{t'}, m_{b'})$ plane and in Figs. 2.9 and 2.10 for $(R_{CKM}, m_{b'})$ plane using different values for $m_{t'}$.

The excluded regions, due to the limits on $Br_{b' \to cW}$, are the stripe centred in $m_{t'}$ in Fig. 2.8 and upper excluded in Figs. 2.9 and 2.10. The remaining excluded regions are due to limits on $Br_{b' \to bZ}$. When $(m_{t'} - m_t) \to 0$, $Br_{b' \to bZ}$ decreases as a consequence of a GIM suppression and $Br_{b' \to cW}$ becomes dominant. In fact, when $m_{t'} - m_t = 0$, $Br_{b' \to cW} \approx 100\%$. Thus, there is always an excluded stripe around m_t. As R_{CKM} grows, $i.e.$, CC dominates, the stripe gets larger and the other two regions in Fig. 2.8 get smaller. This can also be seen in Fig. 2.9 where for $R_{CKM} > 0.0015$ everything is excluded. When $m_{t'} - m_{b'}$ gets smaller, the allowed region grows as can be seen in Fig. 2.10. The reason why there isn't a lower bound close to 96 GeV in Fig. 2.9 is because of the competing NC. Close to the Zb threshold (≈ 96 GeV), $b' \to bg$ dominates over $b' \to bZ$ and the experimental bound on $Br_{b' \to bZ}$ becomes useless. As one moves away from the Zb threshold, $b' \to bZ$ becomes the dominant NC. $Br_{b' \to bZ}$ falls less sharply with $m_{t'}$ than the other neutral currents and that explains why there is a lower bound for e.g. at $m_{b'} = 100$ GeV in Fig. 2.9 but not in Fig. 2.10. After 102 GeV almost all values are allowed because the experiments are not sensitive to those mass values.

Figure 2.11: 95 % CL excluded region in the plane $(m_{t'}, m_{b'})$ with $R_{CKM} = 0.002$, obtained from limits on $Br_{b' \to bZ}$ by the CDF collaboration and $Br_{b' \to cW}$ by the D0 collaboration.

In Figs. 2.11 to 2.13 we show similar plots but using the CDF and the D0 data. The behavior follows the general trend explained for the DELPHI data. The D0 deals with the CC and the CDF deals with the NC. The three curves marked upper, central and lower in Fig. 2.12 and 2.13 are related with the theoretical error bars in the b' production cross section. In Fig. 2.11

Figure 2.12: 95 % CL excluded region in the plane $(R_{CKM}, m_{b'})$ with $m_{t'} - m_{b'} = 50$ GeV, obtained from limits on $Br_{b' \to bZ}$ by the CDF collaboration (bottom) and $Br_{b' \to cW}$ by the D0 collaboration (top). Upper, Central and Lower curves correspond to the values used for the b' production cross-section.

25
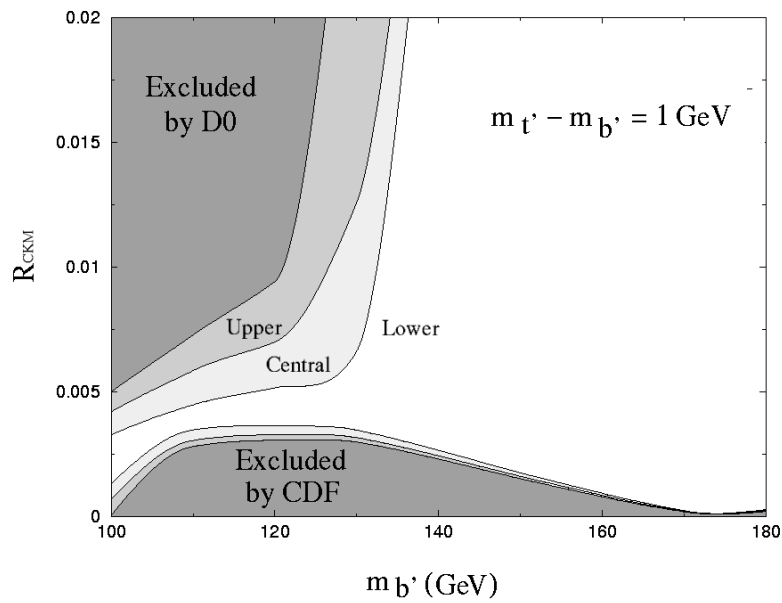
Figure 2.13: 95 % CL excluded region in the plane $(R_{CKM}, m_{b'})$ with $m_{t'} - m_{b'} = 1\,GeV$, obtained from limits on $Br_{b' \to b Z}$ by the CDF collaboration (bottom) and $Br_{b' \to c W}$ by the D0 collaboration (top). Upper, Central and Lower curves correspond to the values used for the b' production cross-section.

we have used central values for the cross sections. Again and for the same reason we see a stripe around m_t in Fig. 2.11. The stripe ends, as it should, for $m_{b'}$ close to 130 GeV which is approximately the D0 bound on $m_{b'}$.

As was seen with DELPHI data, the excluded region grows with $m_{t'} - m_{b'}$. This means that like the constraints from precision electroweak data, the experimental data also disfavors a fourth family with a large mass difference between the two quarks. Notice that whatever the value of $m_{b'}$ is, one can always find an allowed $m_{t'}$ if R_{CKM} is not too large. As $R_{CKM} \rightarrow 0$, $Br_{b' \rightarrow bZ} \approx 100\%$ and we recover the CDF bound [2].

In some cases the allowed regions in the CDF/D0 and DELPHI plots overlap and the excluded region grows. For instance, considering $m_{b'} = 100$ GeV and $m_{t'} - m_{b'} = 50$ GeV we get for DELPHI $4.5 \times 10^{-4} < R_{CKM} < 8.4 \times 10^{-4}$ and for CDF/D0 (lower) $6.7 \times 10^{-4} < R_{CKM} < 1.1 \times 10^{-3}$. Hence, the resulting excluded region is $6.7 \times 10^{-4} < R_{CKM} < 8.4 \times 10^{-4}$.

With the bound $|V_{tb}|^2 + 0.75|V_{t'b}|^2 \leq 1.14$ [13] and assuming $|V_{tb}| \approx 1$, it is possible to limit the value of the matrix element $V_{cb'}$. For the same value of the b' mass, $m_{b'} = 100$ GeV we know that $R_{CKM} < 8.4 \times 10^{-4}$ and so

$$V_{cb'} < 8.4 \times 10^{-4} \sqrt{0.14/0.75} \approx 3.6 \times 10^{-4}$$
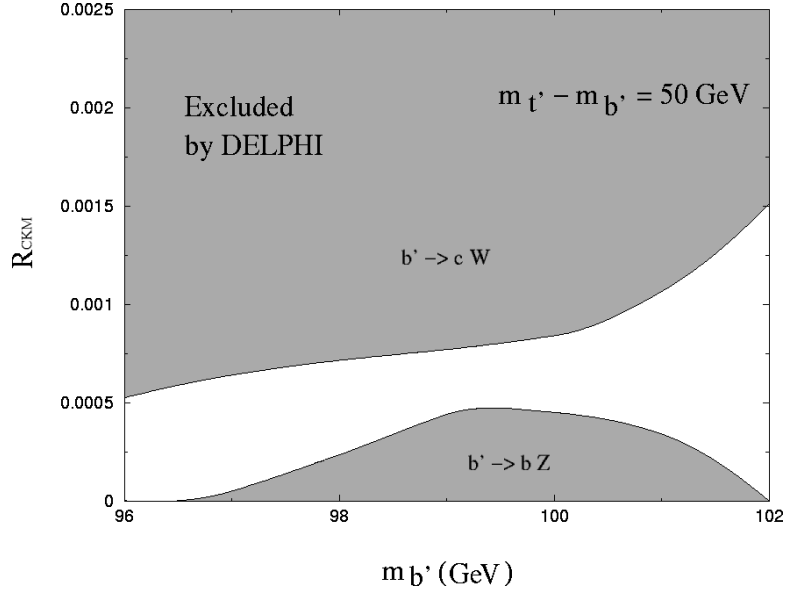
with $m_{t'} = m_{b'}$.
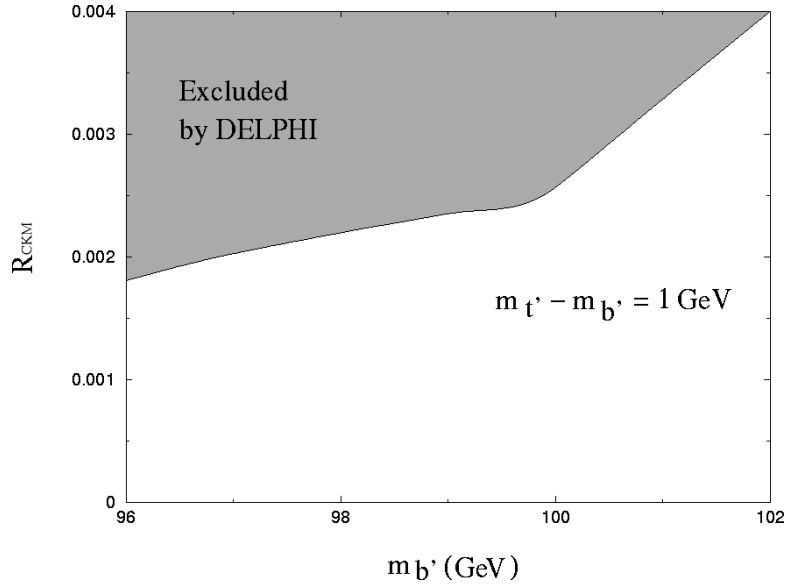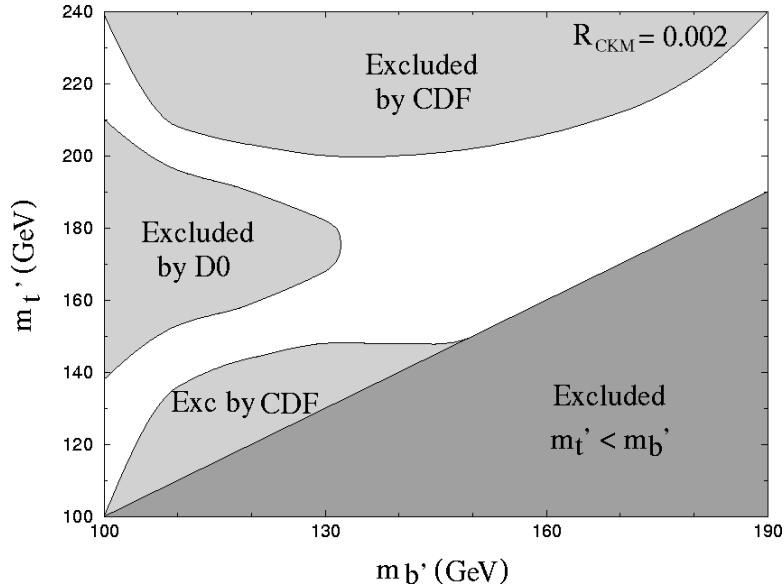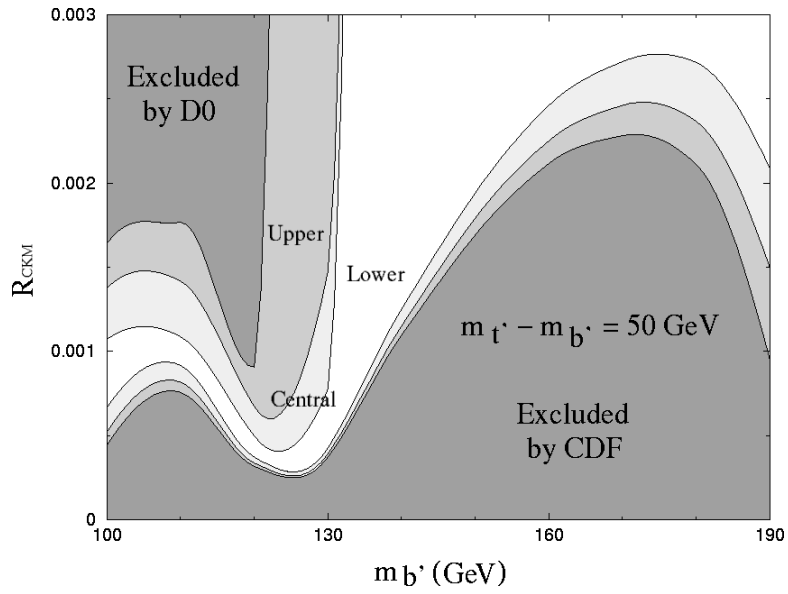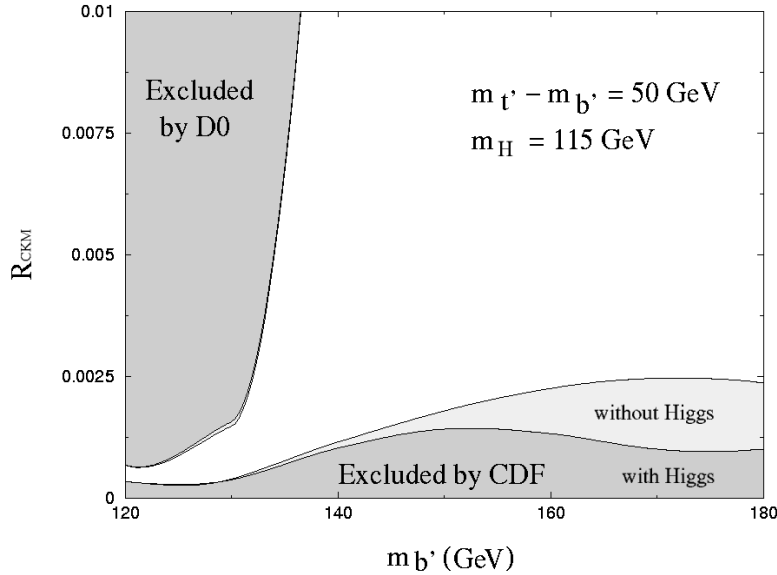

Figure 2.14: 95 % CL excluded region in the plane $(R_{CKM}, m_{b'})$ with $m_{t'} - m_{b'} = 50\,GeV$, obtained from limits on $Br_{b' \rightarrow bZ}$ by the CDF collaboration (bottom) and $Br_{b' \rightarrow cW}$ by the D0 collaboration (top). The darker region is the excluded region with a Higgs boson of 115 GeV. Central values were taken for b' production cross section.

27

Finally, we show an exclusion plot with the Higgs channel opened and a Higgs mass of 115 GeV. As we expected, the inclusion of the Higgs makes the excluded region to shrink. By itself, the inclusion of one more channel always diminishes the branching ratios and consequently less values will be excluded. Like $b' \to b\,Z$, $b' \to b\,H$ is larger for small R_{CKM} and large $m_{b'}$. Hence in this region of parameter space it competes with $b' \to b\,Z$ and $b' \to c\,W$ making the allowed region larger. For a detailed analysis of the so-called cocktail solution see [43].

2.6   Conclusion

We have found the allowed b' mass as a function of the CKM elements of a four generations sequential model. Using all available experimental data for $m_{b'} > 96$ GeV we have shown that there is still plenty of room for a b' with a mass larger than 96 GeV. We have also shown that the allowed region decreases as $m_{t'}$ increases. In fact, as the gap between the fourth generation quark masses increases the allowed region shrinks. Notice that this is in full agreement with the tendency of a small mass gap, if not completely degenerated, favoured by the electroweak precision measurements.

All plots show that R_{CKM} is for sure smaller than $\approx 10^{-2}$ and it can be as small as $\approx 10^{-4}$. This is not surprising because this region is exactly where we expected it to be. In fact, the CKM values we know so far suggest that $V_{cb'} \approx 10^{-4} - 10^{-3}$. If $V_{tb'} \approx 10^{-1}$ then a value of R_{CKM} between 10^{-2} and 10^{-4} is absolutely natural. Moreover, the limit we have obtained for $V_{cb'}$ in the last section makes it even more natural.

In the near future we hope to reduce very much the allowed region in Figs. 2.9 and 2.10. CDF and the D0 collaborations have improved their bounds producing new data for $m_{b'} > 190\,GeV$. We expected to increase the excluded areas using this data. Unfortunately, for $m_{b'} > 190$ the $b' \to W^* t$ channel opens and becomes dominant. So the new data doesn't affect the excluded area. For large $m_{t'} - m_{b'}$, and for some values of $m_{b'}$ the CDF/D0 limits almost shrink the allowed region to zero. Hence, a small improvement in the analysis could disallow a large region of the parameter space.

As for the future, searches in hadron colliders will have to wait for tha analysis of the RunII of the Tevatron and for the Large Hadron Collider (LHC). The $b'\bar{b}'$ production cross section increases by roughly two orders of magnitude at the LHC compared to the Tevatron. Thus LHC will be a copious source of b' pairs. With high values for cross section and luminosity, if background is suppressed exclusion plots can be drawn for a very wide range of b' masses. However, we have to worry about two problems in future searches. From the theoretical point of view we have to take into account all the possible hierarchies in mass, for instance one could have $m_{t'} < m_t < m_{b'}$ or $m_t < m_{t'} < m_{b'}$. A careful study, including also the possibility of finding a Higgs has to be done. From the experimental point of view we have to know how the detectors will perform.

Nobody knows yet if there is going to be a Linear Collider with energies of $\sqrt{s} = 500$ GeV or $\sqrt{s} = 1$ TeV. The planned International Linear Collider (ILC) would allow us to go up

$m_{b'} = 250$ GeV or $m_{b'} = 500$ GeV which is close to the perturbative limit. Depending on the available luminosity, and because a small background is expected, we believe that the excluded region would be very large, probably allowing the exclusion of some values of $m_{b'}$ regardless of the values of the mixing angles. However, if a Higgs boson is found the excluded region will surely be smaller and will depend on the mass and type of Higgs boson found. For a detailed discussion on future searches see [6].

In summary we believe that there is still experimental and theoretical work to be done to find or definitely to exclude a sequential fourth generation of quarks at the electroweak scale.

Chapter 3

Electroweak $2 \to 2$ amplitudes for electron-positron annihilation at TeV energies

3.1 Introduction

The standard theoretical description of e^+e^- annihilation into hadrons at high energies starts with the sub-process of e^+e^- -annihilation into quarks and gluons, which is then studied with perturbative methods. It is usually considered as mediated by the exchange of all electroweak (EW) bosons: $e^+e^- \to \gamma^*, Z, W \to q\bar{q}$+gluons. A successful prediction of the Standard Model is the forward-backward asymmetry, which has been studied for many years both theoretically and experimentally, particularly around the Z boson [31, 32, 33]. Future linear e^+e^- colliders will be operating in a energy domain which is much higher than the electroweak bosons masses, so that the full knowledge of the scattering amplitudes for e^+e^- annihilation into quark and lepton pairs will be needed. As it is well known, pure QED also gives rise to a forward-backward asymmetry even at low energies, albeit small, due to interference of one-photon and two-photon exchange diagrams. This effect persists at asymptotically high energies due to the multiphoton contributions in higher orders in α. Such multiphoton contribution in $e^+e^- \to \mu^+\mu^-$ was studied in Refs. [34] in the double-logarithmic (DL) approximation (DLA). The annihilation process in [34] was considered in the following two kinematic regions:

(i) Forward kinematics, when, in the center of mass frame (cm), the outgoing μ^+ (μ^-) goes in the direction of the initial $e^+(e^-)$.

(ii) Backward kinematics, when the outgoing μ^+ (μ^-) goes in the e^- (e^+) -direction.

These kinematical configurations refer to the case when the initial positive (or negative) electrical charges do not change the direction after the scattering, or they are affected by a major - almost backward - deviation. It was shown in [34] (see also the review [64]) that at high

energies the radiative DL corrections to the Born amplitudes are quite different for the forward and the backward kinematics. As a result, the cross section of the forward annihilation dominates over the backward one and therefore there is a charge forward-backward asymmetry: positive muons tend to go in the e^+ -beam direction and negative muons rather follow the direction of e^-. This forward-backward asymmetry for e^+e^- annihilation into leptons or hadrons produced at energies much greater than the W and Z boson masses has been recently considered in Ref. [20], where the electroweak radiative corrections were calculated to all orders in the double-logarithmic approximation (DLA). It was shown that the effect of the electroweak DL radiative corrections on the value of the forward-backward asymmetry is quite sizable and grows rapidly with the energy. As usual, the asymmetry is defined as the difference between the forward and the backward scattering amplitudes over the sum of them. These amplitudes were calculated in Ref. [20] in DLA, by introducing and solving the Infrared Evolution Equations (IREE). This method is a very simple and the most efficient instrument for performing all-orders double-logarithmic calculations (see Ref. [19] and Refs. therein). In particular, when it was applied in Ref. [19] to calculate the electroweak Sudakov (infrared-divergent) logarithms, it led easily to the proof of the exponentiation of the Sudakov logarithms. At that moment this was in contradiction to the non-exponentiation claimed in Ref. [65] and obtained by other means. This contradiction provoked a large discussion about the exponentiation. The exponentiation was confirmed eventually by the two-loop calculations in Refs. [66]-[67] and by summing up the higher loop DL contributions in Refs. [68] and [69]. These Sudakov logarithms provide the whole set of DL contributions to the $2 \to 2$ amplitudes only when the process is considered in the hard kinematic region where all the Mandelstam variables s, t, u are of the same order. The following equation

$$-t \sim -u \sim s \tag{3.1}$$

corresponds to large cm scattering angles $\theta \equiv \theta_{\mathbf{p_1 p'_1}} \sim 1$. On the other hand, when the kinematics of the $2 \to 2$ processes is of the Regge type, besides the Sudakov logarithms, another kind of DL contributions arises, coming from ladder Feynman graphs. A much more complex expressions for the scattering amplitudes is obtained if the above mentioned contributions (infrared stable) are considered. This was first shown in Ref. [15], where in the framework of pure QED, the scattering amplitudes for the forward and backward $e^+e^- \to \mu^+\mu^-$ annihilation were calculated in the Regge kinematics. One example of high-energy electroweak processes in the Regge kinematics was considered in Ref. [19], where the backward scattering amplitude was calculated, for the annihilation of a lepton pair with same helicities into another pair of leptons. More general calculations of the forward and backward electroweak scattering amplitudes were done in Ref [20]. However, both calculations in Refs. [20] and [19] were done under the assumption that the transverse momenta $k_{i\perp}$ of the virtual photons and virtual W, Z -bosons were much greater than the masses of the weak bosons. In other words, the same infrared cut-off M in the transverse momentum space, was used for all virtual electroweak bosons, i.e.,

$$k_{i\perp} \gg M \geq M_W \approx M_Z. \tag{3.2}$$

32

Obviously, while M is the natural infrared cut-off for the logarithmic contributions involving W, Z bosons, the cut-off for the photons can be chosen independently, in agrement with the experimental resolution in a given observed process. Indeed the assumption (3.2), although simplifying the calculations a lot, is unnecessary and an approach that involves different cut-offs for photons and W, Z weak bosons would be more interesting and suitable for phenomenological applications. This technique involving different cut-offs for photons and for W, Z bosons was applied in Ref. [19], for calculating the double-logarithmic contributions of soft virtual electroweak bosons (the Sudakov electroweak logarithms) but not for the scattering amplitudes in the regions of Regge kinematics.

We generalize the results of Refs. [19] and [20], and obtain new double-logarithmic expressions for the $2 \rightarrow 2$ - electroweak amplitudes in the forward and backward kinematics [70]. These expressions involve therefore different infrared cut-offs for virtual photons and virtual weak bosons. Throughout this chapter we assume that the photon cut-off, μ, and the W, Z boson cut-off, M, satisfy the relations:

$$M \geq M_{W,Z}, \quad \mu \geq m_f \qquad (3.3)$$

where m_f is the largest mass of the quarks or leptons involved in the process. Notice that the values of M and μ could be widely different. Let us remind that in order to study a scattering amplitude $A(s,t)$ in the Regge kinematics $s \gg -t$ (where s and t are the standard Mandelstam variables), it is convenient to represent $A(s,t)$ in the following form:

$$A(s,t) = A^{(+)}(s,t) + A^{(-)}(s,t), \qquad (3.4)$$

with

$$A^{(\pm)}(s,t) = (1/2)[A(s,t) \pm A(-s,t)], \qquad (3.5)$$

called the positive (negative) signature amplitudes. We shall only calculate amplitudes with the positive signatures. The IREE for the negative signature electroweak amplitudes can be obtained in a similar way, see e.g. Ref. [20] for more details.

For those less familiar with the double logs approximation technique an introduction is available in appendix A. This chapter is organized as follows. Instead of calculating amplitudes of $e^+e^- \rightarrow$ quarks directly, we find more convenient to operate with $SU(2)$ - invariant amplitudes of a more general process, the lepton-antilepton annihilation into quark-antiquark pair. In Sect. 3.2 we calculate the invariant amplitude with only one universal cut-off. We start by introduce such invariant amplitudes and show their relation to the forward and backward amplitudes for e^+e^- -annihilation. The IREE for the invariant amplitudes with only one cut-off are constructed in Sub-Sect. 3.2.1 and solved in Sub-Sect. 3.2.2. The solutions are obtained in terms of the Mellin amplitudes corresponding to collinear kinematics. The IREE for the Mellin amplitudes are obtained and solved in Sub-Sect. 3.2.3. Then in Sect. 3.3 we proceed with the two cut-off calculations. In Sub-Sect. 3.3.1, we construct the evolution equations for the invariant amplitudes for the case when in the center mass (cm) frame, the scattering angles are very

small. First, we obtain the IREE equations in the integral form and then we transform them in the simpler, differential form. These differential equations are solved in Sub-Sect. 3.3.2 and explicit expressions for the invariant amplitudes involving the Mellin integrals are obtained. In Sect. 3.4, we consider the case of large scattering angles, or when the Mandelstam variables s, t and u are all large. Sect. 3.5 deals with the expansion of the invariant amplitudes into the perturbative series in order to extract the first-loop and the second-loop contributions. Then we compare these contributions to the analogous terms obtained when one universal cut-off is used and study their difference. The effect of high-order contributions in the two approaches is further studied in Sect. 3.6 where the asymptotic expressions of the amplitudes are compared. Finally, Sect. 3.7 contains our concluding remarks.

3.2 Invariant amplitudes for lepton-antilepton annihilation into $q\bar{q}$ using one universal cut-off

We are going to account for the DL effects of exchanging the EW bosons to e^+e^- -annihilation into quark-antiquark pairs of different flavours. When multiple W - exchange is taken into account, the flavour of the virtual intermediate fermion state is not fixed, though the initial and final states of the annihilation are well-defined. Because the EW theory organizes all fermions into doublets of the left particles and right singlets, this suggests that is more convenient to calculate first the scattering amplitude of a more general process, the annihilation of a lepton and its antiparticle into a quark - antiquark pair, and only after to specify the flavour of the initial and the final states. This turns to be easier because the effects of the violation of the initial $SU(2)U(1)$ symmetry are in many respects neglected within the double-logarithmic accuracy. On the other hand that also means that the DLA can be applied safely only when the energy of the annihilation is much higher than M_Z, M_W. At such energies the propagators of the $SU(2)$ - gauge bosons, W_a $(a = 1, 2, 3)$, are $D_{ab}(k) \sim \delta_{ab}/k^2$. The propagator of the $U(1)$ -gauge boson B is $1/k^2$ in the same approximation. The $SU(2)$ vertices of the W_a interaction with the left fermions are $g\, t^a$, where t^a are the $SU(2)$ generators and g is the coupling, whereas the vertex of the interaction of the field B with the left and the right fermions is $g'\, Y/2$, Y being the hypercharge and g' being the coupling. As in the most general process both the initial and final particles can be left and/or right, we consider all these cases separately.

In this Sect. we consider the general case of the annihilation of the left lepton $l^k(p_1)$ belonging to the doublet (ν, e) and the antilepton $\bar{l}_i(p_2)$ from the charge conjugated doublet into the left quark $q^{k'}(p'_1)$ belonging to the doublet (u, d) and the antiquark $\bar{q}_{i'}(p'_2)$ from the charge conjugated doublet, represented in Fig. 3.1. Therefore, the scattering amplitude A of this process is

$$A = q^{k'}(p'_1)\, \bar{q}_{i'}(-p'_2)\, \widetilde{A}^{ii'}_{kk'}\, l^k(p_1)\, \bar{l}_i(-p_2) \tag{3.6}$$

where the matrix amplitude $\widetilde{A}^{ii'}_{kk'}$ has to be calculated perturbatively. For example: $\widetilde{A}^{21}_{21}$ represents the matrix amplitude for the annihilation of an electron and a positron into quarks u

34

$$p'_1 \qquad\qquad p'_2$$

$$p_1 \qquad\qquad p_2$$
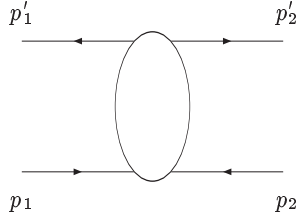
Figure 3.1: Scattering amplitude of the annihilation of Eq. 3.6

and $\bar{u}$. All lepton to quark processes are represented in table 3.2. We consider the kinematics

$$
\begin{array}{llll}
\widetilde{A}^{11}_{11} & \nu\bar{\nu} \to u\bar{u} & \widetilde{A}^{12}_{12} & \nu\bar{\nu} \to d\bar{d} \\
\widetilde{A}^{21}_{21} & e\bar{e} \to u\bar{u} & \widetilde{A}^{22}_{22} & e\bar{e} \to d\bar{d} \\
\widetilde{A}^{11}_{22} & e\bar{\nu} \to d\bar{u} & \widetilde{A}^{22}_{11} & \nu\bar{e} \to u\bar{d}
\end{array}
$$

Table 3.1: Lepton annihilation to quarks processes represented by the amplitudes $\widetilde{A}^{ii'}_{kk'}$.

where, in the cm, both particles of the produced pair move close to the lepton-antilepton beam. It corresponds to two kinematics:

(i) forward kinematics when

$$-t = -(p'_1 - p_1)^2 << s = (p_1 + p_2)^2 \approx -u = -(p'_2 - p_1)^2 \ , \qquad (3.7)$$

(ii) backward kinematics when

$$-u = -(p'_2 - p_1)^2 << s = (p_1 + p_2)^2 \approx -t = -(p'_1 - p_1)^2 \ . \qquad (3.8)$$

Then, replacing in (3.6) the lepton-antilepton pair by e^-, e^+ and the quark-antiquark pair by μ^-, μ^+ respectively, we see immediately that the electric charge almost does not change its direction in the forward kinematics (3.7) while it is reversed in the backward kinematics (3.8). Obviously that does not apply strictly for the annihilation into quarks because the electric charges of u -quarks and d -quarks are different in sign. Therefore t -kinematics is "forward" for the annihilation into a $d\bar{d}$ -pair and at the same moment it is "backward" for the annihilation into $u\bar{u}$ quarks. We will come back to this definition of backward and forward kinematics later, when we shall discuss the annihilation into $u\,\bar{u}$ and $d\,\bar{d}$ pairs, but until then we refer to (3.7) as t - kinematics, and (3.8) as u - kinematics.

In order to simplify the isospin structure, it is convenient to expand the matrix $\widetilde{A}^{ii'}_{kk'}$ into a sum, each term corresponding to some irreducible representation of $SU(2)$. In the t - kinematics

35

(3.7), the initial t - channel state is $l^k(p_1)q_{k'}(p'_1)$. So we can write,

$$
\begin{aligned}
l^k(p_1)q^{k'}(p'_1) &= \left[\frac{1}{2}\delta^k_{k'}\delta^b_a + (\delta^k_a\delta^b_{k'} - \frac{1}{2}\delta^k_{k'}\delta^b_a)\right] l^a(p_1)q^b(p'_1) \\
&= \left[\frac{1}{2}\delta^k_{k'}\delta^b_a + 2\sum_c(t_c)^k_{k'}(t_c)^b_a\right] l^a(p_1)q^b(p'_1)
\end{aligned}
\tag{3.9}
$$

where the first term corresponds to the scalar and the second one – to the triplet representation of $SU(2)$. Eq. (3.9) suggests the representation

$$
\widetilde{A}^{ii'}_{kk'} = (P_1)^{ii'}_{kk'}\widetilde{A}_1 + (P_2)^{ii'}_{kk'}\widetilde{A}_2
\tag{3.10}
$$

where $\widetilde{A}_{1,2}(s, t)$ are scalar functions and the singlet and triplet projection operators correspondingly are :

$$
\begin{aligned}
(P_1)^{ii'}_{kk'} &= \frac{1}{2}\delta^{k'}_k\delta^i_{i'}, \\
(P_2)^{ii'}_{kk'} &= 2(t_c)^{k'}_k(t_c)^i_{i'} .
\end{aligned}
\tag{3.11}
$$

Similarly for the u - kinematics (3.8), where the initial u -channel state is $l^k(p_1)q^{i'}(-p'_2)$, irreducible $SU(2)$ -representations are obtained by symmetrization and antisymmetrization,

$$
\widetilde{A}^{ii'}_{kk'} = (P_3)^{ii'}_{kk'}\widetilde{A}_3(u, s) + (P_4)^{ii'}_{kk'}\widetilde{A}_4(u, s) \ ,
\tag{3.12}
$$

with

$$
\begin{aligned}
(P_3)^{ii'}_{kk'} &= \frac{1}{2}\left[\delta^i_k\delta^{k'}_{i'} - \delta^{k'}_k\delta^i_{i'}\right] , \\
(P_4)^{ii'}_{kk'} &= \frac{1}{2}\left[\delta^i_k\delta^{k'}_{i'} + \delta^{k'}_k\delta^i_{i'}\right] .
\end{aligned}
\tag{3.13}
$$

Using the projectors P_j , $j = 1, 2, 3, 4$, the invariant amplitudes can be easily obtained:

$$
\widetilde{A}_j = \frac{(P_j)^{kk'}_{ii'}(\widetilde{A})^{ii'}_{kk'}}{(P_j)^{kk'}_{ii'}(P_j)^{ii'}_{kk'}} .
\tag{3.14}
$$

Explicitly formulas for A_j are the following:

$$
\begin{aligned}
A_1 &= \frac{1}{2}(A^{11}_{11} + A^{12}_{12} + A^{21}_{21} + A^{22}_{22}) \\
A_2 &= \frac{1}{6}(A^{11}_{11} - A^{11}_{22} + 2A^{12}_{12} + 2A^{21}_{21} - A^{22}_{11} + A^{22}_{22}) \\
A_3 &= \frac{1}{2}(A^{12}_{12} - A^{11}_{22} - A^{22}_{11} + A^{21}_{21}) \\
A_4 &= \frac{1}{6}(2A^{11}_{11} + A^{12}_{12} + A^{21}_{21} + A^{12}_{12} + A^{21}_{21} + 2A^{22}_{22})
\end{aligned}
$$

36

In the Born approximation, the amplitudes $\widetilde{A}_j$ defined in Eqs. (3.10, 3.12) can be written as

$$\widetilde{A}_j^{Born} = R\, A_j^{Born}(s) \; , \tag{3.15}$$

with

$$
\begin{aligned}
A_j^{Born}(s) &= \frac{s}{s + \imath\epsilon}\, a_j \; , \\
R &= \frac{\bar{u}(-p_2)[(1+\gamma_5)/2]\gamma_\nu[(1-\gamma_5)/2]u(p_1)\bar{u}(p_2')[(1+\gamma_5)/2]\gamma_\nu[(1-\gamma_5)/2]u(-p_1')}{s}
\end{aligned}
$$

where R denotes the normalized spinor factor and A_j^{Born} are scalar functions of s, differing only in constant group factors a_j . As we discuss the particular case of the left fermions we can drop the factors $[(1\pm\gamma_5)/2]$ and use the following definition:

$$R = \frac{\bar{u}(-p_2)\gamma_\nu u(p_1)\bar{u}(p_2')\gamma_\nu u(-p_1')}{s} \; . \tag{3.16}$$

For the left particles, the lepton and the quark hypercharges are $Y_l = -1$ and $Y_q = 1/3$ respectively. The group factors a_j for the Born amplitudes can be easily calculated.

$$
\begin{aligned}
a_1 &= \frac{3g^2 + g'^2 Y_l Y_q}{4}, \\
a_2 &= \frac{-g^2 + g'^2 Y_l Y_q}{4}, \\
a_3 &= \frac{-3g^2 + g'^2 Y_l Y_q}{4}, \\
a_4 &= \frac{g^2 + g'^2 Y_l Y_q}{4} \; .
\end{aligned}
\tag{3.17}
$$

The contributions proportional to $Y_l Y_q$ in Eq. (3.17) come from the Born graph where the lepton line is connected to the quark one by the B -field, the other contributions come from the Born graphs with propagators of W_i -fields. Using the explicit expressions for A_j we can include the contributions from the necessary processes. For example, $\nu\bar{\nu} \to u\bar{u}$ represented by $A_{1,1}^{1,1}$, contributes to A_1, A_2 and A_4. In Born approximation there are two possible diagrams to this process, each with a contribution to the group factors: $g^2/4$ from the W_3 exchange and $(g'^2 Y_l Y_q)/4$ from the B exchange.

Accounting for all DL corrections transforms the coefficients a_j into invariant amplitudes A_j,

$$\widetilde{A}_j = R\, A_j(s, u, t) \; , \tag{3.18}$$

where, in DLA, A_j depend on s, t, u through logarithms. When A_j are calculated, Eqs. (3.11, 3.13) allow us to express immediately the amplitudes of $e^+ e^-$ annihilation into quarks in terms of

the invariant amplitudes A_j in both forward(t) -kinematics (3.7) and in backward(u) -kinematics (3.8):

$$
\begin{aligned}
A_F(e^+e^- \to u\bar{u}) &= R\, A_2(s,t), \\
A_F(e^+e^- \to d\bar{d}) &= R\,[A_1(s,t) + A_2(s,t)]/2 \,, \\
A_B(e^+e^- \to u\bar{u}) &= R\,[A_3(s,t) + A_4(s,t)]/2 \,, \\
A_B(e^+e^- \to d\bar{d}) &= R\, A_4(s,t) \,.
\end{aligned}
\tag{3.19}
$$

The amplitudes of e^+e^- annihilation into leptons can also be expressed through the leptonic invariant amplitudes very similarly:

$$
\begin{aligned}
A_F(e^+e^- \to \mu^+\mu^-) &= R\,[A_1(s,t) + A_2(s,t)]/2, \\
A_F(e^+e^- \to \nu_\mu\bar{\nu}_\mu) &= R\,[A_3(s,t) + A_4(s,t)]/2, \\
A_B(e^+e^- \to \mu^+\mu^-) &= R\, A_2(s,t) \,, \\
A_B(e^+e^- \to \nu_\mu\bar{\nu}_\mu) &= R\, A_4(s,t) \,.
\end{aligned}
\tag{3.20}
$$

3.2.1 Evolution equations for the invariant amplitudes A_j

In this section we calculate A_j in the high energy limit, by constructing and solving an IREE for them, as a generalization of the evolution equations derived earlier in QCD. This approach exploits the evolution of scattering amplitudes with respect to the infrared cut-off μ in the transverse momentum space. Transverse momenta of all virtual particles are supposed to obey

$$
k_{i\perp} > \mu, \qquad k_{i\perp} \perp p_1, p_2.
\tag{3.21}
$$

The value of the cut-off μ must not be smaller than any of the involved masses, otherwise it is arbitrary. Introducing μ makes also possible to neglect the masses of all involved quarks and to restrict ourselves to consider the evolution of A_j with respect to μ only. Then one can take in the final formulas μ of order of the largest mass involved. In DLA we can also neglect the difference between the masses of EW bosons M_W and M_Z, putting in the final expressions

$$
\mu = M = M_Z \approx M_W \,.
\tag{3.22}
$$

First we consider the annihilation in t -kinematics and construct the IREE for A_j with $j = 1, 2$. According to (3.7), t is small compared to $u, -s$. To bound it from below we assume that

$$
s \gg -t \gg \mu^2 \,.
\tag{3.23}
$$

The main idea of the IREE consists in evoluting the invariant amplitudes with respect to the infrared cut-off μ by applying to them the differential operator

$$
-\mu^2 \partial/\partial\mu^2 \,,
\tag{3.24}
$$

38

in the form

$$-\mu^2 \frac{\partial A_j}{\partial \mu^2} = \frac{\partial A_j}{\partial \rho} + \frac{\partial A_j}{\partial \eta} \ , \tag{3.25}$$

where we use $u \approx -s$ in this forward kinematics and have introduced the notations

$$\rho = \ln(s/\mu^2), \qquad \eta = \ln(-t/\mu^2) \ . \tag{3.26}$$

In order to obtain the right hand side (rhs) of eq.3.25, we have to take into account the factorization of DL contributions of virtual particles with respect to μ, where μ is the lowest limit of integration over $k_\perp$. In turn, this minimal $k_\perp$ acts as a new cut-off for other virtual momenta (see [16, 22] for details). When the virtual particle with the minimal $k_\perp$ is a EW boson, one can factorize its DL contributions as shown in Fig. 3.2. Applying then the differentiation (3.24) and the projection operators P_j we obtain with the help of Eq. (3.14) the contributions G_1, G_2 to the EW singlet and triplet parts of the IREE respectively.

Before writing the explicit expressions for $G_{1,2}$, we want to discuss the general structure of these contributions. Integration over longitudinal momentum of the factorized boson with momentum k in graphs (a) and (b) in Fig, 3.2 yields $\ln(-s/k_\perp^2)$ whereas the same integration in graphs (c) and (d) yields $\ln(-u/k_\perp^2) \approx \ln(s/k_\perp^2)$. Similarly, graphs (e),(f) yield $\ln(-t/k_\perp^2)$. The different results come from contributions of the propagators evolved. For example in diagram c) the denominator is:

$$[(p_1 - k)^2 - m + i\epsilon][(-p2' - k)^2 - m + i\epsilon][k^2 - i\epsilon] \tag{3.27}$$

Using the Sudakov parametrization:

$$k = \alpha p_2 + \beta p_1 + k_\perp \tag{3.28}$$

We can rewrite this denominator and use the first term to integrate over α using residues theorem. The second term will simplify to $-\beta u - k_\perp^2$. The only region where this will produce a log is when $\beta >> -k_\perp^2/u$. The α integration limits $\beta < 1$, so these two conditions set the limits for β integration. Besides these logarithms, each graph in Fig. 3.2 contains also an integration of $A_j(s/k_\perp^2, t/k_\perp^2)/k_\perp^2$ over $k_\perp^2$, with the lowest limit μ^2. This comes from the third term after α and β integrations. Technical details for different processes can be found on the appendix.

After using differentiation (3.24), we arrive at

$$G_{1,2} = \quad \frac{1}{8\pi^2} \sum_{j=1,2} \left[\left(b_s^{(j)}\right)_{1,2} \ln\left(\frac{-s}{\mu^2}\right) - \left(b_u^{(j)}\right)_{1,2} \ln\left(\frac{-u}{\mu^2}\right) \right] A_j\left(\frac{s}{\mu^2}, \frac{t}{\mu^2}\right)$$
$$- \frac{1}{8\pi^2} h_{1,2} \ln\left(\frac{-t}{\mu^2}\right) A_{1,2}\left(\frac{s}{\mu^2}, \frac{t}{\mu^2}\right) \ , \tag{3.29}$$

where the the quantities $\left(b_s^{(j)}\right)_{1,2}, ..., h_{1,2}$ will be explicitly given later.

39
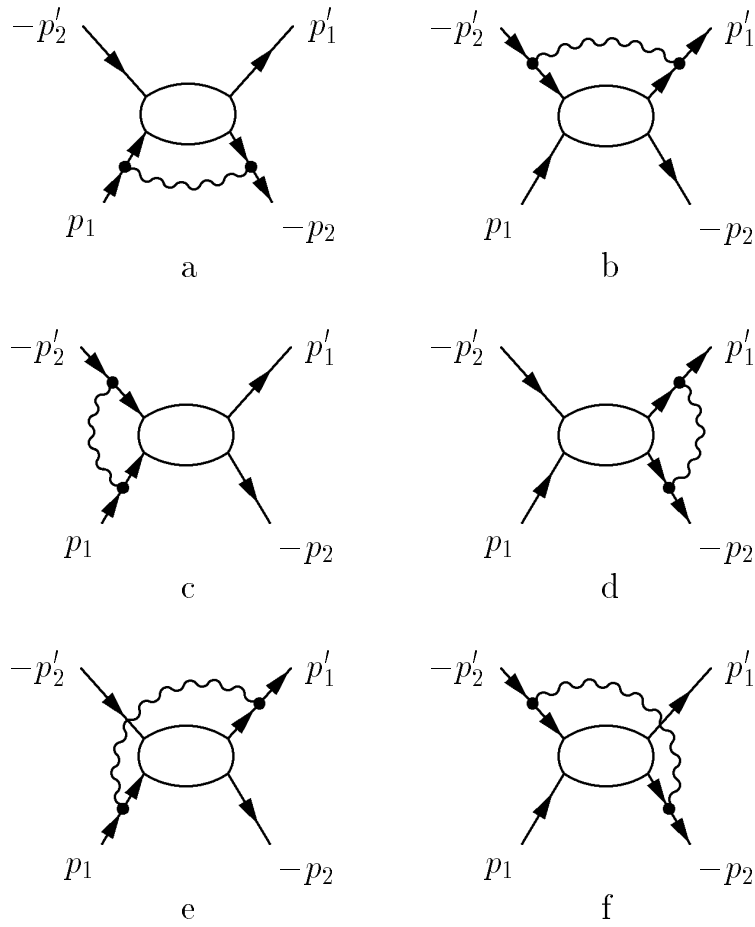
Figure 3.2: Contribution to IREE from soft EW boson factorization in different channels: s-channel – a and b, u-channel – c and d, t-channel – e and f.
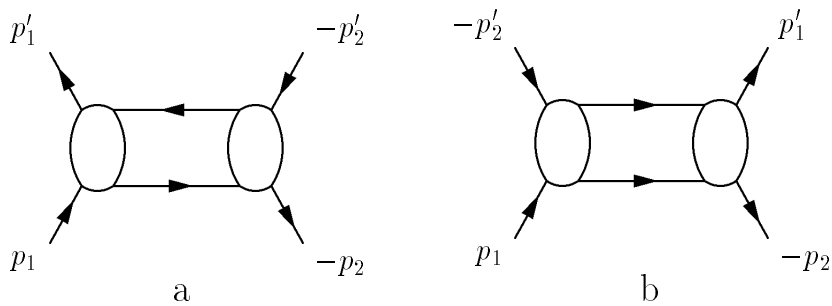
Figure 3.3: Contribution to IREE from soft fermion intermediate state in t-channel – a and in u-channel – b.

Let us introduce

$$\rho^{(\pm)} = \frac{1}{2}\left[\ln\left(\frac{-s}{\mu^2}\right) \pm \ln\left(\frac{-u}{\mu^2}\right)\right] \tag{3.30}$$

so that $\ln(-s/\mu^2) = \rho^{(+)} + \rho^{(-)}$ and $\ln(-u/\mu^2) = \rho^{(+)} - \rho^{(-)}$. Obviously, $\rho^{(+)}$ and $\rho^{(-)}$ are symmetrical and antisymmetrical functions with respect to replacing s by u. It is convenient also to introduce the invariant amplitudes $A_{1,2}^{(\pm)}$ with the same properties [1] :

$$A_{1,2}^{(\pm)} = \frac{1}{2}\left[A_{1,2}\left(\frac{s}{\mu^2}, \frac{t}{\mu^2}\right) \pm A_{1,2}\left(\frac{u}{\mu^2}, \frac{t}{\mu^2}\right)\right] , \tag{3.31}$$

so that $A_{1,2} = A_{1,2}^{(+)} + A_{1,2}^{(-)}$. Then for signature amplitudes $G_{1,2}^{(\pm)}$ defined as

$$G_{1,2}^{(\pm)} = \frac{1}{2}\left[G_{1,2}(s,t) \pm G_{1,2}(u,t)\right] \tag{3.32}$$

from Eq. (3.29) we obtain the following expressions

$$G_{1,2}^{(+)} = \frac{1}{8\pi^2}\sum_{j=1,2}\left[\left(b^{(j)}\right)_{1,2}^{(+)}\rho^{(+)}A_j^{(+)} + \left(b^{(j)}\right)_{1,2}^{(-)}\rho^{(-)}A_j^{(-)}\right] + \frac{1}{8\pi^2}h_{1,2}\,\eta\,A_{1,2}^{(+)} ,$$

$$G_{1,2}^{(-)} = \frac{1}{8\pi^2}\sum_{j=1,2}\left[\left(b^{(j)}\right)_{1,2}^{(+)}\rho^{(+)}A_j^{(-)} + \left(b^{(j)}\right)_{1,2}^{(-)}\rho^{(-)}A_j^{(+)}\right] + \frac{1}{8\pi^2}h_{1,2}\,\eta\,A_{1,2}^{(-)} \tag{3.33}$$

where

$$\left(b^{(j)}\right)_{1,2}^{(\pm)} = \left(b_s^{(j)}\right)_{1,2} \mp \left(b_u^{(j)}\right)_{1,2} . \tag{3.34}$$

Besides an EW boson, in kinematics (3.7) a t-channel virtual fermion pair, as shown in Fig. 3.3, could also attain the minimal transverse momentum. For example, in diagram a) we would have an electron with minimal momentum k and the other with momentum $p_1' - p_1 + k$. This propagator will impose an additional condition to the integration over $k_\perp$. The only region where a log contribution appears is when $k_\perp > t^2$. So DL contributions arising from the integration over this pair momentum could only come from the region $k_\perp^2 > -t \gg \mu^2$. Hence they do not depend on μ in kinematics (3.23) and must vanish when differentiated with respect to μ. The same is true for the Born amplitudes (3.15).

As soon as $\ln(-s/\mu^2) = \ln(s/\mu^2) - \imath\pi$, in kinematics (3.7) with $\rho = \ln(s/\mu^2) \approx \ln(-u/\mu^2)$ we obtain

$$\rho^{(+)} = \rho - \frac{\imath\pi}{2}\,\mathrm{sign}(s) ,$$

$$\rho^{(-)} = -\frac{\imath\pi}{2}\,\mathrm{sign}(s) . \tag{3.35}$$

---

[1] In the Regge theory, amplitudes $A^{(\pm)}$ are called the positive and negative signature amplitudes, and we use these notation below.

It is assumed in DLA that $\ln(s/\mu^2) \gg \pi$. This means that

$$\rho^{(+)} \gg \rho^{(-)} .\tag{3.36}$$

Similarly, in DLA in each order of the perturbative expansion the amplitudes $A_j^{(+)}$ dominate over $A_j^{(-)}$ by one power of $\ln(s/\mu^2)$. By the same reason the amplitudes $A_j^{(+)}$ are mainly real, and we can assume

$$A_j^{(+)} \approx \Re A_j^{(+)} \gg \left| A_j^{(-)} \right| .\tag{3.37}$$

Combining Eqs. (3.25, 3.33) and using Eqs. (3.37, 3.35, 3.36) leads us to the following IREE where the negligible terms, in DLA, $A^{(-)}\rho^{(-)}$ are dropped and terms $A^{(-)}\rho^{(+)} \sim A^{(+)}\rho^{(-)}$ are retained:

$$\frac{\partial A_{1,2}^{(+)}}{\partial \rho} + \frac{\partial A_{1,2}^{(+)}}{\partial \eta} = \frac{1}{8\pi^2}\, \rho \left[\sum_{j=1,2} \left(b^{(j)} \right)_{1,2}^{(+)} A_j^{(+)} \right] + \frac{1}{8\pi^2}\, h_{1,2}\, \eta\, A_{1,2}^{(+)} ,\tag{3.38}$$

$$\frac{\partial A_{1,2}^{(-)}}{\partial \rho} + \frac{\partial A_{1,2}^{(-)}}{\partial \eta} = \frac{1}{8\pi^2}\, \rho \left[\sum_{j=1,2} \left(b^{(j)} \right)_{1,2}^{(+)} A_j^{(-)} \right] + \left(\frac{-\imath\pi}{2} \right) \frac{1}{8\pi^2} \left[\sum_{j=1,2} \left(b^{(j)} \right)_{1,2}^{(-)} A_j^{(+)} \right]$$
$$+ \frac{1}{8\pi^2}\, h_{1,2}\, \eta\, A_{1,2}^{(-)} .\tag{3.39}$$

Let us proceed now to the u - kinematics (3.8). Using projection operators (3.13) instead of (3.11) one can consider the annihilation in the u -kinematics and obtain the IREE for invariant signature amplitudes $A_3^{(\pm)}$, $A_4^{(\pm)}$ introduced in a way similar to that one used for $A_{1,2}^{(\pm)}$. As the amplitudes $A_3^{(\pm)}$, $A_4^{(\pm)}$ correspond to SU(2) singlet and triplet representations, similarly to $A_{1,2}^{(\pm)}$, we can easily obtain IREE for u -kinematics from Eq. (3.38) with the replacement

$$t \longleftrightarrow u , \quad "1" \to "3" , \quad "2" \to "4" , \quad Y_q \to - Y_q .$$

Indeed, adding the restriction

$$s \gg -u \gg \mu^2 \tag{3.40}$$

to Eq. (3.8), the derivation is quite similar to the previous one done for the t - kinematics thus leading to the same structure of the IREE for the amplitudes $A_{3,4}^{(\pm)}$. Therefore one can write down the same IREE for all invariant signature amplitudes $A_j^{(\pm)}$, with $j = 1, 2, 3, 4$, generalizing Eq. (3.38).

The next significant simplification of (3.38) comes from the explicit calculation of the group factors $\left(b^{(j)} \right)_{1,2}^{(\pm)}$. It turns out that

$$\left(b^{(0)} \right)_2^{(+)} = \left(b^{(1)} \right)_1^{(+)} = \left(b^{(-)} \right)_4^{(+)} = \left(b^{(+)} \right)_3^{(+)} = 0,\tag{3.41}$$

and consequently the IREE for the positive signature amplitudes become linear homogenous partial differential equations. They can be written in a more simple general way:

$$\frac{\partial A_j^{(+)}}{\partial \rho} + \frac{\partial A_j^{(+)}}{\partial \eta'} = -\frac{1}{8\pi^2} \left[b_j\rho + h_j\eta' \right] A_j^{(+)} ,\tag{3.42}$$

where b_j, h_j and η' will be specified below, so that the only difference between the equations for different amplitudes comes from the numerical factors b_j, h_j:

$$b_1 = \frac{g'^2(Y_l - Y_q)^2}{4}, \tag{3.43}$$

$$b_2 = \frac{8g^2 + g'^2(Y_l - Y_q)^2}{4},$$

$$b_3 = \frac{g'^2(Y_l + Y_q)^2}{4},$$

$$b_4 = \frac{8g^2 + g'^2(Y_l + Y_q)^2}{4},$$

$$h_1 = \frac{3g^2 + g'^2 Y_l Y_q}{2}, \tag{3.44}$$

$$h_2 = \frac{-g^2 + g'^2 Y_l Y_q}{2},$$

$$h_3 = \frac{3g^2 - g'^2 Y_l Y_q}{2},$$

$$h_4 = \frac{-g^2 - g'^2 Y_l Y_q}{2}.$$

The IREE for the negative signature amplitudes $A_j^{(-)}$ are also linear partial differential equations, but not being homogeneous, they involve positive signature amplitudes through a non-zero matrix $r_{jj'}$:

$$\frac{\partial A_j^{(-)}}{\partial \rho} + \frac{\partial A_j^{(-)}}{\partial \eta'} = -\frac{1}{8\pi^2} \left[(b_j \rho + h_j \eta') A_j^{(-)} + \left(\frac{-\imath\pi}{2}\right) \sum_{j'} r_{jj'} A_{j'}^{(+)} \right]. \tag{3.45}$$

In order to write down the IREE for all $A_j^{(-)}$ and $A_j^{(+)}$ in the same way, we have used in Eqs. (3.42,3.45) the variable η' so that

$$\eta' \equiv \eta = \ln(-t/\mu^2) \tag{3.46}$$

for t - kinematics and

$$\eta' \equiv \chi = \ln(-u/\mu^2) \tag{3.47}$$

for u - kinematics. The non-zero numerical factors $r_{jj'}$ in Eq. (3.45) are :

$$r_{00} = r_{11} = g'^2 \frac{(Y_l + Y_q)^2}{4}$$

$$r_{01} = r_{-+} = 3g^2$$

$$r_{10} = r_{+-} = g^2$$

$$r_{--} = r_{++} = g'^2 \frac{(Y_l - Y_q)^2}{4}. \tag{3.48}$$

43

3.2.2 Solutions to IREE for the invariant amplitudes $A_j^{(\pm)}$

The general solution to Eq. (3.42) is

$$A_j^{(+)} = \Phi_j^{(+)}(\rho - \eta') \exp[-\phi_j(C, \eta')] , \tag{3.49}$$

with

$$\phi_j = \frac{1}{8\pi^2} \left[b_j \, C \, \eta' + (b_j + h_j) \, \frac{\eta'^2}{2} \right] , \tag{3.50}$$

$C = \rho - \eta' = \mathrm{const}$ and Φ_j is an arbitrary function. We can specify it by imposing the boundary condition

$$A_j^{(+)}(\rho, \eta')\Big|_{\eta'=0} = \tilde{A}_j^{(+)}(\rho) , \tag{3.51}$$

where $\tilde{A}_j^{(+)}(\rho)$ are the amplitudes for the annihilation in the "collinear kinematics", i.e. in the kinematics where quarks are produced close to the direction of the beam of initial leptons, with the value of either t or u much smaller than those fixed by Eqs. (3.23,3.40). Of course one must use a separate boundary condition (3.51) for the t and u - kinematics. We define the notation "collinear t -kinematics" for

$$-t < \mu^2 \tag{3.52}$$

and the notation "collinear u -kinematics" for

$$-u < \mu^2 . \tag{3.53}$$

It is convenient to use the Mellin transform[2] to represent signature amplitudes $\tilde{A}_j^{(\pm)}$ in the "collinear kinematics" (3.52,3.53):

$$\tilde{A}_j^{(\pm)}(\rho) = \int_{-\imath\infty}^{\imath\infty} \frac{d\omega}{2\pi\imath} \left(\frac{s}{\mu^2} \right)^{\omega} \xi^{(\pm)}(\omega) \, F_j^{(\pm)}(\omega) \tag{3.54}$$

where

$$\xi^{(\pm)} = \frac{\exp(-\imath\pi\omega) \pm 1}{2} \tag{3.55}$$

are the well known signature factors. At asymptotically high energy s the region of small ω, $\omega \ll 1$, is dominating in integral (3.54). This allows one to exploit the following approximations:

$$\xi^{(+)} \approx 1 , \qquad \xi^{(-)} \approx -\frac{\imath\pi\omega}{2} \tag{3.56}$$

Eq. (3.54) implies that the positive signature amplitudes $A_j^{(+)}(\rho, \eta')$ in the kinematic regions (3.23, 3.40) can be easily expressed through the Mellin amplitudes $F_j^{(\pm)}(\omega)$:

$$A_j^{(+)}(\rho, \eta') = \exp[-\phi_j(C, \eta')] \int_{-\imath\infty}^{\imath\infty} \frac{d\omega}{2\pi\imath} \, e^{(\rho-\eta')\omega} \, \xi^{(+)}(\omega) \, F_j^{(+)}(\omega) . \tag{3.57}$$

---

[2]For a basic introduction on the Mellin transform and the asymptotic form of Sommerfeld-Watson transform see A.3.

On the other hand, as stated earlier, the IREE (3.45) for the negative signature amplitudes $A_j^{(-)}$ are not homogeneous, in contrast to Eq. (3.42). Besides the amplitudes $A_j^{(-)}$, they also involve the positive signature amplitudes $A_j^{(+)}$. In order to solve Eq. (3.45), we have to use again the boundary condition

$$A_j^{(-)}(\rho, \eta')\Big|_{\eta'=0} = \tilde{A}_j^{(-)}(\rho) . \tag{3.58}$$

It is easy to check that the solution to the Eq. (3.45) satisfying Eq. (3.58) is

$$A_j^{(-)}(\rho, \eta') = \exp[-\phi_j(C, \eta')] \times \tag{3.59}$$
$$\left[\tilde{A}_j^{(-)}(\rho - \eta') - \int_0^{\eta'} d\tau \, \exp[\phi_j(C, \tau)] \left(\frac{-\imath\pi}{2} \right) \left(\frac{1}{8\pi^2} \right) \sum_{j'} r_{jj'} \, A_{j'}^{(+)}(C, \tau) \right] .$$

Applying the Mellin transforms (3.54) and (3.57) for the amplitudes in Eq. (3.59) we can rewrite it through the Mellin amplitudes $F_j^{(\pm)}(\omega)$ as well. In order to simplify this procedure we use the substitution

$$\left(\frac{-\imath\pi}{2} \right) \xi^{(+)} \approx \frac{1}{\omega} \xi^{(-)}, \tag{3.60}$$

which follows from the approximation (3.56) and is reasonable when the small ω region is dominating in the integral. Eventually we arrive at

$$A_j^{(-)}(\rho, \eta') = \exp[-\phi_j(C, \eta')] \int_{-\imath\infty}^{\imath\infty} \frac{d\omega}{2\pi\imath} e^{\omega(\rho-\eta')} \xi^{(-)}(\omega) \times \tag{3.61}$$
$$\left[F_j^{(-)}(\omega) - \frac{1}{8\pi^2} \sum_{j'} r_{jj'} \frac{F_{j'}^{(+)}(\omega)}{\omega} \int_0^{\eta'} d\tau \, \exp[\phi_j(C, \tau) - \phi_{j'}(C, \tau)] \right] .$$

Eqs. (3.57,3.61) show how one can obtain the amplitudes $A_j^{(\pm)}$ when the Mellin amplitudes $F_j^{(\pm)}(\omega)$ are calculated.

3.2.3 IREE for the Mellin amplitudes $F_j^{(\pm)}$

In order to calculate $F_j^{(\pm)}$ we have to construct IREE for "collinear kinematics" amplitudes $\tilde{A}_j^{(\pm)}(\rho)$. The IREE for them differ from the IREE for amplitudes $A_j^{(\pm)}$ considered in the previous section, by the following reasons:

(i) The amplitudes $\tilde{A}_j^{(\pm)}$ in the kinematics (3.52, 3.53) depend on $\rho = \ln(s/\mu^2)$ only, and some graphs in Fig. 3.2 do not yield DL contributions to IREE for them. In particular, graphs (e) and (f) with factorized t - channel virtual bosons do not contribute to IREE for $\tilde{A}_{1,2}^{(\pm)}$ while graphs (c),(d) with factorized u - channel bosons do not contribute to IREE for $\tilde{A}_{3,4}^{(\pm)}$. The left hand side (lhs) of the IREE for $\tilde{A}_j^{(\pm)}$ turns to $-\mu^2 \partial \tilde{A}_j^{(\pm)}/\partial\mu^2$ that in terms of the Mellin variable ω results in $\omega F_j^{(\pm)}(\omega)$.

(ii) The DL contributions of the graphs in Fig. 3.2 also depend on μ^2 and therefore do not vanish when differentiated with respect to μ. As these graphs are convolutions of two amplitudes, their contributions become simpler after applying the Mellin transform (3.54). Then the differentiation $-\mu^2 \partial/\partial\mu^2$ of these graphs leads to the following contribution to the IREE for the Mellin transforms $F_j^{(\pm)}$:

$$\frac{c_j}{8\pi^2} \left[F_j^{(\pm)}(\omega) \right]^2 \; , \tag{3.62}$$

with $c_j = 1$ for $j = 1, 2$ and $c_j = -1$ for $j = 3, 4$.

(iii) Though at the first sight the Born amplitudes $\tilde{A}_j^{Born}$ of Eq. (3.15) do not depend on μ^2 it is necessary to replace them by $a_j s/(s - \mu^2 + \iota\epsilon)$. This form explicitly tells that s cannot be smaller than μ^2 and also it makes the Mellin transform for the Born amplitudes to be correctly defined. The Mellin transforms for Born amplitudes are therefore a_j/ω. Applying $-\mu^2\partial/\partial\mu^2$ to them results in multiplying by ω. Hence the contributions of the Born amplitudes to IREE are just the constant terms a_j.

As a result we arrive to the following IREE for Mellin amplitudes $F_j^{(\pm)}(\omega)$.

$$\omega F_j^{(+)}(\omega) \;=\; a_j + \frac{b_j}{8\pi^2} \frac{dF_j^{(+)}(\omega)}{d\omega} + \frac{c_j}{8\pi^2} \left[F_j^{(+)}(\omega) \right]^2 \; , \tag{3.63}$$

$$\omega F_j^{(-)}(\omega) \;=\; a_j + \frac{b_j}{8\pi^2} \frac{1}{\omega} \frac{d\left(\omega F_j^{(-)}(\omega)\right)}{d\omega} + \frac{c_j}{8\pi^2} \left[F_j^{(-)}(\omega) \right]^2 - \sum_{j'} \frac{r_{jj'}}{8\pi^2} F_{j'}^{(+)}(\omega) \; . \tag{3.64}$$

The coefficients a_j, b_j, c_j and $r_{jj'}$ are listed in table 3.2 for t - kinematics and in table 3.3 for u - kinematics.

F	a_j	b_j	h_j	c_j	r_{j0}	r_{j1}	p_j
F_0	$\frac{3g^2+g'^2 Y_l Y_q}{4}$	$g'^2 \frac{(Y_l-Y_q)^2}{4}$	$\frac{3g^2+g'^2 Y_l Y_q}{2}$	1	$g'^2 \frac{(Y_l+Y_q)^2}{4}$	$3g^2$	$\frac{3+Y_l Y_q \tan^2\theta}{(Y_l-Y_q)^2 \tan^2\theta}$
F_1	$\frac{-g^2+g'^2 Y_l Y_q}{4}$	$2g^2+g'^2 \frac{(Y_l-Y_q)^2}{4}$	$\frac{-g^2+g'^2 Y_l Y_q}{2}$	1	g^2	$g'^2 \frac{(Y_l+Y_q)^2}{4}$	$\frac{-1+Y_l Y_q \tan^2\theta}{8+(Y_l-Y_q)^2 \tan^2\theta}$
F_{RR}	$\frac{g'^2 Y_l Y_q}{4}$	$g'^2 \frac{(Y_l-Y_q)^2}{4}$	$\frac{g'^2 Y_l Y_q}{2}$	1	$g'^2 \frac{(Y_l+Y_q)^2}{4}$	0	$\frac{Y_l Y_q}{(Y_l-Y_q)^2}$
F_{LR}	$\frac{g'^2 Y_l Y_q}{4}$	$\frac{3g^2+g'^2 (Y_l-Y_q)^2}{4}$	$\frac{g'^2 Y_l Y_q}{2}$	1	$\frac{3g^2+g'^2(Y_l+Y_q)^2}{4}$	0	$\frac{Y_l Y_q \tan^2\theta}{3+(Y_l-Y_q)^2 \tan^2\theta}$

Table 3.2: The coefficients of IREE Eqs.(3.63,3.64) for t-kinematics. The angle θ here is the Weinberg angle.

Solutions to Eq. (3.63) can be expressed in terms of the Parabolic cylinder functions D_p:

$$F_j^{(+)}(\omega) = \frac{a_j}{\lambda_j} \frac{D_{p_j-1}(\omega/\lambda_j)}{D_{p_j}(\omega/\lambda_j)} \tag{3.65}$$

46

F	a_j	b_j	h_j	c_j	r_{j-}	r_{j+}	p_j
F_-	$\frac{-3g^2+g'^2 Y_l Y_q}{4}$	$g'^2\frac{(Y_l+Y_q)^2}{4}$	$\frac{3g^2-g'^2 Y_l Y_q}{2}$	-1	$g'^2\frac{(Y_l-Y_q)^2}{4}$	$3g^2$	$\frac{3-Y_l Y_q \tan^2\theta}{(Y_l+Y_q)^2 \tan^2\theta}$
F_+	$\frac{g^2+g'^2 Y_l Y_q}{4}$	$2g^2+g'^2\frac{(Y_l+Y_q)^2}{4}$	$\frac{-g^2-g'^2 Y_l Y_q}{2}$	-1	g^2	$g'^2\frac{(Y_l-Y_q)^2}{4}$	$-\frac{1+Y_l Y_q \tan^2\theta}{8+(Y_l+Y_q)^2 \tan^2\theta}$
F_{RR}	$\frac{g'^2 Y_l Y_q}{4}$	$g'^2\frac{(Y_l+Y_q)^2}{4}$	$\frac{-g'^2 Y_l Y_q}{2}$	-1	$g'^2\frac{(Y_l-Y_q)^2}{4}$	0	$-\frac{Y_l Y_q}{(Y_l+Y_q)^2}$
F_{LR}	$\frac{g'^2 Y_l Y_q}{4}$	$\frac{3g^2+g'^2(Y_l+Y_q)^2}{4}$	$\frac{-g'^2 Y_l Y_q}{2}$	-1	$\frac{3g^2+g'^2(Y_l-Y_q)^2}{4}$	0	$-\frac{Y_l Y_q \tan^2\theta}{3+(Y_l+Y_q)^2 \tan^2\theta}$

Table 3.3: The coefficients for IREE Eqs.(3.63,3.64) for u-kinematics. The angle θ here is the Weinberg angle.

where

$$\lambda_j = \sqrt{\frac{b_j}{8\pi^2}}\ , \qquad p_j = \frac{a_j c_j}{b_j}\ . \tag{3.66}$$

In contrast, solutions to Eq. (3.64) can be found only numerically. In QED the negative signature amplitudes for the backward $e^+e^- \to \mu^+\mu^-$ annihilation were solved in Ref. [71]. It is interesting to note that $b_1 = 0$ in the IREE for the forward amplitudes $A_{e\mu}^{(\pm)}$ of $e^+e^- \to \mu^+\mu^-$ -annihilation, and the differential equations (3.63) for $A_{e\mu}^{(\pm)}$ in kinematics (3.52) turn into purely algebraic equations. This result was first obtained in Ref. [34]. Later it was proved[16] that the IREE for the (colourless) scalar components of the $SU(3)$ negative signature amplitudes of quark-antiquark annihilation into another quark-antiquark pair are also algebraic and therefore can be easily solved. The processes mentioned above are the only known examples of solving IREE for negative signature amplitudes [3]. In all those cases the intercepts of the negative signature amplitudes are greater than those for the positive signature amplitudes, though the difference amounts only to a few percents. Equations for the negative signature amplitudes always involve the positive signature amplitudes. It has been observed[20] in a QCD context, that these amplitudes can be approximated by their Born values with good accuracy. Such an approximation can help in solving Eqs. (3.64). We do not consider explicit solutions of Eqs. (3.64) in the present work. Instead, we consider below only contributions of amplitudes with the positive signature $A_j^{(+)}$. Combining Eqs. (3.57,3.65) and introducing variable $x = \omega/\lambda_j$, we arrive at the expression:

$$A_j^{(+)}(\rho,\eta') = a_j\, \exp[-\phi_j(\rho-\eta',\eta')] \int_{-\imath\infty}^{\imath\infty} \frac{dx}{2\pi\imath}\, e^{\lambda_j x(\rho-\eta')}\, \frac{D_{p_j-1}(x)}{D_{p_j}(x)}\ . \tag{3.67}$$

It is useful here to split ϕ_j defined by Eq. (3.50) and to combine its part depending on $\rho-\eta'$ with the exponent of the integrand in Eq. (3.67). Then changing the integration variable x to

---

[3]In the context of the EW theory, the IREE for the backward scattering amplitude with the negative signature was solved in [19] for the unrealistic case of a complex value of the Weinberg angle.

l, where $x = l + \lambda_j \eta'$ we finally obtain

$$A_j^{(+)}(\rho, \eta') = a_j \exp\left[-\frac{b_j + h_j}{8\pi^2} \frac{\eta'^2}{2}\right] \int_{-\imath\infty}^{\imath\infty} \frac{dl}{2\pi\imath} e^{\lambda_j l(\rho - \eta')} \frac{D_{p_j - 1}(l + \lambda_j \eta')}{D_{p_j}(l + \lambda_j \eta')} \tag{3.68}$$

where, for the case of t - kinematics with $j = 1, 2$, $\eta' = \eta = \ln(-t/\mu^2)$ and for the case of u - kinematics with $\eta' = \chi = \ln(-u/\mu^2)$, $j = 3, 4$.

The exponential factor in front of the integral in Eq. (3.68) is of Sudakov type. Actually it is a product of the Sudakov form factors of the left lepton and of the left quark. As can be seen from Eqs. (3.43,3.44), $b_j + h_j = (6g^2 + g'^2(Y_l^2 + Y_q^2))/4$, it does not depend on j, i.e. is same for all invariant amplitudes,

$$S = \exp\left[-\frac{1}{8\pi^2}\left(\frac{3}{2}g^2 + \frac{Y_l^2 + Y_q^2}{4}g'^2\right)\frac{\eta'^2}{2}\right] . \tag{3.69}$$

It corresponds to DL contributions of soft virtual EW bosons and vanishes in the final expressions for the cross sections when bremsstrahlung of soft EW bosons are taken into account. Assuming this to be done we can omit such Sudakov factors.

Until now we have discussed the annihilation $l\bar{l} \to q\bar{q}$ for the case when the both initial and final particles were left, i.e. the spinors in Eq. (3.16) were actually $[(1 + \gamma_5)/2]u$. It is clear that applying the same reasoning it is easy to construct IREE for amplitudes in t and u -kinematics with right fermions. Solutions to such IREE can be presented in the same form of Eq. (3.68) with $j = RR$ for both right leptons and quarks, and $j = LR$ when the initial leptons are left whereas the final quarks are right, or $j = RL$ vice versa, with:

$$\begin{aligned}
a_{RR} &= \frac{g'^2 Y_l Y_q}{4} , & \lambda_{RR} &= \sqrt{\frac{b_{RR}}{8\pi^2}} , & b_{RR} &= \frac{g'^2(Y_l \mp Y_q)^2}{4} , & h_{RR} &= \pm\frac{g'^2 Y_l Y_q}{2} , \\
a_{LR} &= \frac{g'^2 Y_l Y_q}{4} , & \lambda_{LR} &= \sqrt{\frac{b_{LR}}{8\pi^2}} , & b_{LR} &= \frac{3g^2 + g'^2(Y_l \mp Y_q)^2}{4} , & h_{LR} &= \pm\frac{g'^2 Y_l Y_q}{2} ,
\end{aligned} \tag{3.70}$$

where $\mp$ signs in b and $\pm$ signs in h correspond to t and u - kinematics respectively. It is worthwhile to remind here that in the numerical estimations when using Eq. (3.70)) one has to substitute for Y_l, Y_q for right and left fermions the correct EW hypercharges: $Y = 2Q$ for right fermions and $Y = 2(Q - T_3)$ for left fermions. The same formulae for the invariant amplitude $A_{LR}^{(+)}$ in the collinear u -kinematics, with $\chi = 0$, can be also obtained from results of Ref. [19].

3.3 Invariant amplitudes for the annihilation processes with two cut-offs

Let us consider again the general process where the lepton $l^k(p_1)$ and its anti-particle $\bar{l}_i(-p_2)$ annihilate into a quark or a lepton $q^{k'}(p'_1)$ and its anti-particle $\bar{q}_{i'}(-p'_2)$ (see Fig. 3.1):

$$l^k(p_1)\bar{l}_i(-p_2) \to q^{k'}(p'_1)\bar{q}_{i'}(-p'_2) . \tag{3.71}$$

Let us remind that the scattering amplitude A for the annihilation can be written as in eq. 3.6, where the $SU(2)$ matrix amplitude $A_{k'k}^{ii'}$ has to be calculated. As was done in the previous case it is possible to represent $A_{k'k}^{ii'}$ in the following form:

$$A_{k'k}^{ii'} = \frac{\bar{u}(-p'_2)\gamma_\mu u(p'_1)\bar{u}(-p_2)\gamma^\mu u(p_1)}{s}\Big[(P_j)_{kk'}^{ii'}A_j + (P_{j+1})_{kk'}^{ii'}A_{j+1}\Big] , \qquad (3.72)$$

where $j = 1$ for the t-kinematics and $j = 3$ for the u-kinematics.

In order to calculate the amplitudes A_j to all orders in the electroweak couplings in the DLA, we construct and solve some infrared evolution equations (IREE). These equations describe the evolution of A_j, $(j = 1, 2, 3, 4)$ with respect to an infrared cut-off. We now introduce two such cut-offs, μ and M. We presume that $M \approx M_Z \approx M_W$ and use this cut-off to regulate the DL contributions involving soft (almost on-shell) virtual W, Z -bosons. In order to regulate the IR divergences arising from soft photons we use the cut-off μ and we assume that $\mu \approx m_q \ll M$ where m_q is the maximal quark mass involved. Both cut-offs are introduced in the transverse momentum space (with respect to the plane formed by momenta of the initial leptons) so that the transverse momenta k_i of virtual photons obey

$$k_{i\perp} > \mu , \qquad (3.73)$$

while the momenta k_i of virtual W, Z -bosons obey

$$k_{i\perp} > M . \qquad (3.74)$$

Let us first consider A_j in the collinear kinematics where, in the cm frame, the produced quarks or leptons move very close to the e^+e^- -beams. In order to fix such kinematics, we implement Eq. (3.7) by the further restriction on t:

$$s \sim -u \gg M^2 \gg \mu^2 \geq -t \qquad (3.75)$$

and similarly for Eq. (3.8) by

$$s \sim -t \gg M^2 \gg \mu^2 \geq -u . \qquad (3.76)$$

Basically in DLA, the invariant amplitudes A_j depend on s, u and t through logarithms. Under the restriction imposed by Eqs. (3.75, 3.76) then all A_j depend only on logarithms of s, M^2, μ^2 in the collinear kinematics. It is convenient to represent A_j in the following form:

$$A_j(s, \mu^2, M^2) = A_j^{(QED)}(s, \mu^2) + A'_j(s, \mu^2, M^2) , \qquad (3.77)$$

where $A_j^{(QED)}(s, \mu^2)$ accounts for QED DL contributions only, i.e. the contributions of Feynman graphs without virtual W, Z bosons. To calculate $A_j^{(QED)}(s, \mu^2)$ we use the cut-off μ, therefore the amplitudes $A_j^{(QED)}$ do not depend on M. In contrast, the amplitudes $A'_j(s, \mu^2, M^2)$ depend

on both cut-offs. These amplitudes account for DL contributions of the Feynman graphs, with one or more W, Z propagators. By technical reasons, it is convenient to introduce two auxiliary amplitudes. The first one, $\tilde{A}_j^{(QED)}(s, M^2)$, is the same QED amplitude but with a cut-off M. The second auxiliary amplitude, $\tilde{A}_j(s, M^2)$, calculated in the previous section, accounts for all electroweak DL contributions and the cut-off M is used to regulate both the virtual photons and the weak bosons infrared divergences. Beyond the Born approximation, the invariant amplitudes we have introduced depend on logarithms, the arguments of which can be chosen as in the following parametrization:

$$
\begin{aligned}
A_j^{(QED)} &= A_j^{(QED)}(s, \mu^2) = A_j^{(QED)}(s/\mu^2), & (3.78) \\
\tilde{A}_j^{(QED)} &= \tilde{A}_j^{(QED)}(s, M^2) = \tilde{A}_j^{(QED)}(s/M^2), \\
\tilde{A}_j &= \tilde{A}_j(s, M^2) = \tilde{A}_j(s/M^2), \\
A'_j &= A'_j(s, \mu^2, M^2) = A'_j(s/M^2, \varphi) ,
\end{aligned}
$$

with

$$
\varphi \equiv \ln(M^2/\mu^2) . \qquad (3.79)
$$

Our aim is to calculate the amplitudes A'_j, whereas the amplitudes $A_j^{(QED)}, \tilde{A}_j^{(QED)}$ and $\tilde{A}_j(s/M^2)$ where calculated in the previous section. In order to define amplitudes $A'_j, \tilde{A}_j(s, M^2)$, we will follow the same procedure used in the previous section. We rewrite them using the projection operators of Eqs. (3.11, 3.13). The use of these operators is based on the fact that the $SU(2) \times U(1)$ symmetry for the electroweak scattering amplitudes takes place at energies much higher than the weak mass scale M. On the contrary, the QED amplitudes $A_j^{(QED)}$ and $\tilde{A}_j^{(QED)}$ are not $SU(2)$ invariant at any energy. Nevertheless, it is convenient to introduce "the QED invariant amplitudes" $A_j^{(QED)}, \tilde{A}_j^{(QED)}$ by explicit calculation of the forward and backward QED scattering amplitudes. Then inverting Eq. (3.19), we construct the amplitudes $A_j^{(QED)}$ for e^+e^--annihilation into quarks:

$$
\begin{aligned}
A_1^{(QED)} &= 2A_F^{(QED)}(e^+e^- \to d\bar{d}) - A_B^{(QED)}(e^+e^- \to u\bar{u}), & (3.80) \\
A_2^{(QED)} &= A_B^{(QED)}(e^+e^- \to u\bar{u}), \\
A_3^{(QED)} &= 2A_F^{(QED)}(e^+e^- \to u\bar{u}) - A_B^{(QED)}(e^+e^- \to d\bar{d}), \\
A_4^{(QED)} &= A_B^{(QED)}(e^+e^- \to d\bar{d})
\end{aligned}
$$

and inverting Eq. (3.20) allows us to obtain $A_j^{(QED)}$ for e^+e^-- annihilation into leptons:

$$
\begin{aligned}
A_1^{(QED)} &= 2A_F^{(QED)}(e^+e^- \to \mu^+\mu^-), & (3.81) \\
A_2^{(QED)} &= 0, \\
A_3^{(QED)} &= -A_4^{(QED)} = A_B^{(QED)}(e^+e^- \to \mu^+\mu^-).
\end{aligned}
$$

3.3.1 Evolution equations for amplitudes A_j in the collinear kinematics

The IREE with two cut-offs for the electroweak amplitudes in the hard kinematics (3.1) were obtained in Ref. [19]. In the present section we construct the IREE for the $2 \to 2$ - electroweak amplitudes in the Regge kinematics. According to Eqs. (3.73, 3.74), we use two different cut-offs for the virtual photons and for the weak bosons. The amplitude A_j is in the lhs of such an equation. The rhs contains several terms. In the first place, there is the Born amplitude B_j. In order to obtain the other terms in the rhs, we use the Gribov bremsstrahlung theorem that states that the DL contributions of virtual particles with minimal transverse momenta ($\equiv k_\perp$) can be factorized. Furthermore, this $k_\perp$ acts as a new cut-off for the other virtual momenta. The virtual particle with $k_\perp$ (we call such a particle the softest one) can be either an electroweak bosons or a fermion. Let us suppose first that the softest particle is an electroweak boson. In this case, in the Feynman gauge, DL contributions come from the graphs where the softest propagator is attached to the external lines in every possible way whereas $k_\perp$ acts as a new cut-off for the blobs as shown in Fig. 3.4. When the softest electroweak boson is a photon,
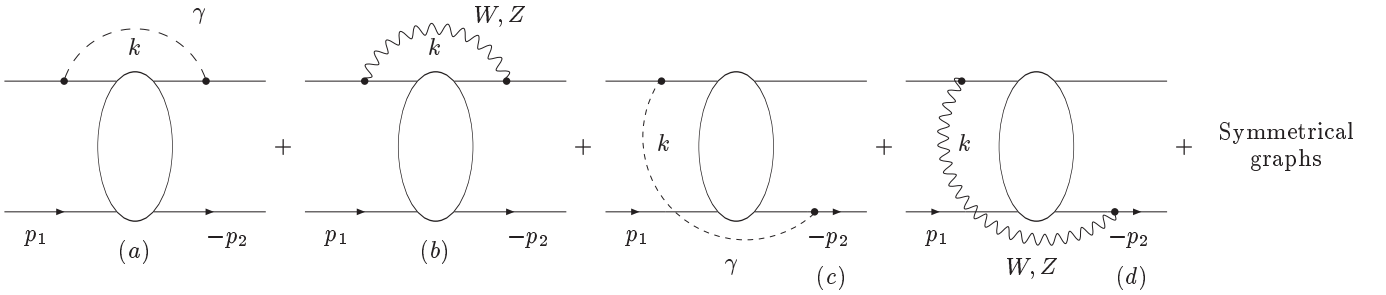
Figure 3.4: Softest boson contributions to IREE to A_j.

the integration region over $k_\perp$ is $\mu^2 \ll k_\perp^2 \ll s$ and its contribution, G_j^γ, to the rhs of the IREE is:

$$G_j^{(\gamma)} = -\frac{1}{8\pi^2} b_j^{(\gamma)} \ \left(\ \int_{\mu^2}^{s} \frac{dk_\perp^2}{k_\perp^2} \ln(s/k_\perp^2) A_j^{(QED)}(s, k_\perp^2) + \right. \tag{3.82}$$

$$\int_{\mu^2}^{M^2} \frac{dk_\perp^2}{k_\perp^2} \ln(s/k_\perp^2) A'_j(s, k_\perp^2, M^2) +$$

$$\left. \int_{M^2}^{s} \frac{dk_\perp^2}{k_\perp^2} \ln(s/k_\perp^2) A'_j(s, k_\perp^2, k_\perp^2) \right) ,$$

where

$$b_1^{(\gamma)} \ = \ g^2 \sin^2 \theta_W \frac{(Y_2 - Y_1)^2}{4}, \tag{3.83}$$

$$b_2^{(\gamma)} = g^2 \sin^2 \theta_W \left[\frac{1}{6} + \frac{(Y_2 - Y_1)^2}{4} \right] ,$$

$$b_3^{(\gamma)} = g^2 \sin^2 \theta_W \frac{(Y_2 + Y_1)^2}{4} ,$$

$$b_4^{(\gamma)} = g^2 \sin^2 \theta_W \left[\frac{1}{6} + \frac{(Y_2 + Y_1)^2}{4} \right] .$$

As in previous sections we have used the standard notations in Eq. (3.83): g, g' are the Standard Model couplings, Y_1 (Y_2) is the hypercharge of the initial (final) fermions and θ_W is the Weinberg angle. The logarithmic factors in the integrands of Eq. (3.82) correspond to the integration in the longitudinal momentum space. The amplitude A' in the last integral of Eq. (3.82) does not depend on μ because $k_\perp^2 > M^2$. Therefore it can be expressed in terms of $\tilde{A}_j(s, k_\perp^2)$ and $\tilde{A}_j^{(QED)}(s, k_\perp^2)$:

$$A'_j(s, k_\perp^2, k_\perp^2) = \tilde{A}_j(s, k_\perp^2) - \tilde{A}_j^{(QED)}(s, k_\perp^2) . \tag{3.84}$$

When the softest boson is either a Z or a W, its DL contribution can be factorized in the region $M^2 \ll k_\perp^2 \ll s$. This yields:

$$G_j^{(WZ)} = -\frac{1}{8\pi^2} b_j^{(WZ)} \int_{M^2}^s \frac{dk_\perp^2}{k_\perp^2} \ln(s/k_\perp^2) \tilde{A}_j(s/k_\perp^2) , \tag{3.85}$$

with

$$b_j^{(WZ)} = b_j - b_j^\gamma \tag{3.86}$$

and the factors b_j can be taken from Eq. (3.43). In Eq. (3.85) we have used the fact that the W and the Z bosons cannot be the softest particles for the amplitudes $A_j^{(QED)}$ since the integrations over the softest transverse momenta in $A_j^{(QED)}$ can go down to μ, by definition. The sum of Eqs. (3.82) and (3.85) , G_j can be written in the more convenient way:

$$
\begin{aligned}
G_j(s, \mu^2, M^2) &= G_j^{(\gamma)}(s, \mu^2, M^2) + G_j^{(WZ)}(s, M^2) \tag{3.87} \\
&= G_j^{(QED)}(s, \mu^2) - \tilde{G}_j^{(QED)}(s, M^2) + \tilde{G}_j(s, M^2) + G'_j(s, \mu^2, M^2) ,
\end{aligned}
$$

where

$$
\begin{aligned}
G_j^{(QED)} &= -\frac{1}{8\pi^2} b_j^{(\gamma)} \int_{\mu^2}^s \frac{dk_\perp^2}{k_\perp^2} \ln(s/k_\perp^2) A_j^{(QED)}(s/k_\perp^2) , \tag{3.88} \\
\tilde{G}_j^{(QED)} &= -\frac{1}{8\pi^2} b_j^{(\gamma)} \int_{M^2}^s \frac{dk_\perp^2}{k_\perp^2} \ln(s/k_\perp^2) \tilde{A}_j^{(QED)}(s/k_\perp^2) , \\
\tilde{G}_j &= -\frac{1}{8\pi^2} b_j \int_{M^2}^s \frac{dk_\perp^2}{k_\perp^2} \ln(s/k_\perp^2) \tilde{A}_j(s/k_\perp^2) , \\
G'_j &= -\frac{1}{8\pi^2} b_j^{(\gamma)} \int_{\mu^2}^{M^2} \frac{dk_\perp^2}{k_\perp^2} \ln(s/k_\perp^2) A'_j(s/k_\perp^2, M^2/k_\perp^2) .
\end{aligned}
$$

Eqs. (3.87, 3.88) account for DL contributions when the softest particle is an electroweak boson. However, the softest particle can also be a virtual fermion. In this case, DL contributions from the integration over the momentum k of the softest fermion arise from the diagram shown in Fig. 3.5 where the amplitudes A_j are factorized into two on-shell amplitudes in the t-channel. We denote this contribution by $Q_j(s, \mu^2, M^2)$. The analytic expression for Q_j is rather cumber-
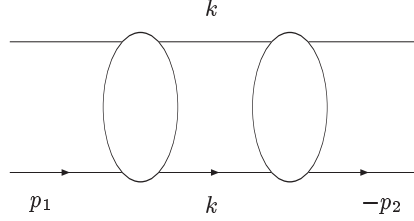
Figure 3.5: Softest fermion contribution.

some. However it looks simpler when the Sudakov parametrization is introduced for the softest quark momentum k (with p_1 and p_2 being the initial lepton momenta).

$$k = \alpha p_2 + \beta p_1 + k_\perp \ . \tag{3.89}$$

After simplifying the spin structure, see appendix A for details, we obtain

$$Q_j(s, \mu^2, M^2) = c_j \int_{\mu^2}^s dk_\perp^2 \int \frac{d\alpha}{\alpha} \frac{d\beta}{\beta} \frac{2k_\perp^2}{(s\alpha\beta - k_\perp^2)^2} A_j(s\alpha, k_\perp^2, M^2) A_j(s\beta, k_\perp^2, M^2) \ , \tag{3.90}$$

where

$$c_1 = c_2 = -c_3 = -c_4 = \frac{1}{8\pi^2} \ . \tag{3.91}$$

Similarly to Eq. (3.87), Q_j of Eq. (3.90) can be divided into the following simple contributions:

$$Q_j = Q_j^{(QED)} - \tilde{Q}_j^{(QED)} + \tilde{Q}_j + Q'_j \ , \tag{3.92}$$

where

$$Q_j^{(QED)}(s/\mu^2) = c_j \int_{\mu^2}^s dk_\perp^2 \int \frac{d\alpha}{\alpha} \frac{d\beta}{\beta} \frac{k_\perp^2}{(s\alpha\beta - k_\perp^2)^2} A_j^{(QED)}(s\alpha/k_\perp^2) A_j^{(QED)}(s\beta/k_\perp^2) \tag{3.93}$$

$$\tilde{Q}_j^{(QED)}(s/M^2) = c_j \int_{M^2}^s dk_\perp^2 \int \frac{d\alpha}{\alpha} \frac{d\beta}{\beta} \frac{k_\perp^2}{(s\alpha\beta - k_\perp^2)^2} \tilde{A}_j^{(QED)}(s\alpha/k_\perp^2) \tilde{A}_j^{(QED)}(s\beta/k_\perp^2) \tag{3.94}$$

$$\tilde{Q}_j(s/M^2) = c_j \int_{M^2}^s dk_\perp^2 \int \frac{d\alpha}{\alpha} \frac{d\beta}{\beta} \frac{k_\perp^2}{(s\alpha\beta - k_\perp^2)^2} \tilde{A}_j(s\alpha/k_\perp^2) \tilde{A}_j(s\beta/k_\perp^2) \ , \tag{3.95}$$

and

$$Q'_j(s/M^2, \varphi) = c_j \int_{\mu^2}^{M^2} dk_\perp^2 \int \frac{d\alpha}{\alpha} \frac{d\beta}{\beta} \frac{2k_\perp^2}{(s\alpha\beta - k_\perp^2)^2} \times \qquad (3.96)$$
$$\left(2A_j^{(QED)}(s\alpha/k_\perp^2) A'_j(s\beta/k_\perp^2, M^2/k_\perp^2) + \right.$$
$$\left. A'_j(s\alpha/k_\perp^2, M^2/k_\perp^2) A'_j(s\beta/k_\perp^2, M^2/k_\perp^2) \right) .$$

Now we are able to write the IREE for amplitudes A_j. The general form is given by:

$$A_j = B_j + G_j + Q_j . \qquad (3.97)$$

Then using Eqs. (3.87) and (3.92) we can rewrite it as

$$\begin{aligned} A'_j + A_j^{(QED)} = \ & B_j^{(QED)} - \tilde{B}_j^{(QED)} + \tilde{B}_j \\ & + G_j^{(QED)} - \tilde{G}_j^{(QED)} + \tilde{G}_j + G'_j \\ & + Q_j^{(QED)} - \tilde{Q}_j^{(QED)} + \tilde{Q}_j + Q'_j . \end{aligned} \qquad (3.98)$$

Let us notice that $A_j^{(QED)}(s/\mu^2)$ obeys the equation

$$A_j^{(QED)} = B_j^{(QED)} + G_j^{(QED)} + Q_j^{(QED)} \qquad (3.99)$$

and therefore $A_j^{(QED)}$ cancels out in Eq. (3.98). Also, the auxiliary amplitudes $\tilde{A}_j$ and $\tilde{A}_j^{(QED)}$, obey similar equations:

$$\begin{aligned} \tilde{A}_j^{(QED)} &= \tilde{B}_j^{(QED)} + \tilde{G}_j^{(QED)} + \tilde{G}_j^{(QED)}, \\ \tilde{A}_j &= \tilde{B}_j + \tilde{G}_j + \tilde{Q}_j . \end{aligned} \qquad (3.100)$$

The solutions to Eqs. (3.99, 3.100) are known. With the notations that we have used they can be taken from the previous section. Hence, we are left with the only unknown amplitude A'_j in Eq. (3.98). Using Eqs. (3.99, 3.100), we arrive at the IREE for A'_j, namely:

$$A'_j(s/M^2, \varphi) = \tilde{A}_j(s/M^2) - \tilde{A}_j^{(QED)}(s/M^2) + G'_j(s/M^2, \varphi) + Q'_j(s/M^2, \varphi) . \qquad (3.101)$$

In order to solve Eq. (3.101), it is more convenient to use the Sommerfeld-Watson transform. As long as one considers the positive signature amplitudes, this transform formally coincides with the Mellin transform. It is convenient to use different forms of this transform for the invariant amplitudes we consider:

$$A_j^{(QED)}(s/\mu^2) = \int_{-\imath\infty}^{\imath\infty} \frac{d\omega}{2\pi\imath} \left(\frac{s}{\mu^2} \right)^\omega f_j^{(0)}(\omega) , \qquad (3.102)$$

54

$$\tilde{A}_j^{(QED)}(s/M^2) = \int_{-\imath\infty}^{\imath\infty} \frac{d\omega}{2\pi\imath} \left(\frac{s}{M^2}\right)^{\omega} f_j^{(0)}(\omega) , \tag{3.103}$$

$$\tilde{A}_j(s/M^2) = \int_{-\imath\infty}^{\imath\infty} \frac{d\omega}{2\pi\imath} \left(\frac{s}{M^2}\right)^{\omega} f_j(\omega) , \tag{3.104}$$

$$A'_j(s/M^2, \varphi) = \int_{-\imath\infty}^{\imath\infty} \frac{d\omega}{2\pi\imath} \left(\frac{s}{M^2}\right)^{\omega} F_j(\omega, \varphi) . \tag{3.105}$$

Combining Eqs. (3.102) to (3.105) with Eq. (3.101) we arrive at the following equation for the Mellin amplitude $F_j(\omega, \varphi)$:

$$\begin{aligned}
\int_{-\imath\infty}^{\imath\infty} \frac{d\omega}{2\pi\imath} \left(\frac{s}{M^2}\right)^{\omega} F_j(\omega, \varphi) &= \int_{-\imath\infty}^{\imath\infty} \frac{d\omega}{2\pi\imath} \left(\frac{s}{M^2}\right)^{\omega} [f_j(\omega) - f_j^{(0)}(\omega)] \\
&\quad - \int_{-\imath\infty}^{\imath\infty} \frac{d\omega}{2\pi\imath} \left(\frac{s}{M^2}\right)^{\omega} \frac{1}{8\pi^2} b_j^{(\gamma)} \int_{\mu^2}^{M^2} \frac{dk_\perp^2}{k_\perp^2} \ln(s/k_\perp^2) F_j(\omega, \varphi') \\
&\quad + \int_{-\imath\infty}^{\imath\infty} \frac{d\omega}{2\pi\imath} \left(\frac{s}{M^2}\right)^{\omega} c_j \int_{\mu^2}^{M^2} \frac{dk_\perp^2}{k_\perp^2} \left(2f_j^{(0)}(\omega) F_j(\omega, \varphi') + F_j^2(\omega, \varphi')\right) ,
\end{aligned} \tag{3.106}$$

where $\varphi' = \ln(M^2/k_\perp^2)$. Differentiating Eq. (3.106) with respect to μ^2 leads to the homogeneous partial differential equation for the on-shell amplitude $F_j(\omega, \varphi)$:

$$\frac{\partial F_j}{\partial \varphi} = -\frac{1}{8\pi^2} b_j^{(\gamma)} \left(-\frac{\partial F_j}{\partial \omega} + \varphi F_j\right) + c_j \left(2f_j^{(0)}(\omega) F_j + F_j^2\right) , \tag{3.107}$$

where we have used the fact that $\ln(s/\mu^2)$, in Eq. (3.106), can be rewritten as $\ln(s/M^2) + \varphi$ and that $\ln(s/M^2)$ corresponds to $-\partial/\partial\omega$.

3.3.2 Solutions to the evolution equations for collinear kinematics

Let us consider first the particular case when $b_1^{(\gamma)} = 0$. It contributes to the forward leptonic, $e^+e^- \to \mu^+\mu^-$ annihilation and corresponds, in our notations, to the option

$$Y_1 = Y_2 = -1. \tag{3.108}$$

Let us notice that A_j with $j = 1$ contributes also to the forward $e^+e^- \to d\bar{d}$ annihilation, though here $Y_1 = -1, Y_2 = 1/3$ and therefore $b_1^{(\gamma)} \neq 0$. In order to avoid confusion between these cases, we change our notations, denoting $\Phi_1 \equiv F_1$, $\phi_1 \equiv f_1$ and $\phi_1^{(0)} \equiv f_1^{(0)}$ when $Y_1 = Y_2 = -1$. We will also use notations $\Phi_{2,3,4}$ instead of $F_{2,3,4}$ when we discuss the annihilation into leptons. Then we denote $c \equiv c_1 = 1/(8\pi^2)$. Therefore, the lepton amplitude $\Phi_1(\omega, \varphi)$ for the particular case (3.108) obeys the Riccati equation

$$\frac{\partial \Phi_1}{\partial \varphi} = c\left(2\phi_1^{(0)}(\omega)\Phi_1 + \Phi_1^2\right) , \tag{3.109}$$

with the general solution

$$\Phi_1 = \frac{e^{2c\phi_1^{(0)}\varphi}}{C\phi_1^{(0)} - e^{2c\phi_1^{(0)}\varphi}/2\phi_1^{(0)}} \ . \tag{3.110}$$

In order to specify C, we use the matching (see Eq. (3.106))

$$\Phi_1 = \phi_1(\omega) - \phi_1^{(0)}(\omega) \ , \tag{3.111}$$

when $\varphi = 0$, arriving immediately at

$$\Phi_1 = \frac{2\phi_1^{(0)}(\phi_1 - \phi_1^{(0)})e^{2c\phi_1^{(0)}\varphi}}{\phi_1^{(0)} + \phi_1 - (\phi_1 - \phi_1^{(0)})e^{2c\phi_1^{(0)}\varphi}} \tag{3.112}$$

and therefore to the following expression for the invariant amplitude $L_1 \equiv A_1$ when $Y_1 = Y_2 = -1$:

$$L_1 = \int_{-\imath\infty}^{\imath\infty} \frac{d\omega}{2\pi\imath} \left(\frac{s}{\mu^2}\right)^\omega \phi_1^{(0)}(\omega) + \int_{-\imath\infty}^{\imath\infty} \frac{d\omega}{2\pi\imath} \left(\frac{s}{M^2}\right)^\omega \frac{2\phi_1^{(0)}(\phi_1 - \phi_1^{(0)})e^{2c\phi_1^{(0)}\varphi}}{\phi_1^{(0)} + \phi_1 - (\phi_1 - \phi_1^{(0)})e^{2c\phi_1^{(0)}\varphi}} \ . \tag{3.113}$$

Obviously, when $\mu \to M$, Eqs. (3.113) converges to the same amplitude obtained with using only one cut-off. Indeed, substituting $\mu = M$ and $\varphi = 0$ leads to

$$L_1 = \int_{-\imath\infty}^{\imath\infty} \frac{d\omega}{2\pi\imath} \left(\frac{s}{M^2}\right)^\omega \phi_1(\omega) \ . \tag{3.114}$$

According to Eqs. (3.81, 3.102), the QED amplitude $\phi_1^{(0)}$ is easily expressed in terms of Mellin amplitude $\phi_F^{(0)}$ for the forward $e^+e^- \to \mu^+\mu^-$ annihilation:

$$\phi_1^{(0)} = 2\phi_F^{(0)} \ . \tag{3.115}$$

The expression for $\phi_F^{(0)}$ can be taken from Refs. [15], [19] and [20]:

$$\phi_F^{(0)} = 4\pi^2(\omega - \sqrt{\omega^2 - \chi_0^2}), \tag{3.116}$$

with

$$\chi_0^2 = 2\alpha/\pi. \tag{3.117}$$

On the other hand, the amplitudes ϕ_j were calculated in Eq. (3.50). In particular,

$$\phi_1 = 4\pi^2(\omega - \sqrt{\omega^2 - \chi^2}) \ , \tag{3.118}$$

where χ^2 is expressed through the electroweak couplings g and g':

$$\chi^2 = [3g^2 + g'^2]/(8\pi^2) \ . \tag{3.119}$$

56

Next, let us solve Eq. (3.107) for the general case of non-zero factor $b_j^{(\gamma)}$. Then, this equation describes the backward e^+e^- annihilation into a lepton pair (e.g. $\mu^+\mu^-$) and also the forward and backward annihilation into quarks. Eq. (3.107) looks simpler when ω, φ are replaced by new variables

$$x = \omega/\lambda_j, \quad y = \lambda_j \varphi , \tag{3.120}$$

with $\lambda_j = \sqrt{b_j^{(\gamma)}/(8\pi^2)}$. Changing to the new variables, we arrive again at the Riccati equation:

$$\frac{\partial F_j}{\partial \tau} = (\sigma - \tau)F_j - 2q_j f_j^{(0)} F_j - q_j F_j^2 , \tag{3.121}$$

where $\sigma = (x+y)/2$, $\tau = (x-y)/2$ and $q_j = c_j/\lambda_j$. The general solution to Eqs. (3.121) is

$$F_j = \frac{P_j(\sigma, \tau)}{C(\sigma) + q_j Q_j(\sigma, \tau)} , \tag{3.122}$$

where $C(\sigma)$ should be specified,

$$P_j(\sigma, \tau) = \exp\left(\sigma\tau - \tau^2/2 - 2q_j \int_\sigma^{\sigma+\tau} d\zeta f_j^{(0)}(\zeta)\right) \tag{3.123}$$

and

$$Q_j(\sigma, \tau) = \int_\sigma^{\sigma+\tau} d\zeta P_j(\sigma, \zeta) . \tag{3.124}$$

The QED amplitudes $f_j^{(0)}$ can be obtained from the known expressions for the backward, $f_B^{(0)}$ and forward $f_F^{(0)}$ QED scattering amplitudes:

$$f_B^{(0)}(x) = (4\pi\alpha e_q/p_B^{(0)})d\ln(e^{x^2/4}D_{p_B^{(0)}}(x))/dx , \tag{3.125}$$

where D_p are the Parabolic cylinder functions with $p_B^{(0)} = -2e_q/(1+e_q)^2$ and $e_q = 1$ for the annihilation into muons, $e_q = 1/3$ (2/3) for the annihilation into d (u)- quarks. Similarly, the QED forward scattering amplitudes for the annihilation into quarks are

$$f_F^{(0)}(x) = (4\pi\alpha e_q/p_F^{(0)})d\ln(e^{x^2/4}D_{p_F^{(0)}}(x))/dx , \tag{3.126}$$

with $p_B^{(0)} = 2e_q/(1-e_q)^2$. Let us stress that the forward amplitudes for the annihilation into leptons are given by Eq. (3.113). The amplitude $f_{F,B}^{(0)}$ was obtained first in Ref. [15] for the backward scattering in QED. Obviously, the only difference between the formulae for $f_j(x)$ and $f_j^{(0)}(x)$ is in the different factors a_j, p_j and λ_j. We can specify $C(\sigma)$, using the matching

$$F_j(\omega) = f_j(\omega) - f_j^{(0)}(\omega) , \tag{3.127}$$

when $\varphi = 0$. The invariant amplitudes f_j were calculated in Ref. [20]:

$$f_j(x) = \frac{a_j}{p_j} \frac{d \ln(e^{x^2/4} D_{p_j}(x))}{dx} = a_j \frac{D_{p_j-1}(x)}{D_{p_j}(x)} .$$ (3.128)

Using Eq. (3.127) we are led to

$$F_j = \frac{(f_j(x+y) - f_j^{(0)}(x+y))P(\sigma,\tau)}{P(\sigma,\sigma) - (f_j(x+y) - f_j^{(0)}(x+y))(Q(\sigma,\sigma) - Q(\sigma,\tau))}$$ (3.129)

and finally to

$$A_j(s/M^2, \varphi) = \int_{-\imath\infty}^{\imath\infty} \frac{d\omega}{2\pi\imath} \left(\frac{s}{\mu^2}\right)^\omega f_j^{(0)}(\omega) +$$ (3.130)

$$\int_{-\imath\infty}^{\imath\infty} \frac{d\omega}{2\pi\imath} \left(\frac{s}{M^2}\right)^\omega \frac{(f_j(x+y) - f_j^{(0)}(x+y))P_j(\sigma,\tau)}{P_j(\sigma,\sigma) - (f_j(x+y) - f_j^{(0)}(x+y))(Q_j(\sigma,\sigma) - Q_j(\sigma,\tau))} .$$

It is easy to check that when $\mu = M$, $A_j(s/M^2, \varphi)$ coincides with the amplitude $\tilde{A}_j(s, M^2)$ obtained with only one cut-off.

Eqs. (3.113, 3.130) describe all invariant amplitudes for e^+e^- -annihilation into a quark or a lepton pair in the collinear kinematics (3.75, 3.76).

3.4 Scattering amplitudes at large values of t and u

In this section we calculate the scattering amplitudes A when the restriction of Eqs. (3.75, 3.76) for the kinematical configurations (3.7, 3.8) are replaced by

$$s \gg M^2 \geq -t \gg \mu^2$$ (3.131)

and

$$s \gg M^2 \geq -u \gg \mu^2 .$$ (3.132)

In this kinematical regions it is more convenient to study the scattering amplitudes A directly, rather than using the invariant amplitudes A_j. In order to unify the discussion for both kinematics (3.131, 3.132), let us introduce

$$\kappa = -t ,$$ (3.133)

when (3.131) is considered and

$$\kappa = -u$$ (3.134)

for the other case (3.132). Using this notation, the same parametrization $A = A(s, \mu^2, M^2, \kappa)$ holds for both kinematics (3.131, 3.132). Let us discuss now the evolution equations for A. As

in the previous case, it is convenient to consider separately the purely QED part, $A^{(QED)}$ and the mixed part, A':

$$A(s, \kappa, \mu^2, M^2) = A^{(QED)}(s, \kappa, \mu^2) + A'(s, \kappa, \mu^2, M^2). \tag{3.135}$$

Generalizing Eq. (3.78), we can parametrize them as follows:

$$
\begin{aligned}
A^{(QED)}(s, \kappa, \mu^2) &= A^{(QED)}(s/\mu^2, \kappa/\mu^2), \\
A'(s, \kappa, \mu^2, M^2) &= A'(s/M^2, s/\mu^2, \kappa/\mu^2, M^2/\mu^2).
\end{aligned}
\tag{3.136}
$$

In order to construct the IREE for $A^{(QED)}$ and A', we should consider again all options for the softest virtual particles. The Born terms for the configurations (3.131) and (3.132) do not depend on μ^2 and vanish after differentiating on μ. The same is true for the softest quark contributions. Indeed, the softest fermion pair yields DL contributions in the integration region $k_\perp^2 \gg \kappa$, which is unrelated to μ. Hence, we are left with the only option for the softest particle to be an electroweak boson. The factorization region for this kinematics is

$$\mu^2 \ll k_\perp^2 \ll \kappa . \tag{3.137}$$

Obviously, only virtual photons can be factorized in this factorization region, which leads to a simple IREE:

$$
\begin{aligned}
\frac{\partial A^{(QED)}}{\partial \rho} + \frac{\partial A^{(QED)}}{\partial z} &= -\lambda(b^{(\gamma)}\rho + h^{(\gamma)}z)A^{(QED)}, \\
\frac{\partial A'}{\partial \rho} + \frac{\partial A'}{\partial z} + \frac{\partial A'}{\partial \varphi'} &= -\lambda(b^{(\gamma)}\rho + h^{(\gamma)}z)A'
\end{aligned}
\tag{3.138}
$$

where we have denoted $\rho = \ln(s/\mu^2)$, $z = \ln(\kappa/\mu^2)$, $\varphi' = \ln(\varphi) = \ln(M^2/\mu^2)$ and $\lambda = \alpha/2\pi$. The factors $b^{(\gamma)}$ and $h^{(\gamma)}$ are:

$$
\begin{aligned}
h^{(\gamma)} &= e_1 e'_1 + e_2 e'_2, \\
b^{(\gamma)} &= e_1 e_2 + e'_1 e'_2 - e_2 e'_1 - e_1 e'_2
\end{aligned}
\tag{3.139}
$$

for the case (3.133), and

$$
\begin{aligned}
h^{(\gamma)} &= -e_2 e'_1 + e_1 e'_2, \\
b^{(\gamma)} &= e_1 e_2 + e'_1 e'_2 + e_2 e'_2 + e_1 e'_1
\end{aligned}
\tag{3.140}
$$

for the other case (3.134).

The notations e_i, e'_i in Eqs. (3.139, 3.140) stand for the absolute values of the electric charges. They correspond to the notations of the external particle momenta introduced in Fig. 3.1. The terms proportional to $h^{(\gamma)}$ in Eq. (3.138) correspond to the Feynman graphs

59

where the softest photons propagate in the κ-channels. Let us notice that for any kinematics we consider it holds

$$b_j^{(\gamma)} + h_j^{(\gamma)} = (1/2)[e_1^2 + e_2^2 + e_1'^2 + e_2'^2] \tag{3.141}$$

due to the electric charge conservation.

In order to solve Eq. (3.138), we use the matching with the amplitude $\hat{A}(s, \mu^2, M^2)$ for the same process, however in the collinear kinematics:

$$\begin{aligned} A^{(QED)}(s, \mu^2, \kappa, M^2) &= \hat{A}^{(QED)}(s, \mu^2), \\ A'(s, \kappa, \mu^2, M^2) &= \hat{A}'(s, \mu^2, M^2) \,, \end{aligned} \tag{3.142}$$

when $\kappa = \mu^2$. The solution to Eq. (3.138) is

$$\begin{aligned} A^{(QED)} &= \psi^{(QED)}(\rho - z)e^{-\lambda b_j^{(\gamma)}\rho^2/2 - \lambda h_j^{(\gamma)}z^2/2}, \\ A' &= \psi'(\rho - z, \varphi' - z)e^{-\lambda b_j^{(\gamma)}\rho^2/2 - \lambda h_j^{(\gamma)}z^2/2}. \end{aligned} \tag{3.143}$$

Using the matching of Eq. (3.142) allows to specify ψ and $\psi^{(QED)}$. After that we obtain:

$$\begin{aligned} A^{(QED)} &= S'\hat{A}^{(QED)}(s/\kappa), \\ A' &= S'\hat{A}'(s/M^2, M^2/\kappa) \,, \end{aligned} \tag{3.144}$$

where

$$S' = e^{-\lambda b_j^{(\gamma)}\rho z + \lambda(b_j^{(\gamma)} - h_j^{(\gamma)})z^2/2} \,. \tag{3.145}$$

We did not change s/M^2 to s/κ in Eq. (3.144) because $M^2 \gg \kappa$. It is convenient to absorb the term $-\lambda b_j^{(\gamma)}\rho z$ into the amplitudes $\hat{A}^{(QED)}$ and $\hat{A}'$. Introducing, instead of ω, the new Mellin variable $l = \omega + \lambda b_j^{(\gamma)}z$ (see Ref. [20] for details), we rewrite Eq. (3.144) as follows (for the sake of simplicity we keep the same notations for these new amplitudes $\hat{A}^{(QED)}$ and $\hat{A}'$):

$$A^{(QED)} = S(\hat{A}^{(QED)}(s/\kappa) + \hat{A}'(s, \kappa, \mu^2, M^2)) \tag{3.146}$$

with S being the Sudakov form factor for the case under discussion. S includes the softest, infrared divergent DL contributions. When the photon infrared cut-off μ is assumed to be greater than the masses of the involved fermions, this form factor is:

$$S = \exp\left(-\frac{\lambda}{2}(b^{(\gamma)} + h^{(\gamma)})\ln^2(\kappa/\mu^2)\right) \,. \tag{3.147}$$

However, in the case of e^+e^- annihilation into quarks (muons), if the cut-off μ is chosen to be very small, less than the electron mass, m_e the exponent in Eq. (3.147) should be changed to:

$$S = \exp\left(-\frac{\lambda}{2}(b^{(\gamma)} + h^{(\gamma)})(\ln^2(\kappa/\mu^2) - \ln^2(m_e^2/\mu^2) - \ln^2(m^2/\mu^2)\right) \,, \tag{3.148}$$

where m is the mass of the produced quark or lepton (cf. Ref. [32]).

If $m > \mu > m_e$, the last term in the exponent of Eq. (3.148) is absent. The kinematics with larger values of κ, e.g. $s \gg \kappa \gg M^2$, can be studied similarly, although it is more convenient to use the invariant amplitudes $\hat{A}_j$. The result is

$$\hat{A}_j = S_j \tilde{A}_j(s/\kappa) \,, \tag{3.149}$$

where

$$S_j = \exp \ \Big[\ -\frac{\lambda}{2}\big((b_j^{(\gamma)} + h_j^{(\gamma)})(\ln^2(\kappa/\mu^2) - \ln^2(m_e^2/\mu^2)$$
$$- \ln^2(m^2/\mu^2) + (b_j - b_j^{(\gamma)} + h_j - h_j^{(\gamma)}) \ln^2(\kappa/M^2)\big)\Big] \tag{3.150}$$

and $\tilde{A}(s/M^2)$ is the scattering amplitude of the same process in the limit of collinear kinematics and using a single cut-off M. These amplitudes were defined in Sect. 2. The factors h_j given below were calculated in Ref [20]:

$$h_1 = g^2(3 + \tan^2\theta_W Y_1 Y_2)/2, \qquad h_2 = g^2(-1 + \tan^2\theta_W Y_1 Y_2)/2 \,, \tag{3.151}$$
$$h_3 = g^2(3 - \tan^2\theta_W Y_1 Y_2)/2, \qquad h_4 = g^2(-1 - \tan^2\theta_W Y_1 Y_2)/2 \,.$$

The form factors S, S_j include the soft DL contributions, with the cm energies of virtual particles ranging from μ^2 to κ. Due to gauge invariance, the sums $b_j^{(\gamma)} + h_j^{(\gamma)}$ and $b_j + h_j$ do not depend on j and S_j is actually the same for every invariant amplitude contributing to $A_{k'k}^{ii'}$ in the forward (backward) kinematics (see Ref. [20]). Obviously, in the case of the hard kinematics where (see Eq. (3.1)) $s \sim -u \sim -t$, i.e. $s \sim \kappa$, ladder graphs do not yield DL contributions. The easiest way to see this, is to notice that the factor $(s/\kappa)^\omega$ in the the Mellin integrals (3.104) for amplitudes $\tilde{A}_j$ does not depend on s in the hard kinematics, therefore all Mellin integrals do not depend on s. So, the only source of DL terms in this kinematics is given by the Sudakov form factor S_j given by Eq. (3.150). Therefore, we easily arrive at the known result

$$A_{k'k}^{ii'} = B_{k'k}^{ii'} S_j \,. \tag{3.152}$$

$B_{k'k}^{ii'}$ in Eq. (3.152) stands for the Born terms. The electroweak Sudakov form factor (3.150) with two infrared cut-offs was obtained in Ref. [19].

3.5 Forward e^+e^- annihilation into leptons

Equations (3.19, 3.20, 3.113) and (3.130) give the explicit expressions for the scattering amplitudes of e^+e^--annihilation into quarks and leptons in the collinear kinematics. These expressions resume the DL contributions to all orders in the electroweak couplings and operate with two infrared cut-offs. In order to estimate the impact of the two-cuts approach, we compare

these results to the formulae for the same scattering amplitudes obtained with one universal cut-off M. We focus on the particular case of the scattering amplitudes for the forward $e^+ e^-$ annihilation into leptons and restrict ourselves, for the sake of simplicity, to the collinear kinematics of Eq. (3.75). Other amplitudes, and other kinematics can be considered in a very similar way. Eqs. (3.20, 3.113) and (3.130) show that the scattering amplitude $L_F^{(\mu)}$ of the forward $e^+ e^-$ into $\mu^- \mu^+$ is

$$
\begin{aligned}
L_F^{(\mu)} &= \int_{-\imath\infty}^{\imath\infty} \frac{d\omega}{2\pi\imath} \left(\frac{s}{\mu^2}\right)^\omega \phi_F^{(0)}(\omega) \\
&+ \frac{1}{2} \int_{-\imath\infty}^{\imath\infty} \frac{d\omega}{2\pi\imath} \left(\frac{s}{M^2}\right)^\omega \frac{4\phi_F^{(0)}(\phi_1 - 2\phi_F^{(0)})e^{4c\phi_F^{(0)}\varphi}}{2\phi_F^{(0)} + \phi_1 - (\phi_1 - 2\phi_F^{(0)})e^{4c\phi_F^{(0)}\varphi}} \\
&+ \frac{1}{2} \int_{-\imath\infty}^{\imath\infty} \frac{d\omega}{2\pi\imath} \left(\frac{s}{M^2}\right)^\omega \frac{\phi_2(x+y)P_2(\sigma,\tau)}{P_2(\sigma,\sigma) - \phi_2(x+y)[Q_2(\sigma,\sigma) - Q_2(\sigma,\tau)]} \ .
\end{aligned}
\tag{3.153}
$$

The first integral in this equation accounts for purely QED double-logarithmic contributions and depends on the QED cut-off μ whereas the next integrals sum up mixed QED and weak double-logarithmic terms and depend on both μ and M. The first and the second integrals in Eq. (3.153) grow with s whilst the last integral rapidly falls when s increases. The point is that this term actually is the amplitude for the backward annihilation into muon neutrinos. It is easy to check that the QED amplitudes $\phi_F^{(0)}$ vanish when $\mu = M$ and the total integrand contains only $[\phi_1(\omega) + \phi_2(\omega)]/2$. In contrast to Eq. (3.153), purely QED contributions are absent in formulae for $e^+ e^-$ annihilation into neutrinos. For example, the scattering amplitude $L_F^{(\nu)}$ of the forward $e^+ e^- \to \nu_\mu \bar{\nu}_\mu$ -annihilation in the collinear kinematics is

$$
L_F^{(\nu)} = \frac{1}{2} \int_{-\imath\infty}^{\imath\infty} \frac{d\omega}{2\pi\imath} \left(\frac{s}{M^2}\right)^\omega \left[\frac{\phi_3(x+y)P_3(\sigma,\tau)}{P_3(\sigma,\sigma) - \phi_3(x+y)[Q_3(\sigma,\sigma) - Q_3(\sigma,\tau)]} + \frac{\phi_4(x+y)P_4(\sigma,\tau)}{P_4(\sigma,\sigma) - \phi_4(x+y)[Q_4(\sigma,\sigma) - Q_4(\sigma,\tau)]} \right] \ .
\tag{3.154}
$$

Similarly to Eq. (3.153), the integrand in Eq. (3.154) is equal to $[\phi_3(\omega) + \phi_4(\omega)]/2$ when $\mu = M$. Although formally Eqs. (3.153, 3.154) correspond to the exclusive $e^+ e^-$ annihilation into two leptons, actually these expressions also describe the inclusive processes when the emission of photons with cm energies $< \mu$ is accounted for.

Let us study the impact of our two-cut-offs approach on the scattering amplitude $L_F^{(\mu)}$ of Eq. (3.153). As the last integral in Eq. (3.153) rapidly falls with s, it is neglected in our estimates and we consider contributions of the first and the second integrals only. First we compare the one-loop and two-loop contributions. Such contributions can be easily obtained expanding the rhs of Eq. (3.153) into a perturbative series. From Eqs. (3.116) and (3.118) one obtains that

$$
\phi_F^{(0)} \approx 2\pi^2 \left(\frac{\chi_0^2}{\omega} + \frac{1}{4}\frac{\chi_0^4}{\omega^3} + \frac{1}{8}\frac{\chi_0^6}{\omega^5} + \ldots\right) ,
\tag{3.155}
$$

$$\phi_1 \approx 2\pi^2\Big(\frac{\chi^2}{\omega} + \frac{1}{4}\frac{\chi^4}{\omega^3} + \frac{1}{8}\frac{\chi^6}{\omega^5} + ...\Big),$$

with χ_0, χ defined in Eqs. (3.117, 3.119). Substituting these series into the first and the second integrals of Eq. (3.153) and performing the integrations over ω, we arrive at

$$L^{(1)} = \gamma_1^{(1)} \ln^2(s/\mu^2) + \gamma_2^{(1)} \ln(s/\mu^2)\ln(s/M^2) + \gamma_3^{(1)} \ln^2(s/M^2) \tag{3.156}$$

for the first-loop contribution to $L_F^{(\mu)}$ and

$$\begin{aligned} L^{(2)} &= \gamma_1^{(2)} \ln^4(s/\mu^2) + \gamma_2^{(2)} \ln^3(s/\mu^2)\ln(s/M^2) + \\ &\quad \gamma_3^{(2)} \ln^2(s/\mu^2)\ln^2(s/M^2) + \gamma_4^{(2)} \ln(s/\mu^2)\ln^3(s/M^2) + \gamma_5^{(2)} \ln^4(s/M^2) \end{aligned} \tag{3.157}$$

for the second-loop contribution. The coefficients $\gamma_i^{(k)}$ are given below:

$$\begin{aligned} \gamma_1^{(1)} &= \frac{\pi^2 \chi_0{}^4}{4}, \tag{3.158}\\ \gamma_2^{(1)} &= \frac{\pi^2 (\chi^4 - 4\chi_0{}^4)}{4}, \\ \gamma_3^{(1)} &= -\frac{\pi^2 (\chi^4 - 6\chi_0{}^4)}{8}, \\ \gamma_1^{(2)} &= \frac{\pi^2 \chi_0{}^6}{96}, \\ \gamma_2^{(2)} &= 0, \\ \gamma_3^{(2)} &= \frac{\pi^2 \chi^2 (\chi^4 - 4\chi_0{}^4)}{32}, \\ \gamma_4^{(2)} &= -\frac{\pi^2 (\chi^6 - 6\chi^2\chi_0{}^4 + 2\chi_0{}^6)}{24}, \\ \gamma_5^{(2)} &= \frac{\pi^2 (3\chi^6 - 24\chi^2\chi_0{}^4 + 14\chi_0{}^6)}{192}. \end{aligned}$$

Let us compare the above results with those obtained with one universal cut-off M only. We introduce the notation $\tilde{L}(s/M^2)$ for amplitude $L_F^{(\mu)}$ when one cut-off M is used. The ratio $R^1 = L^1(s, \mu, M)/\tilde{L}^{(1)}(s, M)$ of the first loop contributions to the amplitudes $L_F^{(\mu)}$ and $\tilde{L}$ is

$$R^{(1)} = \frac{L^{(1)}}{\tilde{\gamma}^1 \ln^2(s/M^2)} \tag{3.159}$$

where $\tilde{\gamma}^1 = \pi^2 \chi^4/8$. Similarly the ratio $R^{(2)}$ of the second-loop contributions is

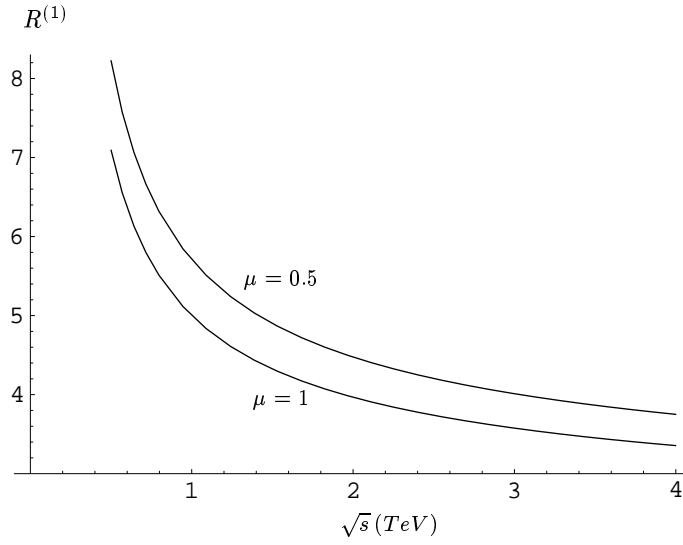$$R^{(2)} = \frac{L^{(2)}}{\tilde{\gamma}^2 \ln^4(s/M^2)}, \tag{3.160}$$

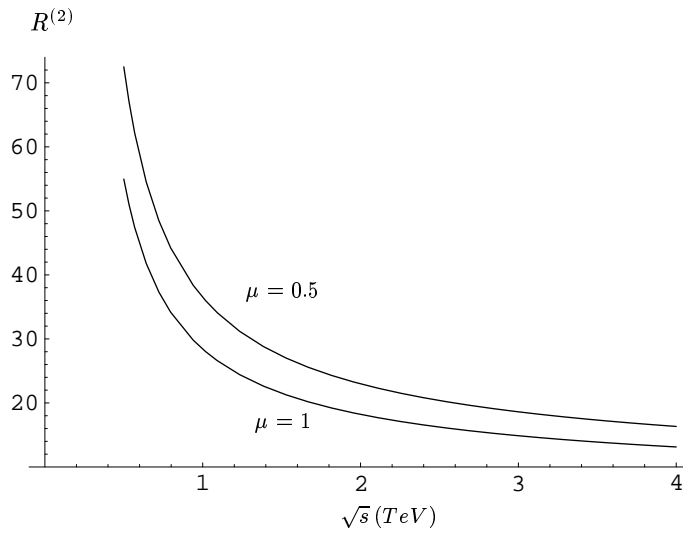Figure 3.6: Dependence of $R^{(1)}$ on s for different values of μ(GeV).

Figure 3.7: Dependence of $R^{(2)}$ on s for different values of μ(GeV).

where $\tilde{\gamma}^2 = \pi^2 \chi^6 / 64$. The comparison between figs. 3.6 and 3.7 show explicitly that the difference between the one cut-off amplitude $\tilde{L}$ and the two cut-off amplitude $L_F^{(\mu)}$ grows with the order of the perturbative expansion, though rapidly decreasing with s. We can expect therefore that a sizable difference between $L_F^{(\mu)}$ and $\tilde{L}$ when all orders of the perturbative series are resumed.

3.6 Asymptotics of the forward scattering amplitude for e^+e^- annihilation into $\mu^+\mu^-$

In order to estimate the effect of higher order DL contributions on the difference between the one-cut-off and two-cut-off amplitudes, it is convenient to compare their high-energy asymptotics. For the sake of simplicity, we present below such asymptotical estimates for the amplitude L_F^μ of the forward e^+e^- annihilation into $\mu^+\mu^-$ in the collinear kinematics (3.75). Calculations for the other amplitudes (3.130) can be done in a similar way. As well-known, the leading contribution to the asymptotic behavior is $L_F^\mu \sim s^{\omega_0}$, with ω_0 being the rightmost singularity of the amplitude L_F^μ. This amplitude contains the amplitudes $\phi_{1,2}^{(0)}$ and $\phi_{1,2}$ and therefore also their singularities. Eqs. (3.118, 3.116) show that the singularities of both ϕ_1 and $\phi_1^{(0)}$ are the square root branching points. The rightmost singularity of $\phi_1^{(0)}$ is χ_0 and the rightmost singularity of ϕ_1 is χ. They are defined in Eqs. (3.117, 3.119). Obviously,

$$
\begin{aligned}
\phi_1^{(0)}(\chi_0) &= 4\pi^2 \chi_0, \\
\phi_1^{(0)}(\chi) &= 4\pi^2 \left(\chi - \sqrt{\chi^2 - \chi_0^2}\right) \equiv 4\pi^2 (\chi - \chi'), \\
\phi_1(\chi) &= 4\pi^2 \chi .
\end{aligned}
\tag{3.161}
$$

Combining Eqs. (3.153) and (3.161) and neglecting the last integral in Eq. (3.153), we obtain the asymptotic formula for the forward leptonic invariant amplitude A:

$$
L_F^\mu \sim 4\pi^2 \left(\frac{s}{\mu^2}\right)^{\chi_0} \chi_0 + 4\pi^2 \left(\frac{s}{M^2}\right)^{\chi} \frac{2(\chi - \chi')(2\chi' - \chi)e^{2\varphi(\chi - \chi')}}{3\chi - 2\chi' - (2\chi' - \chi)e^{2\varphi(\chi - \chi')}}.
\tag{3.162}
$$

The first term in Eq. (3.162) represents the asymptotic contribution of the QED Feynman graphs, the second term the mixing of QED and weak DL contributions. On the other hand, when the one-cut-off approach is used, the new amplitude $\tilde{L}_F^\mu$ asymptotically behaves as:

$$
\tilde{L}_F^\mu \sim 4\pi^2 \frac{\chi}{2} \left(\frac{s}{M^2}\right)^{\chi} .
\tag{3.163}
$$

Then defining $Z(s, \varphi)$, as:

$$
L_F^\mu = \tilde{L}_F^\mu (1 + Z(s, \varphi)) ,
\tag{3.164}
$$

it is easy to see that

$$Z(s, \varphi) \sim \left(\frac{s}{M^2}\right)^{-\chi+\chi_0} \frac{2\chi_0}{\chi} e^{\varphi\chi_0} - 1 + \frac{4(\chi - \chi')(2\chi' - \chi)e^{2\varphi(\chi-\chi')}}{\chi[3\chi - 2\chi' - (2\chi' - \chi)e^{2\varphi(\chi-\chi')}]} \ . \tag{3.165}$$

As $\chi_0 < \chi$, $Z(s)$ falls when s grows. So, the one-cut-off and the two-cut-off approach lead to the same asymptotics, although at very high energies, say $\sqrt{s} \geq 10^6$ TeV the value of Z is 0.3. At lower energies, accounting for Z, the amplitude $L_F^{(\mu)}$ is increased by a factor of order 2. On the other hand, Z strongly depends on the ratio M/μ, which, of course, is related to the actual phenomenological conditions. To illustrate this dependence, we take $M = 100$ GeV and choose different values for μ, ranging from 0.1 to 1 GeV. Then in Fig. 3.8 we plot $Z(s, \mu)$ for $\mu = 1$ GeV and $\mu = 0.5$ GeV. This shows that the variation is approximately 1.5 at energies in the interval from 0.5 to 5 TeV.
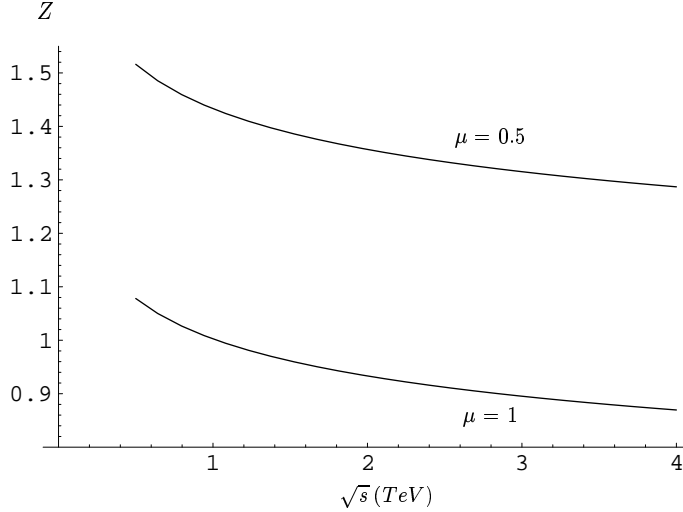
Figure 3.8: Dependence of Z on s for different values of μ (GeV).

It is also interesting to estimate the difference between the purely QED asymptotics of L_F^μ (the first term in the rhs of Eq. (3.162)) and the full electroweak asymptotics. To this aim, we introduce Δ_{EW}:

$$L_F^{(\mu)} = (L_F^{(\mu)})^{(QED)}(1 + \Delta_{EW}) \ . \tag{3.166}$$

From Eq. (3.162) we immediately get the following asymptotic behavior for Δ_{EW}:

$$\Delta_{EW} \sim \left(\frac{s}{M^2}\right)^{\chi-\chi_0} \frac{2(\chi - \chi')(2\chi' - \chi)e^{2\varphi(\chi-\chi')}}{3\chi - 2\chi' - (2\chi' - \chi)e^{2\varphi(\chi-\chi')}} \tag{3.167}$$

As $\chi > \chi_0$, Δ_{EW} grows with s, as shown in Fig. 3.9. Therefore the weak interactions contribution is approximately of the same size of the QED contribution, and their ratio rapidly increases as μ decreases.
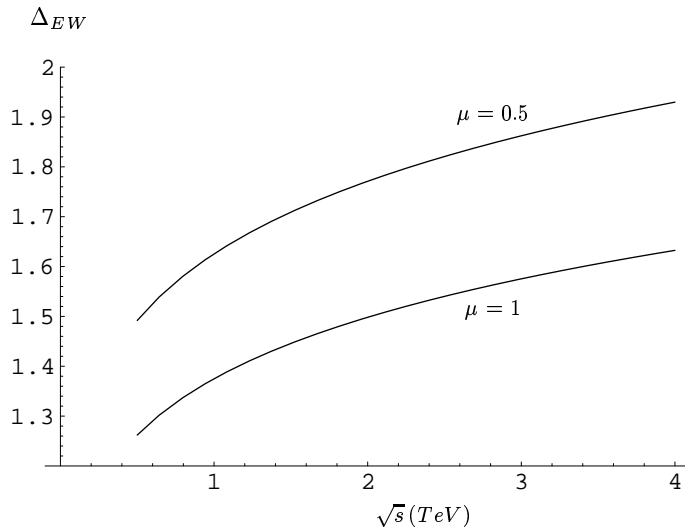
Figure 3.9: Dependence of Δ_{EW} on s for different values of μ (GeV).

3.7   Summary and Outlook

Next future linear e^+e^- colliders will be operating in a energy domain which is much higher than the electroweak bosons masses, so that the full knowledge of the scattering amplitudes for e^+e^- annihilation into fermion pairs will be needed. In the present work we have considered the high-energy non-radiative scattering amplitudes for e^+e^- annihilation into leptons and quarks in the Regge kinematics (3.7) and (3.8). We have calculated these amplitudes in the DLA, using a cut-off M, with $M \geq M_Z \approx M_W$, for the transverse momenta of virtual weak bosons and an infrared cut-off μ for regulating DL contributions of virtual soft photons. We have obtained explicit expressions (3.112, 3.130) for these amplitudes in the collinear kinematics (3.75, 3.76) and Eqs. (3.146, 3.149) for the configuration where all Mandelstam variables are large. The basic structure of the expressions in the limit of collinear kinematics is quite clear. They consist of two terms: the first term presents the purely QED contribution, i.e. the one with virtual photon exchanges only, whereas the next term describe the combined effect of all electroweak boson exchanges. Obviously, in the limit when the cut-off $\mu \to M$, our expressions for the scattering amplitude converge to the much simpler expressions obtained in Ref [20] with one universal cut-off for all electroweak bosons. In order to calculate the electroweak scattering amplitudes, we derived and solved infrared equations for the evolution of the amplitudes with respect to the cut-offs M and μ.

In order to illustrate the difference between the two methods, we have considered in more detail the scattering amplitude $L_F^{(\mu)}$ of the forward e^+e^- annihilation into $\mu^+\mu^-$ and studied the ratios of the results obtained in the two approaches, first in one- and two-loop approximation and then to all orders to DLA. The ratios of the first- and second-loop DL results are plotted

in Figs. 3.6 and 3.7. The total effect of higher-loop contributions is estimated comparing the asymptotic behaviors of the amplitudes. This is shown in Fig. 3.8. The effect of all electroweak DL corrections compared the QED ones is plotted in Fig. 3.9. It follows that accounting for all electroweak radiative corrections $L_F^{(\mu)}$ increases by up to factor of 2.6 at $\sqrt{s} \leq 1$ TeV, depending on the value of M/μ. In formulae for the $2 \to 2$ - electroweak cross sections, one can put $M = M_W \approx M_Z$ whereas the value of μ is quite arbitrary. However it vanishes, when these expressions are combined with cross sections of the radiative $2 \to 2 + X$ processes.

In the present chapter we have considered the most complex case of both the initial electron and the final quark or lepton being heft-handed (and their antiparticles right-handed). Studying other combinations of the helicities of the initial and final particles can be done quite similarly. We intend to use the results obtained in the present work for further studying the forward-backward asymmetry at TeV energies, by including also the real radiative contributions.

Chapter 4

Production of electroweak bosons in e^+e^- annihilation at high energies

4.1 Introduction

Annihilation of e^+e^- in the double-logarithmic approximation (DLA) was considered first in Ref. [15]. In this work it was shown that when the total energy of the annihilation is high enough, the most sizable radiative QED corrections to e^+e^- annihilation into $\mu^+\mu^-$ are double-logarithmic (DL). These corrections were calculated in Ref. [15] to all orders in α. The DL contributions to this process appear when the final $\mu^+\mu^-$ -pair is produced in the Regge kinematics, i.e. when the muons move (in cm) closely to the initial e^+e^- -beam direction. According to the terminology introduced in Ref. [15], the process where μ^+ moves in the e^+ (e^-) -direction is called forward (backward) annihilation. Generalisation of these results to QCD (the forward and backward annihilation of quarks into quarks of other flavours) and to the EW theory (the backward annihilation of the left handed leptons into the right handed leptons) was obtained in Ref. [16] and Ref. [19] respectively. The forward and backward annihilation of e^+e^- into quarks, all chiralities accounted for, was considered recently in Ref. [20]. One of the features obtained in Refs [15]-[20] is that the forward scattering amplitudes in DLA are greater than the backward ones in QED, in QCD and in EW theory.

Besides these $2 \to 2$, i.e. elastic processes, it is interesting also to study the $2 \to 2 + n$ -exclusive processes accounting for emission of n bosons accompanying the elastic $2 \to 2$ annihilation. The point is that besides the conventional, (soft) bremsstrahlung there can be emitted harder bosons. Emission of such bosons can be also studied in DLA to all orders in the couplings, providing the hard bosons are emitted in cones with opening angles $\ll 1$ around the initial e^+e^- beams, i.e. in the multi-Regge kinematics. In this case, the most important part of the inelastic scattering amplitudes accounting for emission of n bosons consists of the kinematic factor $\sim (1/k_{1\perp})\dots(1/k_{n\perp})$ multiplied by some function M which is called the multi-Regge amplitude of the process. The energy dependence of M is controlled by $n+1$

electroweak Reggeons propagating in the crossing channel. Description of the multi-Regge photon production in the backward $e^+e^- \to \mu^+\mu^-$ -annihilation was considered in Ref. [21] and in Ref. [22]. The multi-Regge amplitudes for gluon production in the backward annihilation of quark-antiquark pairs were considered in Ref. [23].

In the present chapter we calculate the scattering amplitudes for electroweak boson production in e^+e^- annihilation into quarks and leptons assuming that the bosons are emitted in the multi-Regge kinematics. We use the approach of Refs. [22],[23] and account for electroweak double-logarithmic contributions to all orders in the electroweak couplings. This chapter is organised as follows: in Sect. 4.2 we consider emission of one EW boson in e^+e^- -annihilation into a quark-antiquark pair. We compose the infrared evolution equations (IREE) for the amplitudes of these processes. The IREE are solved in Sect. 4.3 . A generalisation of these results to the case of emission of n bosons is given in Sect. 4.4 . Emission of the EW bosons in e^+e annihilation into leptons is considered in Sect. 4.5 . Results of numerical calculations are presented and discussed in Sect. 4.6 . Finally, Sect. 4.7 is for conclusive remarks.

4.2 Emission of one electroweak boson in the multi-Regge kinematics

Let us start by considering the process $e^+(p_2)e^-(p_1) \to q(p'_1)\,\bar{q}(p'_2)$ accompanied by emission of one electroweak boson with momentum k. Energies of the bosons are assumed to be $\gg M_Z$. There are two kinematics for this process that yield DL radiative corrections. First of them is the kinematics where $p'_1 \sim p_1$, $p'_2 \sim p_2$. Obviously,

$$ s = (p_1 + p_2)^2 \gg t_{1,2} \,, \qquad t_1 = q_1^2 = (p'_1 - p_1)^2 \,, \qquad t_2 = q_2^2 = (p_2 - p'_2)^2 \qquad (4.1) $$

in this region. Eq. (4.1) means that the final particles are in cones with opening angles $\theta \ll 1$ around the e^+e^- beams. The second kinematics is the one where $p'_1 \sim p_2$, $p'_2 \sim p_1$ and therefore

$$ s = (p_1 + p_2)^2 \gg u_{1,2} \,, \qquad u_1 = q'^2_1 = (p'_2 - p_1)^2 \,, \qquad u_2 = q'^2_2 = (p_2 - p'_1)^2. \qquad (4.2) $$

Eq. (4.2) means that the final particles are also in cones with the cm opening angles $\pi - \theta \ll 1$ around the e^+e^- beams. Through this chapter we call kinematics (4.1) the t -kinematics and the kinematics (4.2) - the u -kinematics. Both of them are of the Regge type and studying them is similar in many respects.

Instead of directly calculating inelastic amplitudes $A^{(\gamma,Z,W)}$ describing emission of any of γ, Z, W, it is possible to calculate first the amplitudes $A^{(0)}$ and $A^{(r)}$ $(r = 1, 2, 3)$ describing emission of the isoscalar and the isovector bosons respectively. When expressions for such amplitudes are obtained, the standard relations between the fields γ, Z, W and the fields corresponding to the unbroken $SU(2) \otimes U(1)$ can be used in order to express $A^{(\gamma,Z,W)}$ in terms of A_0, A_r. This way of calculating $A^{(\gamma,Z,W)}$ is technically simpler than the direct one because when the radiative corrections are taken into account in DLA, contributions proportional to

masses in propagators of all virtual EW bosons are neglected and therefore both the isoscalar and the isovector fields act as independent ones. It makes more convenient operating with virtual isoscalar and isovector bosons than with γ, Z, W -bosons.

It is also convenient to discuss a more general process where lepton $l^i(p_1)$ (instead of e^-) and its antiparticle $\bar{l}_{i'}(p_2)$ (instead of e^+) annihilate into the quark-antiquark pair $q^j(p_1')$ $\bar{q}_{j'}(p_2')$ and a boson. The emitted boson can be either the isoscalar boson A_c, with $c = 0$ or an isovector one A_c, with $c = 1, 2, 3$. We consider first the most difficult case when both l^i and q^j are left-handed particles, transitions to the other chiralities are easy to do. The scattering amplitude of this process is $q_j\bar{q}^{j'}(M^c)_{ij'}^{i'j}\bar{l}_{i'}l^i$ where the matrix amplitude $(M^c)_{ij'}^{i'j}$ is the object to calculate. In order to simplify the isospin matrix structure of $(M^c)_{ij'}^{i'j}$, it is convenient to regard the process in the crossing channel, i.e. in the t -channel for kinematics (4.1) and in the u -channel for kinematics (4.2). When the process $l^i\bar{l}_{i'} \to q^j\bar{q}_{j'}A_c$ is considered in the t -channel, its amplitude can be expressed through the same matrix $(M^c)_{ij'}^{i'j}$, however with initial (final) t-state being $q_j l^i(A_c\bar{q}^{j'}\bar{l}_{i'})$:

$$M = \frac{2}{k_\perp^2} A_c\bar{q}^{j'}\bar{l}_{i'}(M^c)_{ij'}^{i'j}q_jl^i \ . \tag{4.3}$$

We have extracted the kinematic factor $2/k_\perp^2$ in order to simplify the matching condition (4.34) we will use. The initial cross-channel state $q_j l^i$ in Eq. (4.3) can be expanded into the sum of the isoscalar and of the isovector irreducible $SU(2)$ representations:

$$q_j l^i = \left[\frac{1}{2}\,\delta_j^i\delta_b^a + 2\,(t_m)_j^i(t_m)_a^b\right]q_b l^a \ . \tag{4.4}$$

The same is true for the final $\bar{q}^{j'}$ $\bar{l}_{i'}$ -pair. Therefore, $(M^c)_{ij'}^{i'j}$ can be represented as the sum

$$(M^c)_{ij'}^{i'j} = \sum_{k=0}^{4}(P_k^c)_{ij'}^{i'j}M_k \ . \tag{4.5}$$

of the invariant amplitudes M_k ($k = 0, 1, 2, 3, 4$), each multiplied the projection operator $(P_k^c)_{ij'}^{i'j}$ corresponding to an irreducible $SU(2)$ -representation. $k = 0, 1$ correspond to emission of the isoscalar field and $k = 2, 3, 4$ correspond to the isovector fields emission. Then, the projection operator $(P_0^c)_{ij'}^{i'j}$ describes the case (see Fig.4.1) when both the initial t -channel fermion state and the final one are $SU(2)$ singlets. Obviously, in this case the emitted boson can be isoscalar only, i.e. $c = 0$. Therefore

$$(P_0^c)_{ij'}^{i'j} = \frac{1}{2}\delta_0^c\delta_{j'}^{i'}\delta_i^j \ . \tag{4.6}$$

The projection operators P_k, with ($k = 1, 2$) describe the cases when both the initial and the final t -channel states are the isovector $SU(2)$ states. However, P_1 corresponds to the case when the emitted boson is isoscalar,

$$(P_1^c)_{ij'}^{i'j} = 2\,\delta_0^c(t_m)_i^j(t_m)_{j'}^{i'} \tag{4.7}$$

71
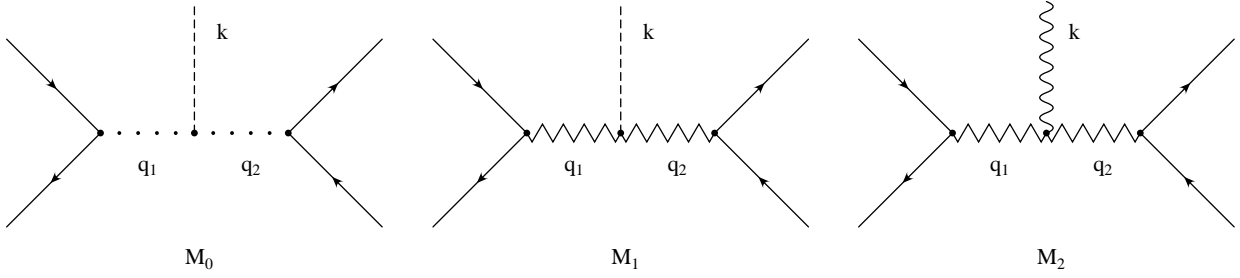
Figure 4.1: The multi-Regge invariant amplitudes M_r (and the projector operators) in kinematics (1). The dotted lines correspond to the isoscalar Reggeons; whereas the zigzag lines stand for the isovector ones. The dashed lines denote isoscalar vector bosons and the waved line correspond to the isovector boson.

whereas P_2 describes emission of isovector fields:

$$(P_2^c)_{ij'}^{i'j} = (t_b)_i^j (T^c)_{ba} (t_a)_{j'}^{i'} . \tag{4.8}$$

T^c (c = 1,2,3) in Eq. (4.8) stands for $SU(2)$ generators in the adjoint (vector) representation. Projector P_3 correspond to the case when the initial fermion state is the $SU(2)$ singlet whereas the final one is the $SU(2)$ vector. Projector P_4 describes the opposite situation. The emitted boson is isovector in both these cases. Therefore,

$$(P_3^c)_{ij'}^{i'j} = (t_c)_i^j \delta_{j'}^{i'} , \qquad (P_4^c)_{ij'}^{i'j} = \delta_i^j (t_c)_{j'}^{i'} . \tag{4.9}$$

All operators in Eqs. (4.6, 4.9) are orthogonal:

$$(P_A)_{ij'}^{i'j} (P_B)_{ij'}^{i'j} \sim \delta^{AB} . \tag{4.10}$$

Below (see Eq. (4.34)) we will show that the invariant amplitudes M_3, M_4 do not have DL contributions. It leaves us with amplitudes $M_{0,1,2}$ to calculate. These invariant amplitudes account for radiative corrections to all powers in the EW couplings in the DLA. The arguments of M_k are

$$\begin{aligned} s_1 &= (p_1' + k)^2 \approx 2p_1 k , & t_1 &= q_1^2 = (p_1 - p_1')^2, \\ s_2 &= (p_2' + k)^2 \approx 2p_2 k , & t_2 &= q_2^2 = (p_2' - p_2)^2 , \end{aligned} \tag{4.11}$$

so that

$$s_1 s_2 = s k_\perp^2 \tag{4.12}$$

The kinematics is the t-channel multi-Regge kinematics when

$$s_{1,2} \gg t_{1,2} \geq M_Z^2 . \tag{4.13}$$

72

Similarly, in order to simplify the isotopic structure of $(M^c)_{ij'}^{i'j}$ of Eq. (4.3) in kinematics (4.2), it is convenient to consider it in the u -channel where it can be expressed through u -channel invariant amplitudes M'_k:

$$(M^c)_{ij'}^{i'j} = \sum_{k=0}^{2} (P'^c_k)_{ij'}^{i'j} M'_k .$$

(4.14)

Operators $(P'^c_k)_{ij'}^{i'j}$ describe irreducible $SU(2)$ representations, which for this channel are either symmetrical or antisymmetrical two-quark states:

$$
\begin{aligned}
P'^c_0 &= \frac{1}{2}\delta^c_0 \left[\delta^{i'}_i \delta^j_{j'} - \delta^j_i \delta^{i'}_{j'} \right] , \\
P'^c_1 &= \frac{1}{2}\delta^c_0 \left[\delta^{i'}_i \delta^j_{j'} + \delta^j_i \delta^{i'}_{j'} \right] , \\
P'^c_2 &= \frac{1}{2} \left[\delta^{i'}_i (t^c)^j_{j'} + (t^c)^{i'}_i \delta^j_{j'} + \delta^{i'}_{j'} (t^c)^j_i + (t^c)^{i'}_{j'} \delta^j_i \right] .
\end{aligned}
$$

(4.15)

Operators P'_0, P'_1 describe emission of the isoscalar field whereas P'_2 describes the isovector field emission. Let us note that the operator

$$P'^c_3 = \frac{1}{2} \left[\delta^{i'}_i (t^c)^j_{j'} + (t^c)^{i'}_i \delta^j_{j'} - \delta^{i'}_{j'} (t^c)^j_i - (t^c)^{i'}_{j'} \delta^j_i \right]$$

(4.16)

in principle, should be included (cf Ref. [23]). However, the invariant amplitude M'_3 related to P' does not yield DL contributions in the case of $SU(2)$ though it does in the case of $SU(N)$ with $N > 2$. It leaves us with three invariant amplitudes $M'_{0,1,2}$ (just like it was in the case of the t -kinematics). They depend on $s_{1,2}$ and on $u_{1,2}$. In the multi-Regge kinematics (4.2)

$$s_{1,2} \gg u_{1,2} \geq M_Z^2 .$$

(4.17)

In order to specify the multi-Regge t (u) -kinematics completely, we assume that

$$t_1 \gg t_2 , \qquad (u_1 \gg u_2).$$

(4.18)

The opposite case can be considered similarly. The kinematics where $t_1 \sim t_2$ $(u_1 \sim u_2)$ means emission of soft electroweak bosons. This kinematics will be considered below separately. From the point of view of the Regge theory, accounting for radiative corrections in kinematics (4.13,4.17) can be expressed through exchange of Reggeons propagating in the cross channels. Therefore operators P_0, (P'_0) of Eq. (4.6) (Eq. (4.15)) imply that amplitude M_0 (M'_0) is controlled by two isoscalar Reggeons whereas the projection operators $P_{1,2}$ of Eqs. (4.7,4.8) (operators $P'_{1,2}$ of Eqs. (4.15)) imply that the energy dependence of amplitudes $M_{1,2}(M'_{1,2})$ is controlled by two isovector Reggeons. In contrast to it, one of the Reggeons in amplitudes $M_{3,4}$ is isoscalar and the other is isovector.

73

Besides $s_{1,2}$ and $t_{1,2}$ ($u_{1,2}$), invariant amplitudes $M_{0,1,2}$ ($M'_{0,1,2}$) depend also on the infrared (IR) cut-off μ introduced in order to avoid IR singularities from integrating over virtual particle momenta. We use the IR cut-off μ in the transverse space. However, definition of μ for radiative amplitudes differs from the definition for elastic amplitudes. In this chapter we introduce μ the same way as it was done in [24]. Let us denote $k'^{ab}_{l\perp}$ to be the component of a virtual particle momenta k'_l transverse to the plane formed by momenta a and b, with $a \neq b$. Then, the IR cut-off μ obeys

$$\mu < k'^{ab}_{l\perp} \tag{4.19}$$

for all $l = 1, \dots$ when $a, b = p_1, p_2, p'_1, p'_2, k$. In the present chapter we assume that $\mu \approx M_Z$.

In order to calculate M_r we generalise to the EW theory the technique applied earlier to investigation of the similar inelastic processes in QED[22] and in QCD[23]. The essence of the method is factorizing DL contributions from the virtual particles with minimal $k'^{ab}_{l\perp}$ and differentiating with respect to $\ln \mu^2$. At $t_1, t_2 \gg \mu^2$, such particles can only be virtual EW bosons. Factorizing their contributions leads to the IREE for amplitude $(M^c)^{i'j}_{ij'}$. This equation is depicted in Fig.4.2.
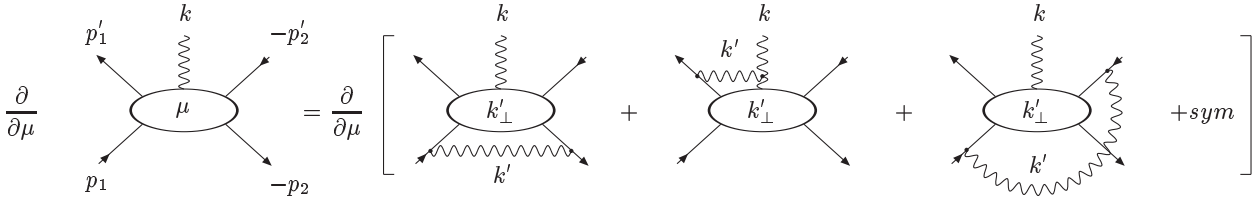
Figure 4.2: IREE for M_Z. Letters inside the blobs stand for infrared cutoffs.

Applying to it the projector operators of Eqs. (4.6 - 4.9, 4.15) leads to the following IREE for M_r (see Refs. [22],[23], [20] for technical details):

$$\frac{\partial M_r}{\partial \rho_1} + \frac{\partial M_r}{\partial \rho_2} + \frac{\partial M_r}{\partial y_1} + \frac{\partial M_r}{\partial y_2} = -\frac{1}{8\pi^2}[b_r \ln(s/\mu^2) + h_r(y_1 + y_2) + m_k y_1]M_r \ . \tag{4.20}$$

We have used in Eq. (4.20) the fact that, according to our assumption Eq. (4.18), $k_\perp^2 \approx t_1(u_1)$ and introduced the logarithmic variables

$$\rho_{1,2} = \ln(s_{1,2}/\mu^2) \ , \qquad y_{1,2} = \ln(t_{1,2}/\mu^2) \ . \tag{4.21}$$

The numerical factors b_r, h_r and m_r in Eq. (4.20) are:

$$b_0 = \frac{g'^2(Y - Y')^2}{4} \ , \tag{4.22}$$

$$b_1 = b_2 = 2g^2 + \frac{g'^2(Y - Y')^2}{4} \ ,$$

$$h_0 = \frac{3g^2}{4} + \frac{g'^2 Y Y'}{4} \,,$$

$$h_1 = h_2 = -\frac{g^2}{4} + \frac{g'^2 Y Y'}{4} \,,$$

$$m_0 = m_1 = 0 \,,$$

$$m_2 = g^2 \,.$$

The IREE for the invariant amplitudes $M'_{0,1,2}$ can be obtained similarly. It has the same structure as Eq. (4.20), though everywhere $t_{1,2}$ should be replaced by $u_{1,2}$. It means in particular that $y_{1,2}$ should be replaced by $y'_{1,2} = \ln(u_{1,2})/\mu^2$. This replacement and replacement of operators $P_{0,1,2}$ by $P'_{0,1,2}$ results in replacement of the factors b_r, h_r by b'_r, h'_r :

$$b'_0 = \frac{g'^2 (Y + Y')^2}{4} \,, \tag{4.23}$$

$$b'_1 = b'_2 = 2g^2 + \frac{g'^2 (Y + Y')^2}{4} \,,$$

$$h'_0 = \frac{3g^2}{4} - \frac{g'^2 Y Y'}{4} \,,$$

$$h'_1 = h'_2 = -\frac{g^2}{4} - \frac{g'^2 Y Y'}{4} \,.$$

Factors m'_r in the IREE for M'_r coincide with factors m_r in Eq. (4.22). Therefore after replacements $y_{1,2} \to y'_{1,2}$, and $b_{0,1,2} \to b'_{0,1,2}$, $h_{0,1,2} \to h'_{0,1,2}$ Eq. (4.20) for amplitudes M_r in kinematics (4.13) holds for amplitudes M'_r describing $e^+ e^- \to q\bar{q}$ -annihilation in kinematics (4.17).

4.3 Solving the evolution equations for M_r

In order to solve Eq. (4.20), it is convenient to operate with the Mellin amplitude F_r related to M_r through the Mellin transform:

$$M_r = \int_{-\imath\infty}^{\imath\infty} \frac{d\omega_1}{2\imath\pi} \frac{d\omega_2}{2\imath\pi} e^{\omega_1 \rho_1 + \omega_2 \rho_2} F_r(\omega_1, \omega_2, y_1, y_2) \,. \tag{4.24}$$

In the ω -representation, multiplying by ρ_i corresponds to $-\partial/\partial\omega_i$. Using this and Eqs. (4.12, 4.24), we can rewrite Eq. (4.20) as

$$\omega_1 F_r + \omega_2 F_r + \frac{\partial F_r}{\partial y_1} + \frac{\partial F_r}{\partial y_2} = b_r \Big(\frac{\partial F_r}{\partial \omega_1} + \frac{\partial F_k}{\partial \omega_2} \Big) + \Big(\frac{1}{8\pi^2} \Big) [(b_r - h_r - m_r) y_1 - h_r y_2] F_r \,. \tag{4.25}$$

For further simplification, it is convenient to introduce variables $x_{1,2}$ and $z_{1,2}$:

$$x_{1,2} = \omega_{1,2}/\lambda_r \,, \qquad z_{1,2} = -\lambda_r y_{1,2} \tag{4.26}$$

where $\lambda_r = \sqrt{b_r/8\pi^2}$. In terms of x_i, z_i, the differential operator in the left hand side of Eq. (4.25) acquires symmetrical and simple form. Thus, we arrive at

$$\frac{\partial F_r}{\partial x_1} + \frac{\partial F_r}{\partial x_2} + \frac{\partial F_r}{\partial z_1} + \frac{\partial F_r}{\partial z_2} = [(x_1 + x_2) + (1 + \beta_r)z_1 + \gamma_r z_2]F_r \tag{4.27}$$

where $\beta_r = -(h_r + m_r)/b_r$, $\gamma_r = -h_r/b_r$.

The general solution to Eq. (4.27) can be written as

$$F_r = \Phi_r(x_1 - z_2, x_2 - z_2, z_1 - z_2) \exp\left[\frac{x_1^2 + x_2^2}{2} + (1 + \beta_r)\frac{z_1^2}{2} + \gamma_r\frac{z_2^2}{2}\right] \tag{4.28}$$

where unknown function Φ_r has to be specified. It can be done in particular through matching

$$F_r(x_1, x_2, z_1, z_2)|_{z_2=0} = \tilde{F}_r(x_1, x_2, z_1) \tag{4.29}$$

where $\tilde{F}_r$ is related through the Mellin transform (4.24) to amplitude $\tilde{M}_r$ of the same process in the kinematics Eqs. (4.13,4.18) though with $q_2^2 \sim \mu^2$. The IREE (4.30) for $\tilde{F}_r$ differs from the IREE of Eq. (4.27) for F_r in the following two respects. First, there is no z_2 dependence in Eq. (4.30). Second, in contrast to Eq. (4.27), the IREE for $\tilde{F}_r$ contains an additional term (that we denote $dQ_r(x)/dx$) (and will specify below in Eq. (4.32)) in the rhs:

$$\frac{\partial \tilde{F}_r}{\partial x_1} + \frac{\partial \tilde{F}_r}{\partial x_2} + \frac{\partial \tilde{F}_r}{\partial z_1} = [(x_1 + x_2) + (1 + \beta_r)z_1 + \frac{dQ_r(x_2)}{dx_2}]\tilde{F}_r \tag{4.30}$$

This new term corresponds to the situation when the particles with the minimal transverse momenta are the t_2-channel virtual quark pair (see Fig.4.3). This contribution is μ-dependent
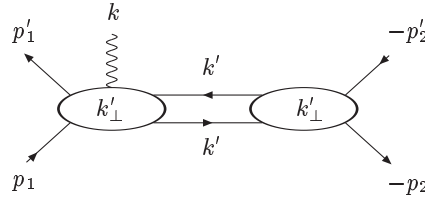
Figure 4.3: The soft fermion contribution to the IREE for $\tilde{M}_Z$

only when $t_2 \approx \mu^2$. The intermediate two-particle state in Fig.4.3 factorizes amplitude $\tilde{M}_r$ into a convolution of the same amplitude and the elastic amplitude E_r. The explicit expressions for the elastic electroweak amplitude E_r were obtained in the last chapter (Ref. [20]). The particular case where the produced particles were a right handed lepton and its antiparticle was studied in Ref. [19]. For all cases, the Mellin amplitude f_r is related to E_r through the Mellin transform

$$E_r = \int_{-\imath\infty}^{\imath\infty} \frac{d\omega}{2\imath\pi} e^{\omega\rho} f_r(\omega) , \tag{4.31}$$

76

with $\rho = \ln(s/\mu^2)$, can be expressed through the Parabolic cylinder functions $D_{p_r}(x)$ with different values of p_r:

$$f_r(x) = \frac{1}{p_r} \frac{d[\ln(e^{x^2/4} D_{p_r}(x))]}{dx} = \frac{D_{p_r-1}(x)}{D_{p_r}(x)} \equiv \frac{1}{p_r} \frac{dQ_r(x)}{dx}. \tag{4.32}$$

The term $dQ_r(x_2)/dx_2$ in the rhs of Eq. (4.30) corresponds to the contribution of the right blob in Fig. 4.3 to the IREE (4.30). The general solution to Eq. (4.30) is

$$\tilde{F}_r = \tilde{\Phi}_r(x_1 - z_1, x_2 - z_1) \frac{1}{D_{p_r}(x_2) \exp(x_2^2/4)} \exp\left[\frac{x_1^2 + x_2^2}{2} + (1 + \beta_r)\frac{z_1^2}{2}\right] \tag{4.33}$$

where there is, again, an unknown function $\tilde{\Phi}_r$. In order to specify $\tilde{\Phi}_r$, we use the factorisation of bremsstrahlung bosons with small $k_\perp$ which takes place (see Refs. [64],[16],[24],[72]) both in Abelian and in non-Abelian field theories. In the context of the problem under consideration it states that when $z_1 = 0$, the radiative amplitude $\tilde{M}_r$ and the elastic amplitude E_r are related:

$$\tilde{M}_r|_{z_1=0} = E_r G_r \ . \tag{4.34}$$

E_r in Eq. (4.34) are the invariant amplitudes of the elastic annihilation process (see [20]); $G_r = g'(Y \pm Y')/2$ for $r = 0$ (for invariant amplitude $M_0(M_0')$ the sign is "+" ("-")); $G_r = g$ for $r = 1, 2, 3$.

Eq. (4.34) means that when $z_1 = 0$, the two Reggeons in every amplitude M_r converge into one Reggeon that controls E_r energy dependence. However, such convergence is possible in the DLA only when both Reggeons are either isoscalar or isovector. This rules amplitudes $M_{3,4}$ out of consideration. Obviously, this property of the multi-Regge amplitudes holds for the more complicated cases when the number of involved Reggeons is more than two. This property was first obtained in Ref. [23] and was called "Reggeon diagonally".

The matching (4.34) can be rewritten in terms of Mellin amplitudes $f_r(\omega)$ and $\phi_r(x_1, x_2) \equiv \tilde{F}_r(\omega_1, \omega_2, z_1)|_{z_1=0}$:

$$\int_{-\imath\infty}^{\imath\infty} \frac{d\omega}{2\imath\pi} e^{\omega_1\rho_1 + \omega_2\rho_2} \phi_r(\omega_1, \omega_2) = G_r \int_{-\imath\infty}^{\imath\infty} \frac{d\omega}{2\imath\pi} e^{\omega(\rho_1+\rho_2)} f_r(\omega) \ . \tag{4.35}$$

We have used in Eq. (4.35) that according to Eq. (4.12) $\rho = \rho_1 + \rho$ when $z_1 = 0$. For the amplitudes with positive signatures that we discuss in the present chapter, the transform inverse to Eq. (4.24) can be written as

$$M_r(\rho_{1,2}, y_{1,2}) = \int_0^\infty d\rho_1 d\rho_2 e^{-\omega_1\rho_1 - \omega_2\rho_2} F_r(\omega_1, \omega_2, y_{1,2}) \ . \tag{4.36}$$

Applying this transform to Eq. (4.35) at $z_1 = 0$ leads to

$$\begin{aligned}
\phi_r(\omega_1, \omega_2) &= G_r \int_{-\imath\infty}^{\imath\infty} \frac{d\omega}{2\imath\pi} \int_0^\infty d\rho_1 d\rho_2 e^{(\omega-\omega_1)\rho_1 + (\omega-\omega_2)\rho_2} f_r(\omega) = \\
&\quad G_r \int_{-\imath\infty}^{\imath\infty} \frac{d\omega}{2\imath\pi} \frac{1}{(\omega - \omega_1)(\omega - \omega_2)} f_r(\omega) \ .
\end{aligned} \tag{4.37}$$

Choosing the integration contours in Eq. (4.37) so that $\Re\omega < \Re\omega_{1,2}$ allows us to integrate over ω by closing the contour to the right, which does not involve dealing with singularities of f_r. When this integration is done, we arrive at

$$\phi_r = \frac{f_r(\omega_1) - f_r(\omega_2)}{\omega_2 - \omega_1} \ . \tag{4.38}$$

After that it is easy to obtain the following expression for M_r:

$$
\begin{aligned}
M_r \ = \ & G_r \int_{-\imath\infty}^{\imath\infty} \frac{d\omega_1}{2\imath\pi} \frac{d\omega_2}{2\imath\pi} \left(\frac{s_1}{q_1^2}\right)^{\omega_1} \left(\frac{s_2}{\sqrt{q_1^2 q_2^2}}\right)^{\omega_2} \left[\frac{f_r(x_1) - f_r(x_2)}{\omega_2 - \omega_1}\right] . \\
& \frac{D_{p_r}(x_2 - z_1)}{D_{p_r}(x_2 - z_2)} \exp\left[-\frac{(1 - 2\beta_r)}{4}z_1^2 - \frac{(1 - 2\gamma_r)}{4}z_2^2\right] .
\end{aligned}
\tag{4.39}
$$

If we choose $\Re x_1 < \Re x_2$, Eq. (4.39) takes simpler form:

$$M_r = G_r R_r \tag{4.40}$$

where

$$
\begin{aligned}
R_r \ = \ & \int_{-\imath\infty}^{\imath\infty} \frac{d\omega_1}{2\imath\pi} \frac{d\omega_2}{2\imath\pi} \left(\frac{s_1}{q_1^2}\right)^{\omega_1} \left(\frac{s_2}{\sqrt{q_1^2 q_2^2}}\right)^{\omega_2} \frac{1}{\omega_2 - \omega_1} \frac{D_{p_r-1}(x_1 - z_1)}{D_{p_r}(x_1 - z_1)} . \\
& \frac{D_{p_r}(x_2 - z_1)}{D_{p_r}(x_2 - z_2)} \exp\left[-\frac{(1 - 2\beta_r)}{4}z_1^2 - \frac{(1 - 2\gamma_r)}{4}z_2^2\right] .
\end{aligned}
\tag{4.41}
$$

The amplitudes $M^{(\gamma)}, M^{(Z)}, M^{(W^\pm)}$ of the electroweak boson production are easily expressed through R_r:

$$
\begin{aligned}
M^{(\gamma)} \ &= \ \cos\theta_W M^{(0)} + \sin\theta_W M^{(3)} = g\cos\theta_W(R_0 + R_1) + g\sin\theta_W R_2 \ , \\
M^{(Z)} \ &= \ -\sin\theta_W M^{(0)} + \cos\theta_W M^{(3)} = -g\sin\theta_W(R_0 + R_1) + g\cos\theta_W R_2 \ , \\
M^{(W^\pm)} \ &= \ (1/\sqrt{2})[M^{(1)} \pm \imath M^{(2)}] = (g/\sqrt{2})R_2
\end{aligned}
\tag{4.42}
$$

when the boson are produced in kinematics (4.13). For kinematics (4.17), the boson production amplitudes are expressed through R_r':

$$
\begin{aligned}
M^{(\gamma)} \ &= \ g\cos\theta_W(R_0' + R_1') + g\sin\theta_W R_2' \ , \\
M^{(Z)} \ &= \ -g\sin\theta_W(R_0' + R_1') + g\cos\theta_W R_2' \ , \\
M^{(W^\pm)} \ &= \ (g/\sqrt{2})R_2' \ .
\end{aligned}
\tag{4.43}
$$

The exponent in Eq. (4.41) is the Sudakov form factor for this process. It accumulates the soft DL contributions, with virtualities $\leq z_1^2$. The harder DL contributions are accounted

78

through D_p -functions. It is convenient to perform integration over $\omega_{1,2}$ by taking residues. Such residues are actually zeros $\bar{x}_k(r)$ $(k = 1, \ldots)$ of involved D_{p_r} -functions, so

$$R_r \sim \sum_{k=1} \left(\frac{s_1}{q_1^2}\right)^{\lambda_r \bar{x}_k(r)} \left(\frac{s_2}{\sqrt{q_1^2 q_2^2}}\right)^{\lambda_r \bar{x}_k(r)} . \qquad (4.44)$$

Position of $\bar{x}_k(r)$ depend on values of p_r in such a way that the greater p_r, the greater are $\Re \bar{x}_k(r)$. In particular, the real part of the rightmost zero $\equiv \bar{x}(r)$ is positive when $p_r > 1$. In other words, R_r increase with the total energy when $p_r > 1$. Ref. [20] states that

$$
\begin{aligned}
p_0' &= \frac{3 - YY' \tan^2 \theta_W}{(Y + Y')^2 \tan^2 \theta_W}, \qquad (4.45) \\
p_1' = p_2' &= -\frac{1 + YY' \tan^2 \theta_W}{8 + (Y + Y')^2 \tan^2 \theta_W}
\end{aligned}
$$

and

$$
\begin{aligned}
p_0 &= \frac{3 + YY' \tan^2 \theta_W}{(Y - Y')^2 \tan^2 \theta_W}, \qquad (4.46) \\
p_1 = p_2 &= -\frac{1 - YY' \tan^2 \theta_W}{8 + (Y - Y')^2 \tan^2 \theta_W}.
\end{aligned}
$$

Therefore, only M_0 and M_0' grow with increase of the annihilation energy whereas the amplitudes $M_{1,2}$ and $M'_{1,2}$ are falling.

Let us discuss the asymptotics of R_r first. The asymptotics of the energy dependence of each R_r is controlled by two identical isoscalar (isovector) leading Reggeons. Intercepts Δ_j $(j = S, V, S', V')$ of these Reggeons are related to the position of the rightmost zero $\bar{x}(j)$ of the D_{p_r} -functions so that

$$\Delta_S = \lambda_0 \bar{x}(p_0) , \qquad \Delta_{S'} = \lambda_0' \bar{x}(p_0') , \qquad \Delta_V = \lambda_1 \bar{x}(p_1) , \qquad \Delta_{V'} = \lambda_1' \bar{x}(p_1') . \qquad (4.47)$$

We remind that $\lambda_j = \sqrt{b_j/8\pi^2}$. Therefore we arrive at the following asymptotics:

$$
\begin{aligned}
M_0 &\sim g' s^{\Delta_S} , \qquad M_1 \sim g' s^{\Delta_V} , \qquad M_2 \sim g s^{\Delta_V} , \\
M_0' &\sim g' s^{\Delta_{S'}} , \qquad M_1' \sim g' s^{\Delta_{V'}} , \qquad M_2' \sim g s^{\Delta_{V'}} . \qquad (4.48)
\end{aligned}
$$

As the intercepts of the isoscalar Reggeons are greater than the ones of the isovector Reggeons, the asymptotics of the exclusive cross sections $\sigma^{(\gamma)}$ and $\sigma^{(Z)}$ of the photon and Z -production is given by contributions of the isoscalar Reggeons with intercepts Δ_S and $\Delta_{S'}$. Therefore, the only difference between these cross sections is the different couplings of these fields to the isoscalar Reggeons. So, we conclude (see Eqs. (4.42),(4.43)) that asymptotically

$$\frac{\sigma^{(Z)}}{\sigma^{(\gamma)}} \approx \tan^2 \theta_W . \qquad (4.49)$$

79

Accounting for contributions of other zeros, $\bar{x}^{(r)}$ changes the values of $\sigma^{(\gamma)}$ and $\sigma^{(Z)}$ but does not change Eq. (4.49). In contrast to Eq. (4.49), the asymptotics of the ratio $\sigma^{(\gamma)}/\sigma^{(W)}$ depends on s. The point is that the exclusive cross section $\sigma^{(W)}$ of W -production involves the isovector Reggeons with smaller intercepts. So, asymptotically this cross section obeys the following relation:

$$\frac{\sigma^{(\gamma)}}{\sigma^{(W)}} \sim s^{2(\Delta_S - \Delta_V)} = s^{-0.36} . \tag{4.50}$$

However, contributions of other zeros of D_p -functions change this asymptotic relation. Results of numerical calculation of $\sigma^{(W^\pm)}$, $\sigma^{(Z)}$ and $\sigma^{(\gamma)}$, and accounting for non-leading DLA contributions are discussed in Sect. 4.6.

4.4 Emission of n vector bosons in the multi-Regge kinematics

The arguments of the previous Sects. can be extended in a straightforward way to the case when the e^+e^- -annihilation into quarks is accompanied by emission of n isoscalar or isovector bosons with momenta $k_1, ..., k_n$ in the multi-Regge kinematics. It is not difficult to generalise expressions of Eqs. (4.6-4.8, 4.15) for projection operators to the case of the n boson emission and obtain new projector operators. First of all, let us note that all non-diagonal projectors should be ruled out of consideration by the same reason as it was done in Sect. 1. Therefore, the invariant amplitudes of emission of n bosons involve $n+1$ identical intermediate Reggeons. The isotopic quantum numbers of the Reggeons depend on the initial fermion state and on the isospin of the emitted bosons. If the initial fermion state is isoscalar (or antisymmetric), the same is true for all intermediate Reggeons and therefore only isoscalar bosons can be emitted in these cases. The projector operators for this case are again $P_{0,1}$ ($P'_{0,1}$) with trivial adding factors $\delta_{c_i 0}$ for every isoscalar boson. If the initial fermion state is isovector (or symmetrical), the emitted bosons can be both isoscalar or isovector gauge fields. Accounting for emission of the isoscalar bosons does not require any changes of the projectors. When r ($r \leq n$) isovector bosons $c_1, c_2, .., c_r$ are emitted in the t -kinematics, the operators P_2 of Eq. (4.8) should be replaced by

$$(P_2^{(c_1, c_2, ..., c_n)})_{ij}^{i'j'} = (t_b)_{i'}^{j'}(T^{c_r})_{ba_r} \dots (T^{c_2})_{a_2 a_1}(T^{c_1})_{a_2 a_1}(t_{a1})_j^i . \tag{4.51}$$

A similar generalisation of operator P'_2 is also easy to obtain. The new invariant amplitudes $M_j(M'_j)$ corresponding to these operators depend on $n+1$ variables s_i:

$$s_1 = 2p_1 k_1 , \qquad s_2 = 2k_1 k_2 , \dots , \qquad s_{n+1} = 2k_n p_2 \tag{4.52}$$

and on $t_i(u_i)$ in the case of the t (u) - kinematics:

$$t_i = q_i^2 , \qquad u_i = q'^2_i \tag{4.53}$$

where

$$q_1 = p_1' - p_1 \,, \qquad q_2 = q_1 - k_1 \,, \ldots \,, \qquad q_{n+1} = q_n - k_n = p_2 - p_2'$$
$$q_1' = p_2' - p_1 \,, \qquad q_2' = q_1' - k_1 \,, \ldots \,, \qquad q_{n+1}' = q_n' - k_n = p_2 - p_1' \,. \qquad (4.54)$$

The kinematics is the multi-Regge t -kinematics if

$$s_i \gg t_j \geq M_Z^2 \qquad (4.55)$$

and it is the multi-Regge u -kinematics if

$$s_i \gg u_j \geq M_Z^2, \qquad (4.56)$$

with $i, j = 1, \ldots, n+1$. In order to define these kinematics completely, one should fix relations between different t_i (different u_i). In this chapter we consider the simplest case of the monotonic ordering. We assume that

$$t_1 \gg t_2 \gg \ldots \gg t_{n+1} \qquad (4.57)$$

for the case of the multi-Regge t -kinematics and the similar monotonic ordering

$$u_1 \gg u_2 \gg \ldots \gg u_{n+1} \qquad (4.58)$$

for the case of the multi-Regge u -kinematics [1]. Eqs. (4.52,4.53) read that in the both kinematics

$$s_1 \ldots s_{n+1} = s k_{1\,\perp}^2 \ldots k_{n\,\perp}^2 \,. \qquad (4.59)$$

It is also convenient to introduce variables $\rho_i = \ln(s_i/\mu^2)$ and y_i where $y_i = \ln(t_i/\mu^2)$ for the forward kinematics ($y_i' = \ln(u_i/\mu^2)$ for the case of the backward one). In these terms, the IREE for $M_j^{(n)}$ looks quite similar to Eq. (4.20):

$$\frac{\partial M_j^{(n)}}{\partial \rho_1} + \ldots + \frac{\partial M_j^{(n)}}{\partial \rho_{n+1}} + \frac{\partial M_j^{(n)}}{\partial y_1} + \ldots + \frac{\partial M_j^{(n)}}{\partial y_{n+1}} =$$
$$-\frac{1}{8\pi^2} \left[b_j \ln(s/\mu^2) - h_j(y_1 + y_{n+1}) + \sum_l m_l y_l \right] M_j^{(n)} \,, \qquad (4.60)$$

where b_j, h_j are given by Eqs. (4.22,4.23); $m_l = g^2$ if the boson l with momentum k_l is isovector, otherwise $m = 0$. Let us consider for simplicity the case of emission of isoscalar bosons. Introducing the Mellin amplitude F_n through the transform

$$M_n = \int_{-\imath\infty}^{\imath\infty} \frac{d\omega_1..d\omega_{n+1}}{2\pi\imath} e^{\omega_1\rho_1 + \ldots + \omega_{n+1}\rho_{n+1}} F_n(\omega_1, \ldots, \omega_{n+1}, y_1, \ldots, y_{n+1}) \qquad (4.61)$$

---

[1] Scattering amplitudes for other multi-Regge kinematics can be calculated similarly (see Ref. [23]). It is worth to mention that amplitudes for kinematics (4.57) and (4.58) yield main contributions to the inclusive cross section when integration over the EW boson momenta is performed.

and using notations x_i, z_i defined as

$$x_i = \omega_i/\lambda , \qquad z_i = -\lambda y_i , \tag{4.62}$$

we transform Eq. (4.61) into the following one:

$$\frac{\partial F_n}{\partial x_1} + \ldots + \frac{\partial F_n}{\partial x_{n+1}} + \frac{\partial F_n}{\partial z_1} + \ldots + \frac{\partial F_n}{\partial z_{n+1}} =$$
$$[(x_1 + \ldots + x_{n+1}) + z_1 + \ldots + z_n + h(z_1 + z_{n+1})] F_n , \tag{4.63}$$

with the general solution

$$F_n = \Phi_n \left(x_1 - z_{n+1}, x_2 - z_{n+1}, \ldots, x_{n+1} - z_{n+1}; z_1 - z_{n+1}, \ldots, z_n - z_{n+1} \right) \cdot$$
$$\exp\left[S_{n+1}(x) + S_n(z) + h\left(\frac{z_1^2 + z_{n+1}^2}{2}\right) \right] \tag{4.64}$$

where we have denoted $S_r(a) \equiv \sum_1^r a_i^2/2$. An unknown function Φ_n can be specified through the matching

$$F_n|_{z_{n+1}=0} = \tilde{F}_n \tag{4.65}$$

where the Mellin amplitude $\tilde{F}_n$ describes the same process in the multi-Regge kinematics (4.52,4.54,4.57) though with $q_{n+1}^2 = \mu^2$. The IREE for $\tilde{F}_n$ is

$$\frac{\partial \tilde{F}_n}{\partial x_1} + \ldots + \frac{\partial \tilde{F}_n}{\partial x_{n+1}} + \frac{\partial \tilde{F}_n}{\partial z_1} + \ldots + \frac{\partial \tilde{F}_n}{\partial z_{n+1}} =$$
$$\left[(x_1 + \ldots + x_{n+1}) + z_1 + \ldots + z_{n+1} + hz_1 + \frac{dQ_r(x_{n+1})}{dx_{n+1}} \right] \tilde{F}_1 \tag{4.66}$$

where Q is defined by Eq. (4.32). The general solution to Eq. (4.66) can be obtained quite similar to the one of Eq. (4.63):

$$\tilde{F}_n = \tilde{\Phi}_n \left(x_1 - z_n, x_2 - z_n, \ldots, x_{n+1} - z_n; z_1 - z_n, \ldots, z_{n-1} - z_n \right) \cdot$$
$$\exp[S_{n+1}(x) + S_n(z) + h\frac{z_1^2}{2}] . \tag{4.67}$$

It also contains an unknown function $\tilde{\Phi}$. In order to specify it we use factorisation of the photons with small $k_\perp$:

$$\tilde{M}_n|_{z_n=0} = \tilde{M}_{n-1}(s_1, \ldots, s_n; q_1^2, \ldots, q_{n-1}^2, \mu^2) . \tag{4.68}$$

Rewriting this equation in terms of the Mellin amplitudes and performing the transform inverse to Eq. (4.61), we express $\tilde{F}_n$ through amplitude $\tilde{F}_{n-1}$:

$$\tilde{F}_n|_{z_n=0} = \frac{1}{(\omega_n - \omega_{n+1})} \left[\tilde{F}_{n-1}(x_1, \ldots, x_{n-1}, x_n; z_1, \ldots, z_{n-1}) - \right.$$
$$\left. \tilde{F}_{n-1}(x_1, \ldots, x_{n-1}, x_{n+1}; z_1, \ldots, z_{n-1}) \right] . \tag{4.69}$$

82

Combining this equation with Eqs. (4.61,4.67) leads to the following recurrent formula for F_n:

$$F_n(x_1, \ldots, x_{n+1}; z_1, \ldots, z_{n+1}) = \tag{4.70}$$

$$\frac{1}{\omega_n - \omega_{n+1}} \tilde{F}_{n-1}(x_1 - z_n, \ldots, x_n - z_n; z_1 - z_n, \ldots, z_{n-1} - z_n) \cdot \frac{D_p(x_{n+1} - z_n)}{D_p(x_{n+1} - z_{n+1})}$$

$$\exp\left[S_{n+1}(x) - S_{n+1}(x - z_n) + S_n(z) - S_{n-1}(z - z_n) + \frac{h}{2}[z_1^2 + z_{n+1}^2 - (z_1 - z_n)^2]\right] .$$

Using this formula leads to the following expression for the amplitude $M_j^{(n)}$ of emission of n isoscalar bosons in the ordered kinematics (4.57,4.58):

$$M_r^{(n)} = \left(g'\frac{(Y \pm Y')}{2}\right)^n \int_{-\imath\infty}^{\imath\infty} \frac{d\omega_1}{2\imath\pi} \cdots \frac{d\omega_{n+1}}{2\imath\pi} \left(\frac{s_1}{q_1^2}\right)^{\omega_1} \cdots \left(\frac{s_{n+1}}{\sqrt{q_n^2 q_{n+1}^2}}\right)^{\omega_{n+1}} \frac{D_{p_r-1}(x_1 - z_1)}{D_{p_r}(x_1 - z_1)} \cdot$$

$$\frac{D_{p_r}(x_2 - z_1)}{D_{p_r}(x_2 - z_2)} \cdots \frac{D_{p_r}(x_{n+1} - z_n)}{D_{p_r}(x_{n+1} - z_{n+1})} \exp\left[-\frac{(b_r - 2h_r)}{4b_r}(z_1^2 + z_2^2)\right] . \tag{4.71}$$

where $Y \pm Y'$ corresponds to the kinematics (4.57,4.58) respectively. Eq. (4.71) implies that the contours of integrations obey $\Re x_1 < .. < \Re x_{n+1}$. After that one can perform integration in Eq. (4.71) by taking residues in the D_{p_r} zeros.

When k of the isoscalar bosons are replaced by the isovector ones, $(g'(Y \pm Y')/2)^n$ in Eq. (4.71) should be replaced by $g^k(g'(Y \pm Y')/2)^{n-k}$; the factor $(m/2b_r)z_l^2$ for each of the emitted isovector bosons should be added to the last exponent. Using the standard relation between gauge fields A_r and γ, Z, W, one can easily rewrite the gauge boson production amplitudes of Eq. (4.71) in terms of amplitudes for the electroweak bosons production. Asymptotics of the scattering amplitudes of the photon and Z-production are governed by the isoscalar Reggeons whereas W-production involves the isovector Reggeons. Eq. (4.71) can be used for obtaining different relation between cross sections of different radiative processes in the multi-Regge kinematics. For example,

$$\frac{\sigma^{(nZ)}}{\sigma^{(n\gamma)}} \approx \tan^{2n}\theta_W . \tag{4.72}$$

whereas the energy dependence of the ratio $\sigma^{(n\gamma)}/\sigma^{(nW)}$ is less trivial. Asymptotically,

$$\frac{\sigma^{(n\gamma)}}{\sigma^{(nW)}} \sim s^{-0.36}. \tag{4.73}$$

Results of accounting for the non-leading Reggeon contributions for $\sigma^{(n\gamma)}/\sigma^{(nW)}$ can be obtained from Fig. 6 because $\sigma^{(n\gamma)}/\sigma^{(nW)} = (e\sqrt{2}/g)^{n-1}\sigma^{(\gamma)}/\sigma^{(W)}$. In obtaining Eqs. (4.72,4.73) from Eq. (4.71) we have used that according to Eq. (4.59), $(s_1)^\Delta \ldots s_{n+1}^\Delta \sim s^\Delta$.

4.5 Emission of EW bosons in e^+e^- -annihilation into leptons

Inelastic annihilation of e^+e^-, with the e^- being left handed, into another left handed lepton l' (i.e. into μ or τ) and its antiparticle $\bar{l}'$ can be considered quite similarly to the annihilation into quarks discussed above. In particular, explicit expressions for the new invariant amplitudes, $L_r^{(n)}$ of this process [2] can be obtained from Eqs. (4.39),(4.40),(4.71) by putting $Y' = Y = -1$ in Eqs. (4.22),(4.23) for the factors b_r, h_r, b'_r, h'_r. However having done it, we obtain that $b_0 = 0$ (see Eq. (4.22)). It means that the IR evolution equations for the scattering amplitude $L_0^{(n)}$ of the inelastic annihilation $e^+e^- \to l'\bar{l}' + n_1\gamma + (n - n_1)Z$ in the kinematics (4.1) do not contain contributions proportional to $\ln(s/\mu^2)$ in the rhs and therefore the Mellin amplitudes $f_0^{(n)}$ (related to L_0 through the Mellin transform (4.24), Eq. (4.74)) do not have the partial derivatives with respect to ω_j (cf Eq. (4.71)). In order to obtain expressions for the new scattering amplitudes $L_0^{(n)}$, let us consider first the simple case of emission of one isoscalar boson accompanying the forward $e^+e^- \to l'\bar{l}'$ -annihilation, assuming that both e^- and l' are left particles. It is obvious that for this case, the IREE of Eq. (4.20) for scattering amplitude M_0 has to be replaced by the simpler one,

$$\frac{\partial L_0^{(1)}}{\partial \rho_1} + \frac{\partial L_0^{(1)}}{\partial \rho_2} + \frac{\partial L_0^{(1)}}{\partial y_1} + \frac{\partial L_0^{(1)}}{\partial y_2} = -\frac{1}{8\pi^2}\bar{h}_0(y_1 + y_2)L_0^{(1)} \tag{4.74}$$

where we have denoted $\bar{h}_0 = (3g^2 + g'^2)/4$.

In terms of the Mellin amplitude $f_0^{(1)}$, Eq. (4.74) takes the following form:

$$(\omega_1 + \omega_2)f_0^{(1)} + \frac{\partial f_0^{(1)}}{\partial y_1} + \frac{\partial f_0^{(1)}}{\partial y_2} = \bar{h}_0(y_1 + y_2)f_0^{(1)} . \tag{4.75}$$

The solution to Eq. (4.75) respecting the matching condition (4.24) is (cf Eq. (4.39):

$$L_0^{(1)} = \frac{g'Y}{2} \int_{-\imath\infty}^{\imath\infty} \frac{d\omega_1}{2\imath\pi} \frac{d\omega_2}{2\imath\pi} \left(\frac{s_1}{q_1^2}\right)^{\omega_1} \left(\frac{s_2}{q_2^2}\right)^{\omega_2} \frac{(\bar{f}_0(x_1) - \bar{f}_0(x_2))}{(\omega_2 - \omega_1)}$$
$$e^{(1/8\pi^2)\bar{f}_0(\omega_2)(y_1 - y_2)}e^{-(\bar{h}_0/2)(y_1^2 + y_2^2)} \tag{4.76}$$

where the Mellin amplitude $\bar{f}_0 =$ for the elastic $e^+e^- \to \mu^+\mu^-$ annihilation is (see [16, 19, 20])

$$\bar{f}_0 = 4\pi^2 \left[\omega - \sqrt{\omega^2 - (3g^2 + g'^2)/8\pi^2}\right] . \tag{4.77}$$

The last exponent in Eq. (4.76) is the Sudakov form factor accumulating the DL contribution of the soft virtual EW bosons only. The other terms in the integrand account for harder

---

[2]the kinematic factor $2/k_\perp$ is also extracted from $A_r^{(n)}$ like it was done for amplitudes $M_r^{(n)}$.

contributions. The leading singularity (intercept), ω_0 of the integrand of Eq. (4.76) is given by the position of the branch point of the rhs of Eq. (4.77). Therefore we obtain

$$\omega_0 = \sqrt{\frac{\alpha}{2\pi}\Big(\frac{3}{\sin^2\theta_W} + \frac{1}{\cos^2\theta_W}\Big)} = 0.13 \ , \tag{4.78}$$

so asymptotically

$$L_0 \sim s^{0.13} \ . \tag{4.79}$$

The invariant amplitudes $L_0^{(n)}$ for production of n isoscalar bosons in the kinematics (4.57) when e^+e^- annihilate into another lepton pair can be obtained similarly. The IREE for the amplitudes $L_0^{(n)}$ is

$$\Big[\frac{\partial L_0^{(n)}}{\partial \rho_1} + ... + \frac{\partial L_0^{(n)}}{\partial \rho_{n+1}}\Big] + \Big[\frac{\partial L_0^{(n)}}{\partial y_1} + ... + \frac{\partial L_0^{(n)}}{\partial y_{n+1}}\Big] = -\frac{1}{8\pi^2}\bar{h}_0(y_1 + ... + y_{n+1})L_0^{(n)} \tag{4.80}$$

and its solution is

$$L_0^{(n)} = \Big(\frac{g'Y}{2}\Big)^n \int_{-\imath\infty}^{\imath\infty} \frac{d\omega_1}{2\imath\pi}...\frac{d\omega_{n+1}}{2\imath\pi}\Big(\frac{s_1}{q_1^2}\Big)^{\omega_1}\Big(\frac{s_2}{q_1^2}\Big)^{\omega_2}....\Big(\frac{s_{n+1}}{q_n^2}\Big)^{\omega_{n+1}} \tag{4.81}$$

$$\frac{\bar{f}_0(\omega_1)}{(\omega_{n+1} - \omega_n)...(\omega_2 - \omega_1)} \, e^{(1/8\pi^2)\big[\bar{f}_0(\omega_2)(y_1 - y_2) + ... + \bar{f}_0(\omega_{n+1})(y_n - y_{n+1})\big]}e^{-(\bar{h}_0/2)(y_1^2 + .. + y_{n+1}^2)}$$

when $\Re(\omega_i) < \Re(\omega_{i+1}), i = 1, .., n$. Their asymptotic s-dependence is also given by Eq. (4.79). The results of numerical calculations for the cross section of γ, Z and W production in $e^+e^- \to l'\bar{l}'$ are presented in Fig. 6.

4.6 Numerical results

In order to estimate at what energy scale one might hope to observe the predicted asymptotical behaviour of cross sections of exclusive $W^\pm$ and Z, γ production we have first to account for all non-leading DLA amplitudes for left and right chiralities of initial e^+e^- and final $q\bar{q}$ or $l\bar{l}$ pairs. There are many such amplitudes, but all of them can be easily calculated as described in previous sections. The results for Regge intercepts for the forward (t-channel) and backward (u-channel) kinematics are collected in table 4.1 for the final $q\bar{q}$ and in table 4.2 for the final $l\bar{l}$.

Evidently, in far asymptotics the leading contribution for $W^\pm$ production comes from F_1 (isotriplet) of the backward $e_L^+e_L^- \to q_L\bar{q}_L$ whereas the leading contribution to (Z, γ) production comes from F_0 (isosinglet) of the forward $e_L^+e_L^- \to q_L\bar{q}_L$. However differences between the non-leading and leading intercepts are small, and one can expect the role of the first to be essential at real energies scales. Moreover, the effects of non-leading intercepts of the same amplitude can be also large enough at real energies. Therefore it seems reasonable to numerically compute the energy dependent amplitudes, M_r, by taking the inverse transform of the IREE solutions

$F_r(\omega)$	forward kinematics			
	p	x_0	λ	ω_0
F_{LLS}	5.796	3.23	0.026	0.083
F_{LLT}	-0.129	-2.52±1.62$\imath$	0.106	-0.267±0.171$\imath$
F_{LRu}	-0.083	-2.65±1.48$\imath$	0.077	-0.205±0.115$\imath$
F_{LRd}	0.062	-2.25	0.063	-0.142
F_{RL}	-0.042	-2.87±1.31$\imath$	0.077	-0.222±0.102$\imath$
F_{RRu}	-0.24	-2.33±1.86$\imath$	0.064	-0.15 ±0.12 $\imath$
F_{RRd}	0.75	-0.34	0.026	-0.009
$F_r(\omega)$	backward kinematics			
	p	x_0	λ	ω_0
F_{LLS}	24.68	8.65	0.013	0.111
F_{LLT}	-0.805	-1.98±2.62$\imath$	0.039	-0.076±0.101$\imath$
F_{LRu}	0.124	-1.85	0.063	-0.117
F_{LRd}	-0.05	-2.81±1.35$\imath$	0.071	-0.199±0.095$\imath$
F_{RL}	0.05	-2.365	0.071	-0.167
F_{RRu}	6.	3.32	0.013	0.0428
F_{RRd}	-0.188	-2.40±1.76$\imath$	0.051	-0.124±0.090$\imath$

Table 4.1: Rightmost zeros x_0 of parabolic cylinder functions $D_p(x)$ determining the values of the leading singularities ω_0 of different Mellin transform amplitudes $F_r(\omega)$ for $e^+e^- \to q\bar{q}$ annihilation in forward and backward kinematics.

$F_r(\omega)$	forward kinematics			
	p	x_0	λ	ω_0
F_{LLS}	∞	—	—	0.132
F_{LLT}	-0.090	-2.63±1.50$\imath$	0.103	-0.270±0.154$\imath$
$F_{LR\nu}$	—	—	—	—
$F_{LR\mu}$	0.172	-1.64	0.066	-0.108
F_{RL}	0.172	-1.64	0.066	-0.108
$F_{RR\nu}$	—	—	—	—
$F_{RR\mu}$	∞	—	—	0.077
$F_r(\omega)$	backward kinematics			
	p	x_0	λ	ω_0
F_{LLS}	2.41	1.32	0.039	0.051
F_{LLT}	-0.602	-2.06±2.40$\imath$	0.053	-0.109±0.127$\imath$
$F_{LR\nu}$	—	—	—	—
$F_{LR\mu}$	-0.102	-2.59±1.54$\imath$	0.086	-0.221±0.132$\imath$
F_{RL}	-0.102	-2.59±1.54$\imath$	0.086	-0.221±0.132$\imath$
$F_{RR\nu}$	—	—	—	—
$F_{RR\mu}$	-0.25	-2.32±1.88$\imath$	0.077	-0.179±0.145$\imath$

Table 4.2: Rightmost zeros x_0 of parabolic cylinder functions $D_p(x)$ determining the values of the leading singularities ω_0 of different Mellin transform amplitudes $F_r(\omega)$ for $e^+e^- \to l\bar{l}$ annihilation in forward and backward kinematics. Notations for isodublet components of l are taken as for muon doublet.

$F_r(\omega)$, and to calculate with them the inelastic cross sections of boson production in central region (in cm) with $k_\perp^2 \sim \mu^2 = M_Z^2$. It seems also suitable to sum over the final $q\bar{q}$ or $l\bar{l}$ isotopic states, fixing only the emitted boson isotopic state. $W^\pm$ production in the forward and backward kinematics is described by the same formula (though with different amplitudes involved!):

$$\frac{\sigma(W^\pm)}{\sigma_0} = g^2 \left[|M_{LLT}|^2 + |M_{RL}|^2 \right] , \qquad (4.82)$$

where σ_0 is the common Born cross section of the elastic process (see [15]), M_{LLT} denotes M_2 amplitude of $e_L^+ e_L^- \to q_L \bar{q}_L$ and M_{RL} denotes the amplitude of $e_R^+ e_R^- \to q_L \bar{q}_L$ (and similar for annihilation to leptons). Let us remind that $W^\pm$ are produced first as isovector boson A_1, A_2 states and then transform to observable boson states. In contrast, (Z, γ) are being produced first as isoscalar B or isovector A_3 fields, and then transform to the observable states, Z mainly comes from A_3 and γ - from B. Cross sections for production of B and A_3 bosons can be written as:

$$\sigma(Z, \gamma) = \sigma(A_3) + \sigma(B) , \qquad (4.83)$$

$$\frac{\sigma(A_3)}{\sigma_0} = g^2 \left[|M_{LLT}|^2 + \frac{1}{4} \left(|M_{LRu}|^2 + |M_{LRd}|^2 \right) + \frac{1}{2} |M_{RL}|^2 \right] \qquad (4.84)$$

where again the amplitudes M involved are either forward or backward amplitudes: $M_{LLT} = M_2$ of $e_L^+ e_L^- \to q_L \bar{q}_L$, M_{LRu} stands for $e_L^+ e_L^- \to u_R \bar{u}_R$, M_{LRd} stands for $e_L^+ e_L^- \to d_R \bar{d}_R$ and M_{RL} for $e_R^+ e_R^- \to q_L \bar{q}_L$, and

$$\begin{aligned}
\frac{\sigma(B)}{\sigma_0} &= g'^2 \left[\frac{(Y_{e_L} \mp Y_{q_L})^2}{4} \left(\frac{1}{4} |M_{LLS}|^2 + \frac{5}{4} |M_{LLT}|^2 + \frac{1}{2} |M_{LLS} M_{LLT}| \right) \right. \qquad (4.85) \\
&\quad + \frac{(Y_{e_L} \mp Y_{u_R})^2}{4} |M_{LRu}|^2 + \frac{(Y_{e_L} \mp Y_{d_R})^2}{4} |M_{LRd}|^2 + \frac{(Y_{e_R} \mp Y_{q_L})^2}{4} 2|M_{RL}|^2 \\
&\quad + \left. \frac{(Y_{e_R} \mp Y_{u_R})^2}{4} |M_{RRu}|^2 + \frac{(Y_{e_R} \mp Y_{d_R})^2}{4} |M_{RRd}|^2 \right] ,
\end{aligned}$$

where "$\mp$" denotes that "-" sign corresponds to forward amplitudes and "+" sign to backward amplitudes denoted above.

The same formulae can be used for $e^+ e^- \to l\bar{l}$ annihilation channel: one has to substitute the appropriate amplitudes M_r and to replace electro-weak charge Y_q with the appropriate Y_l. As the Regge kinematics is dominating in the cross sections, we sum the contributions of forward and backward kinematics in what follows. The results of numerical calculations presented in Figs. 4.4, 4.5 show that at energies $\sqrt{s} < 10^6$ GeV $W^\pm$ and (Z, γ) are mainly produced in $e^+ e^- \to l\bar{l}$ annihilation. And only at $\sqrt{s} > 10^6 - 10^7$ GeV their yields from $e^+ e^- \to q\bar{q}$ annihilation become greater (see Fig. 4.5).

The explicit asymptotical dominance of exclusive channel $q\bar{q} + (Z, \gamma)$ over the channel $l\bar{l} + (Z, \gamma)$ stems from the fact that despite the leading F_{LLS} amplitude in the table 4.2 has
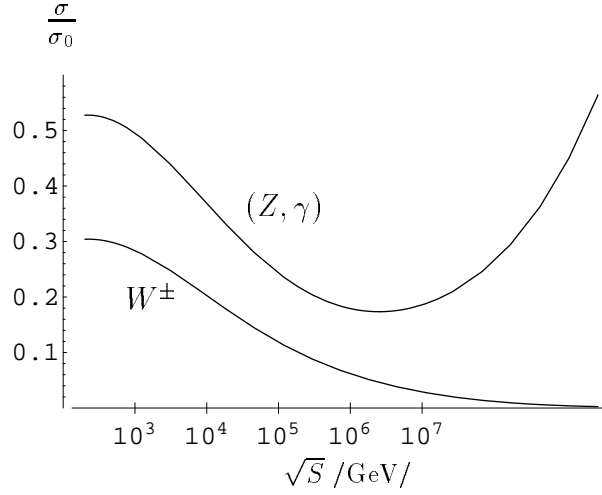
88

Figure 4.4: Dependence of exclusive $W^{\pm}$ and (Z, γ) production on the total energy of e^+e^- annihilation. The cross sections are divided by the differential elastic Born cross section σ_0 to make differences in energy dependencies more clear.
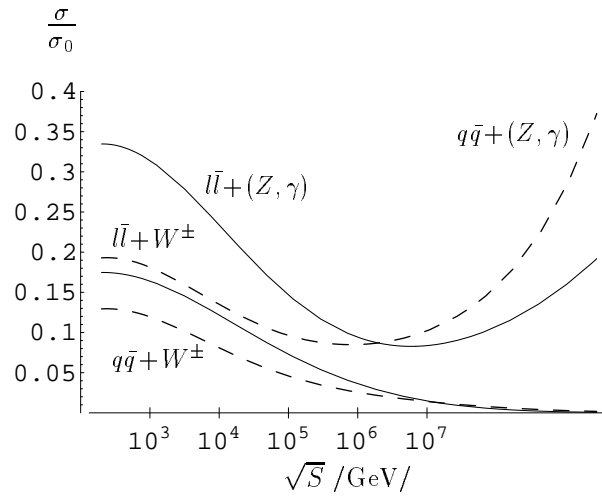

Figure 4.5: Total energy dependence of $W^{\pm}$ and (Z, γ) production in different channels of e^+e^- annihilation: $e^+e^- \to l\bar{l}$ – solid curves and $e^+e^- \to q\bar{q}$ – dashed curves.

89

the greater intercept $\omega_0 \approx 0.132$ than $\omega_0 \approx 0.111$ of the leading F_{LLS} in the table 4.1, its contribution is multiplied by the zero factor in Eq. (4.85).

The numerical calculation for the ratio of $W^\pm$ to (Z, γ) production summed over the both annihilation channels $e^+ e^- \to l\bar{l}$ and $e^+ e^- \to q\bar{q}$ is shown in Fig. 4.6. Thus the DLA predicts rather slow energy dependence of the ratio till $\sqrt{s} \sim 10^4 \mathrm{GeV}$ and then its relatively rapid decrease.
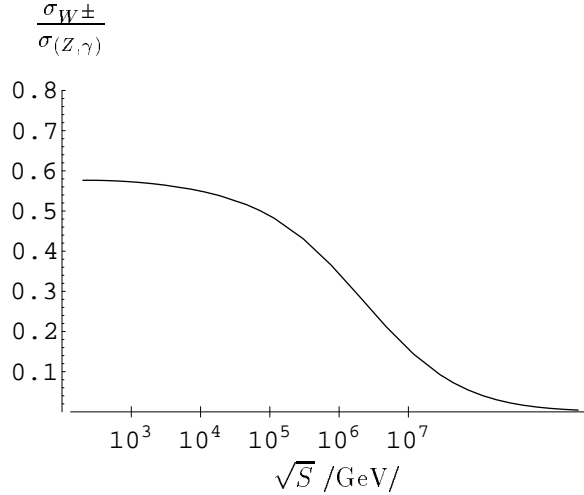

Figure 4.6: Total energy dependence of $W^\pm$ to (Z, γ) rate in $e^+ e^-$ annihilation.

The energy dependence of the ratio Z to γ,

$$\frac{\sigma(Z)}{\sigma(\gamma)} = \frac{\sigma(A_3) + \sigma(B) \tan^2 \theta_W}{\sigma(A_3) \tan^2 \theta_W + \sigma(B)} \; , \tag{4.86}$$

is shown in Fig. 4.7. In far asymptotics radiation of isoscalar field B dominates over radiation of isovector field A and the ratio tends to the fixed value $\tan^2 \theta_W \approx 0.28$.

It is worthwhile to note that apart from the results of [15] for pure QED, the figures of the table 4.2 show that backward $e_L^+ e_L^- \to l_L \bar{l}_L$ amplitude (i.e. when antilepton follows the direction of initial electron) for isoscalar channel in EW theory has the positive intercept though small enough if compared to forward annihilation amplitude.

Let us emphasise that the demonstrated in Fig. 4.7 excess of Z production over γ production at $\sqrt{s} < 10^3 \div 10^5$ GeV as well as excess of (Z, γ) emission over $W^\pm$ emission in the same energy range shown in Fig. 4.4, and the dominance of $l\bar{l}$ channel over $q\bar{q}$ channel shown in Fig. 4.5 may all happen to be just artifacts of the DLA. To get more reliable predictions for the cross sections one has at least to account for single logarithmic corrections as well. The presented figures show that the observation of the theoretically correct predictions (4.49) and (4.50) is hardly possible even in far future.
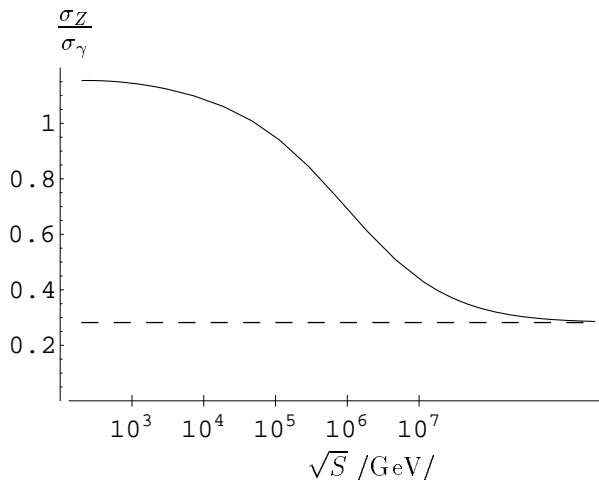
90

Figure 4.7: Total energy dependence of Z to γ rate in e^+e^- annihilation. The dashed line shows the asymptotical value of the ratio: $\tan^2 \theta_W \approx 0.28$.

4.7   Conclusion

In the present chapter we have obtained explicit expressions for the scattering amplitudes for the e^+e^- annihilation into quarks and into leptons at the annihilation energies $\sqrt{s} \gg 100$ Gev accompanied by the emission of n electroweak bosons in the multi-Regge kinematics, i.e. in the kinematics where the final particles are in cones with opening angles $\ll 1$ around the initial e^+e^- beams. We accounted for the double-logarithmic contributions to this process to all orders in the EW couplings. We have shown that it is convenient to calculate amplitudes for this process in terms of the isoscalar and of the isovector amplitudes. The isoscalar amplitudes describe production of the isoscalar gauge fields. They are controlled by $n + 1$ isoscalar Reggeons propagating in the crossing channel. The leading intercepts of these Reggeons are positive ($\Delta_{S'} = 0.11$ and $\Delta_S = 0.08$) and therefore such scattering amplitudes grow when s increases. The isovector amplitudes bring sub-leading contributions to the production of the isoscalar bosons and at the same time give the leading contributions to the production of the isovector gauge fields. They are governed by $n + 1$ isovector Reggeons with negative intercepts $\Delta_{V'} = -0.08$ and $\Delta_V = -0.27$. It means that the amplitudes for isovector production decreases when s grows. These results lead in particular to the fact that production of each Z boson is always accompanied by production of a hard photon with the same energy $\gg 100$ Gev. In DLA, such hard photons are never produced without Z bosons. The cross sections of production of these photons and the Z bosons have identical energy dependence, however they are different numerically due to difference in the couplings. They are related by Eq. (4.72) at asymptotically high energies ($\geq 10^7$ Gev). The s -dependence of the ratio $\sigma^{nZ}/\sigma^{n\gamma}$ for lower energies is given

91

in Fig. 4.7. The energy dependence of the cross section for the W production is weaker than the one for the photons and the Z bosons by factor $s^{-0.36}$ at asymptotically high energies. The s -dependence of these cross sections is shown in Figs. 4.4-4.6. Through this chapter we consider only the monotonically ordered multi-Regge kinematics (4.57) and (4.58). Accounting for the other kinematics can be done in a similar way. Though it is likely to bring corrections to explicit formulae for the invariant amplitudes $M_r^{(n)}$, it cannot change the asymptotic relation of Eq. (4.72) and the fact (see Eq. (4.73)) that $\sigma^{(n\gamma)}/\sigma^{(nW)}$ decreases with s.

Appendix A

Double Logs Approximation

The double log approximation technique is used to extract the main DL contribution of some process in the very high energy regime. One of the easiest process to illustrate this technique is the electron positron or quark anti-quark creation. This is not a physical process, there is no energy momentum conservation, but due to its simplicity it is a good example to illustrate the technical details used in this technique.

A.1 $\quad \gamma \to e^- e^+$ creation in QED

The interaction of an electron or quark with an electromagnetic field is described in terms of two independent form factors f e g:

$$\Gamma_\mu = \bar{u}(p_2) \left[\gamma_\mu f(q^2) - \frac{\sigma_{\mu\nu} q^\nu}{2m} g(q^2) \right] u(p_1) \tag{A.1}$$

where $\sigma_{\mu\nu} = (\gamma_\mu \gamma_\nu - \gamma_\nu \gamma_\mu)/2$, $q = p_2 - p_1$ is the momentum transferred to the electron or the quark, m is the electron or the quark mass and both the f and g depend on q^2.

In the Born approximation $f = 1$ and $g = 0$. In the fifties V.V. Sudakov showed[14], for QED, that in the limit of large momentum transfer, the most sizable contributions to f are the double logarithmic (DL) ones. This Sudakov form factor f has been calculated in QCD[27, 73, 74, 29, 75, 76] and recently in the electroweak theory (EW)[19],[65],[68]. In the next sections I will illustrate the calculations performed by Sudakov in the fifties for f using the DLA technique in QED.

A.1.1 Calculations of f with one-loop corrections in QED

The aim of this section is the calculation of the f form factor for the process $\gamma \to e^- e^+$ with one-loop corrections, this can be represented as $f^{(1)}$. As already stated the most sizable contributions are double logarithmic. The DLA technique uses this knowledge as a orientation for the calculations.

In figure A.1 there is a graphical representation of the one-loop corrections to the process that we need to calculate. I would like to remind the reader that due to practice in this field the feynman graphs are represented bottom up contrary to the usual left to right. The amplitude
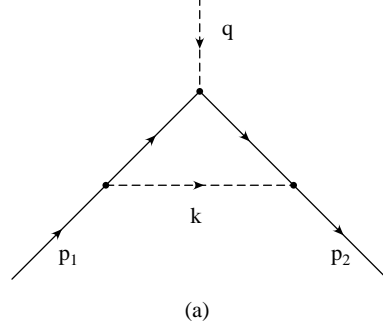

(a)

Figure A.1: Electron positron creation with one-loop corrections.

for this process can be written as :

$$
\begin{aligned}
-i\Gamma_\mu &= (-i)^3(-i)i^2\frac{\alpha}{4\pi^3}\delta_{ij}\int d^4k\frac{\bar{u}_2\gamma^\nu(\hat{p}_2-\hat{k}+m)\gamma_\mu(\hat{p}_1-\hat{k}+m)\gamma_\nu u_1}{[(p_2-k)^2-m+i\varepsilon][(p_1-k)^2-m+i\varepsilon][k^2+i\varepsilon]} \\
\Gamma_\mu &= -i\frac{\alpha}{4\pi^3}\int\dots
\end{aligned}
\tag{A.2}
$$

where $\hat{k} = k_\mu\gamma^\mu$ is the usual $\not{k}$. We can write the numerator as:

$$
\mathcal{N} = \bar{u}_2\gamma^\nu(\hat{p}_2-\hat{k}+m)\gamma_\mu(\hat{p}_1-\hat{k}+m)\gamma_\nu u_1,
\tag{A.3}
$$

and divide it into 4 different parts:

$$
\begin{aligned}
\mathcal{N}_1 &= \bar{u}_2\gamma^\nu(\hat{p}_2+m)\gamma_\mu(\hat{p}_1+m)\gamma_\nu u_1 \\
\mathcal{N}_2 &= -\bar{u}_2\gamma^\nu(\hat{p}_2+m)\gamma_\mu\hat{k}\gamma_\nu u_1 \\
\mathcal{N}_3 &= -\bar{u}_2\gamma^\nu\hat{k}\gamma_\mu(\hat{p}_1+m)\gamma_\nu u_1 \\
\mathcal{N}_4 &= \bar{u}_2\gamma^\nu\hat{k}\gamma_\mu\hat{k}\gamma_\nu u_1.
\end{aligned}
\tag{A.4}
$$

The most trivial case is when the electrons or quarks are on-shell. Using the same ideas one can calculate the off-shell case.

The on-shell case

On the on-shell case we know that $p_1^2 = p_2^2 = m^2$. Then we can simplify $\mathcal{N}_1$ by commuting both γ_ν matrices with p_1 and p_2.

$$
\mathcal{N}_1 = \bar{u}_2(2p_2^\nu - \hat{p}_2\gamma^\nu + m\gamma^\nu)\gamma_\mu(2p_{1\nu} - \gamma_\nu\hat{p}_1 + \gamma_\nu m)\gamma_\nu u_1
\tag{A.5}
$$

94

By means of the Dirac equation

$$\begin{aligned}
\bar{u}_i(\hat{p}_i - m) &= 0 \\
(\hat{p}_j - m)u_j &= 0
\end{aligned} \qquad (A.6)$$

this equation can be simplified to

$$\mathcal{N}_1 = 2s\bar{u}_2\gamma_\mu u_1 \qquad (A.7)$$

where $s = 2p_1 p_2$.

Applying the same trick on $\mathcal{N}_2$ we get

$$\mathcal{N}_2 = -\bar{u}_2 2p_2^\nu \gamma_\mu \hat{k}\gamma_\nu u_1 = -2\bar{u}_2\gamma_\mu \hat{k}\hat{p}_2 u_1. \qquad (A.8)$$

Commuting $\hat{k}$ with $\hat{p}_2$ we obtain

$$\mathcal{N}_2 = -2\bar{u}_2\gamma_\mu(2kp_2 - \hat{p}_2\hat{k})u_1. \qquad (A.9)$$

Using Sudakov parametrization [14] where the momentum k of the soft virtual particle is expressed through the longitudinal variables α, β and the transverse momentum by $k_\perp$:

$$k = \alpha p_2' + \beta p_1' + k_\perp \qquad (A.10)$$

where $(k_\perp p_1) = (k_\perp p_2) = 0$, $p_1' = p_1 + x_2 p_2$ and $p_2' = p_2 + x_1 p_1$. We impose that $(p_1')^2 = (p_2')^2 = 0$ so it is possible to calculate x_1 and x_2 ($x_1 = -p_2^2/s$ e $x_2 = -p_1^2/s$). Using this, k can be rewritten as

$$\begin{aligned}
k &= \alpha(p_2 + x_1 p_1) + \beta(p_1 + x_2 p_2) + k_\perp \\
&= p_1(\alpha x_1 + \beta) + p_2(\alpha + x_2\beta) + k_\perp
\end{aligned} \qquad (A.11)$$

This change of variable has to be also taken into account in the integration. So we must change

$$\int d^4k \rightarrow \frac{s}{2} \int d^2k_\perp d\alpha d\beta \qquad (A.12)$$

Further more we can change

$$\int d^2k_\perp \rightarrow \int k_\perp dk_\perp \int_{-\pi}^{\pi} d\phi = \int 2\pi k_\perp dk_\perp = \pi \int dk_\perp^2 \qquad (A.13)$$

So

$$\int d^4k \rightarrow \frac{s\pi}{2} \int d\alpha d\beta dk_\perp^2 \qquad (A.14)$$

Applying A.11 to $\mathcal{N}_2$ we get:

$$\begin{aligned}
\mathcal{N}_2 &= -2\left(s(\alpha x_1 + \beta) + 2m^2(\alpha + x_2\beta)\right)\bar{u}_2\gamma_\mu u_1 \\
&\quad + 2\bar{u}_2\gamma_\mu\hat{p}_2(\hat{p}_1(\alpha x_1 + \beta) + \hat{p}_2(\alpha + x_2\beta) + \hat{k}_\perp)u_1
\end{aligned} \qquad (A.15)$$

using Dirac equation and simplifying

$$\begin{aligned}
\mathcal{N}_2 = {}& -2\left(s(\alpha x_1 + \beta) + 2m^2(\alpha + x_2\beta)\right)\bar{u}_2\gamma_\mu u_1 \\
& +2m^2(\alpha + x_2\beta)\bar{u}_2\gamma_\mu u_1 \\
& +2m(\alpha x_1 + \beta)\bar{u}_2\gamma_\mu\hat{p}_2 u_1 \\
& +2\bar{u}_2\gamma_\mu\hat{p}_2\hat{k}_\perp u_1.
\end{aligned}$$
(A.16)

We can simplify and rewrite this in terms of q

$$\begin{aligned}
\mathcal{N}_2 = {}& -2\left(s(\alpha x_1 + \beta) + m^2(\alpha + x_2\beta)\right)\bar{u}_2\gamma_\mu u_1 \\
& +2m(\alpha x_1 + \beta)\bar{u}_2\gamma_\mu(\hat{q} - \hat{p}_1)u_1 \\
& -2\bar{u}_2\gamma_\mu\hat{k}_\perp\hat{p}_2 u_1 \\
\\
= {}& -2\left((s + m^2)(\alpha x_1 + \beta) + m^2(\alpha + x_2\beta)\right)\bar{u}_2\gamma_\mu u_1 \\
& +2m(\alpha x_1 + \beta)\bar{u}_2\gamma_\mu\hat{q}u_1 \\
& -2\bar{u}_2\gamma_\mu\hat{k}_\perp\hat{p}_2 u_1
\end{aligned}$$
(A.17)

The last term will not produce DL so we can neglect it.[1]

We are calculating the f form factor at very large momentum transfer. If we look at the previous equation only the first line has a suitable structure for f. Because the momentum transfer is very large we can neglect the m^2 terms compared to s.

Then we can write:

$$\mathcal{N}_2 \approx -2\left(s(\alpha x_1 + \beta) + m^2(\alpha + x_2\beta)\right)\bar{u}_2\gamma_\mu u_1$$
(A.18)

$\mathcal{N}_3$ can be simplified following the procedure we did before. So we can write this term as

$$\begin{aligned}
\mathcal{N}_3 = {}& -2\left((s + m^2)(\alpha + \beta x_2) + m^2(\alpha x_1 + \beta)\right)\bar{u}_2\gamma_\mu u_1 \\
& +2m(\alpha + \beta x_2)\bar{u}_2\hat{q}\gamma_\mu u_1 \\
& -2\bar{u}_2\hat{p}_2\hat{k}_\perp\gamma_\mu u_1
\end{aligned}$$
(A.19)

and by the same reasons as before we can simplify it to

$$\mathcal{N}_3 \approx -2\left(s(\alpha + \beta x_2) + m^2(\alpha x_1 + \beta)\right)\bar{u}_2\gamma_\mu u_1$$
(A.20)

Now for $\mathcal{N}_4$ we have

$$\begin{aligned}
\mathcal{N}_4 = {}& \bar{u}_2\gamma^\nu\hat{k}\gamma_\mu\hat{k}\gamma_\nu u_1 \\
= {}& -2\bar{u}_2\hat{k}\gamma_\mu\hat{k}u_1
\end{aligned}$$
(A.21)

---

[1] As will be shown later the denominator is proportional to $k_\perp^2$. The existence of a $k_\perp$ in the numerator will produce a single log.

where we have used the γ-matrices identity $\gamma_\nu \gamma^\alpha \gamma^\mu \gamma^\beta \gamma^\nu = -2\gamma^\beta \gamma^\mu \gamma^\alpha$.

Using Sudakov parametrization

$$\mathcal{N}_4 = -2\bar{u}_2 \left(\hat{p}_1(\alpha x_1 + \beta) + \hat{p}_2(\alpha + x_2\beta) + \hat{k}_\perp \right) \gamma_\mu \left(\hat{p}_1(\alpha x_1 + \beta) + \hat{p}_2(\alpha + x_2\beta) + \hat{k}_\perp \right) u_1 \quad (A.22)$$

and Dirac equation

$$\mathcal{N}_4 = -2\bar{u}_2 \left(\hat{p}_1(\alpha x_1 + \beta) + m(\alpha + x_2\beta) + \hat{k}_\perp \right) \gamma_\mu \left(m(\alpha x_1 + \beta) + \hat{p}_2(\alpha + x_2\beta) + \hat{k}_\perp \right) u_1. \quad (A.23)$$

Keeping only terms that are not proportional neither to mass or to single $\hat{k}_\perp$

$$\begin{aligned} \mathcal{N}_4 &= -2(\alpha x_1 + \beta)(\alpha + x_2\beta)\bar{u}_2 \hat{p}_1 \gamma_\mu \hat{p}_2 u_1 \\ &\quad -2\bar{u}_2 \hat{k}_\perp \gamma_\mu \hat{k}_\perp u_1 \end{aligned} \quad (A.24)$$

Applying some basic algebra it is possible to simplify this equation to

$$\begin{aligned} \mathcal{N}_4 &= -2s(\alpha\beta(1 + x_1 x_2) + \alpha^2 x_1 + \beta^2 x_2)\bar{u}_2 \gamma_\mu u_1 \\ &\quad -2\bar{u}_2 \hat{k}_\perp \gamma_\mu \hat{k}_\perp u_1 \end{aligned} \quad (A.25)$$

$x_1 x_2$ is very small compared to 1 so we can neglect it. The last term of this expression is a contribution to g.

We are now in a position to write the full numerator as:

$$\mathcal{N} \approx 2s \left(1 - \alpha(1 + x_1) - \beta(1 + x_2) - \frac{m^2}{s}(\alpha + x_2\beta + \alpha x_1 + \beta) - \alpha\beta - \alpha^2 x_1 - \beta^2 x_2 \right) \bar{u}_2 \gamma_\mu u_1 \quad (A.26)$$

Due to the fact that x_1 and x_2 are very small compared to 1 we can neglect them. We will see later that $\alpha < 1$ and $\beta < 1$ to get DL contributions, with this we can neglect the terms proportional to α^2, β^2 and $\alpha\beta$ compare with α and β.

$$\mathcal{N} \approx 2s \left(1 - \alpha - \beta \right) \bar{u}_2 \gamma_\mu u_1 \quad (A.27)$$

The next step is the calculation of the denominator. This can be divided in three parts:

$$\begin{aligned} \mathcal{D}_1 &= [(p_2 - k)^2 - m + i\varepsilon] \\ \mathcal{D}_2 &= [(p_1 - k)^2 - m + i\varepsilon] \\ \mathcal{D}_3 &= [k^2 + i\varepsilon] \end{aligned} \quad (A.28)$$

Starting with $\mathcal{D}_3$ we need to calculate k^2 using the Sudakov parametrization:

$$\begin{aligned} k^2 &= (p_1(\alpha x_1 + \beta) + p_2(\alpha + x_2\beta) + k_\perp)^2 \\ &= p_1^2(\alpha x_1 + \beta)^2 + p_2^2(\alpha + x_2\beta)^2 + s(\alpha x_1 + \beta)(\alpha + x_2\beta) - k_\perp^2 \\ &= s(-x_2(\alpha x_1 + \beta)^2 - x_1(\alpha + x_2\beta)^2 + (\alpha x_1 + \beta)(\alpha + x_2\beta)) - k_\perp^2 \\ &\approx s\alpha\beta - k_\perp^2 \end{aligned} \quad (A.29)$$

We can write $\mathcal{D}_3$ as:

$$\mathcal{D}_3 \approx s\alpha\beta - k_\perp^2 + i\varepsilon. \tag{A.30}$$

Next let's rewrite $\mathcal{D}_1$ as:

$$\mathcal{D}_1 = (p_2 - k)^2 - m = p_2^2 + k^2 - 2p_2 k - m^2 + i\varepsilon \tag{A.31}$$

and $-2p_2 k$ can be simplified by

$$
\begin{aligned}
-2p_2 k &= -2p_2 \left(p_1(\alpha x_1 + \beta) + p_2(\alpha + x_2\beta) + k_\perp\right) \\
&= -s\left(\alpha x_1 + \beta - 2x_1(\alpha + x_2\beta)\right) \\
&\approx -s(\alpha x_1 + \beta)
\end{aligned} \tag{A.32}
$$

$$
\begin{aligned}
\mathcal{D}_1 &= p_2^2 + s\alpha\beta - k_\perp^2 - s(\alpha x_1 + \beta) - m^2 + i\varepsilon \\
&\approx -s(x_1 + \beta - \alpha\beta) - k_\perp^2 + i\varepsilon
\end{aligned} \tag{A.33}
$$

By the same line of reasoning we can simplify $\mathcal{D}_2$ as:

$$\mathcal{D}_2 \approx -s(x_2 + \alpha - \alpha\beta) - k_\perp^2 + i\varepsilon \tag{A.34}$$

The full denominator $\mathcal{D}$ is them given by:

$$\mathcal{D} \approx \left[-s(x_1 + \beta - \alpha\beta) - k_\perp^2 + i\varepsilon\right]\left[-s(x_2 + \alpha - \alpha\beta) - k_\perp^2 + i\varepsilon\right]\left[s\alpha\beta - k_\perp^2 + i\varepsilon\right] \tag{A.35}$$

We can integrate over α using the residues theorem. So we have three poles for α, one for each denominator. The following table shows the poles:

	α
D_1	$\dfrac{k_\perp^2 + s(x_1 + \beta) - i\varepsilon}{s\beta}$
D_2	$\dfrac{-k_\perp^2 - sx_2 + i\varepsilon}{s(1 - \beta)}$
D_3	$\dfrac{k_\perp^2 - i\varepsilon}{s\beta}$

$$\tag{A.36}$$

The imaginary part of α depends on the value of β. So we have three different scenarios depending on the possible values for β:

98

i. if $\beta > 1$ implies that for all the poles $Im(\alpha) < 0$, then the 3 poles are on the lower half plane and we can close the integral by the upper half plane. So the result of this integral in this case is 0.

ii. if $0 < \beta < 1$ in this case pole 1 and 3 are in the lower half plane but pole 2 is in the upper half plane. So to simplify we can close the integration by the upper half plane. To do this we need to calculate the *Residue* of pole 2.

iii. if $\beta < 0$ implies that for all the poles $Im(\alpha) > 0$, then the 3 poles are on the upper half plane and we can close the integral by the lower half plane. So the result of this integral in this case is 0.

Since the only non zero case is when $0 < \beta < 1$ we can define the denominator as a function f defined as:

$$f(\alpha) = \frac{1}{\mathcal{D}} = \frac{h(\alpha)}{g(\alpha)}, \tag{A.37}$$

where

$$h(\alpha) = \frac{1}{\left[-s(x_1 + \beta - \alpha\beta) - k_\perp^2 + i\varepsilon\right]\left[s\alpha\beta - k_\perp^2 + i\varepsilon\right]} \tag{A.38}$$

$$g(\alpha) = \left[-s(x_2 + \alpha - \alpha\beta) - k_\perp^2 + i\varepsilon\right]. \tag{A.39}$$

Using the residue theorem we have to calculate

$$Res\left\{f(\alpha), a = \frac{-k_\perp^2 - sx_2 + i\varepsilon}{s(1-\beta)}\right\} = \frac{h(a)}{g'(a)} \tag{A.40}$$

Then

$$\frac{1}{h(a)} = \left[-s(x_1 + \beta - \frac{-k_\perp^2 - sx_2 + i\varepsilon}{s(1-\beta)}\beta) - k_\perp^2 + i\varepsilon\right]\left[s\frac{-k_\perp^2 - sx_2 + i\varepsilon}{s(1-\beta)}\beta - k_\perp^2 + i\varepsilon\right]$$

$$= \left[-s(x_1 + \frac{x_2}{1-\beta}) - s\beta - \frac{k_\perp^2}{1-\beta}\right]\left[-\frac{k_\perp^2}{1-\beta} - \frac{sx_2\beta}{1-\beta}\right] \tag{A.41}$$

$$g'(a) = \left[-s(x_2 + \alpha(1-\beta)) - k_\perp^2 + i\varepsilon\right]' = -s(1-\beta) \tag{A.42}$$

Since x_1 and x_2 are small we can neglect terms proportional to them. To get the major contributions that are log's we need to have $s\beta \gg \frac{k_\perp^2}{1-\beta}$. Since $0 < \beta < 1$ we get

$$s\beta(1-\beta) \gg k_\perp^2 \Rightarrow \beta \gg \frac{k_\perp^2}{s} \Rightarrow \frac{k_\perp^2}{s} < \beta < 1 \tag{A.43}$$

This gives us new limits for the integration of β. In $g'(a)$ the value of β can be neglected compared to 1 so we get $g'(a) \approx s$. We know that $0 < k_\perp^2 < s$ witch sets the integration limits to $k_\perp^2$. Putting it all together,

$$Res\left\{f(\alpha), a\right\} \approx \frac{1}{-s[-s\beta][-k_\perp^2]} = \frac{1}{-s^2\beta k_\perp^2} \tag{A.44}$$

The full expression can be written as

$$\begin{aligned}
\int d^4k \frac{\mathcal{N}}{\mathcal{D}} &\approx \frac{s\pi}{2}\frac{2s}{-s^2}(2i\pi)\bar{u}_2\gamma_\mu u_1 \int_0^s \frac{dk_\perp^2}{k_\perp^2}\int_{k_\perp^2/s}^1 \frac{d\beta}{\beta} \\
&\approx -2i\pi^2\bar{u}_2\gamma_\mu u_1 \int_0^s \frac{dk_\perp^2}{k_\perp^2}\ln\frac{s}{k_\perp^2}
\end{aligned} \tag{A.45}$$

It is easy to see that this integral in IR divergent so we can solve this problem by inserting μ^2 as a cut off.

$$\begin{aligned}
\int d^4k \frac{\mathcal{N}}{\mathcal{D}} &\approx -2i\pi^2\bar{u}_2\gamma_\mu u_1 \int_{\mu^2}^s \frac{dk_\perp^2}{k_\perp^2}\ln\frac{s}{k_\perp^2} \\
&\approx -i\pi^2\bar{u}_2\gamma_\mu u_1 \ln^2\frac{s}{\mu^2}
\end{aligned} \tag{A.46}$$

So the final result is the well known expression:

$$f^{(1)} = -\frac{\alpha}{4\pi}\ln^2\frac{s}{\mu^2} \tag{A.47}$$

A.1.2   All orders: Infrared Evolution Equation

Its possible to calculate f in all orders without the need of graph-by-graph calculations. This can be achieved by obtaining f as a solution of some integral equation. For that we build and solve a Infrared Evolution Equation (IREE). This equation is based on the evolution of f with the parameter μ, the infrared cutoff. We are looking for virtual photons with minimal $k_\perp$. The region where all virtual photons have the same momentum ($k_{1\perp} = k_{2\perp} = k_{3\perp}...$) yields no contributions. The rest of the phase space can be divided in different non overlapping region where there is always a photon with minimum $k_\perp$. Using Gribov bremsstrahlung theorem witch states that the photon with minimum $k_\perp$ can be factorized in DLA, we can write the Sudakov form factor in a graphical form as:

We can write this equation as:

$$M_B f(s/\mu^2) = M_B - \frac{\alpha}{2\pi}M_B \int_{\mu^2}^s \frac{dk_\perp^2}{k_\perp^2}\int_{k_\perp^2}^s \frac{d\beta}{\beta}f(s/k_\perp^2) \tag{A.48}$$

Substituting $s/\mu^2 \to \rho$ we can rewrite this as :

$$f(\rho) = 1 - \frac{\alpha}{2\pi}\int_{\mu^2}^s \frac{dk_\perp^2}{k_\perp^2}\ln\frac{s}{k_\perp^2}f\left(\frac{s}{k_\perp^2}\right) \tag{A.49}$$
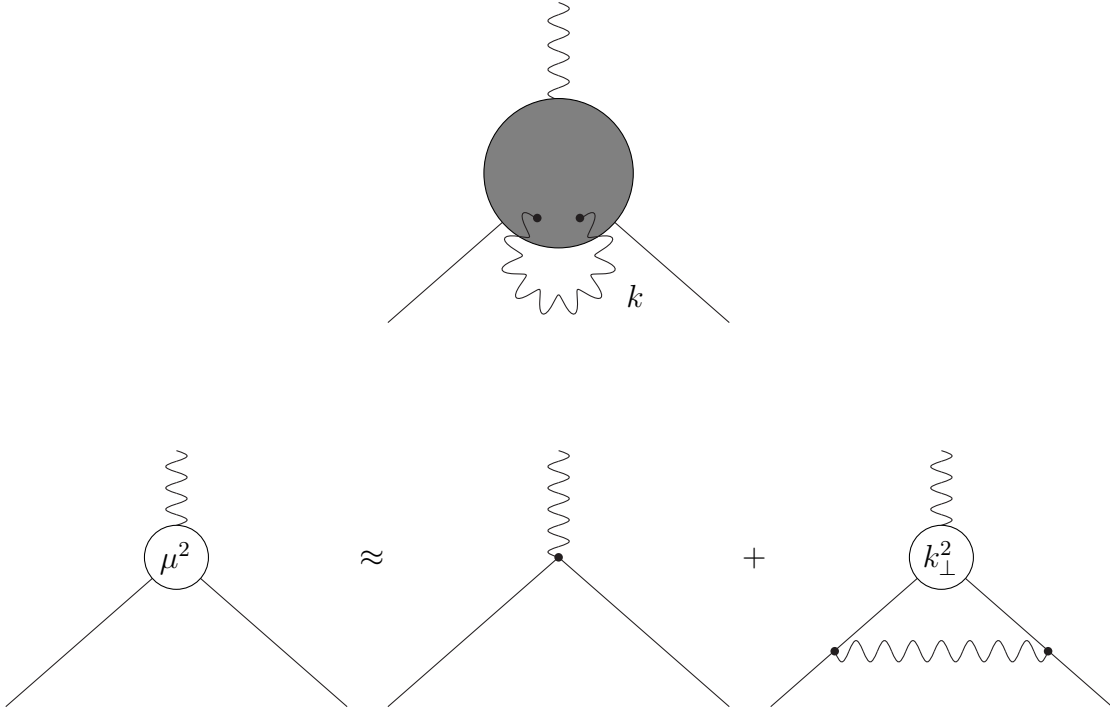
Applying the differential operator $\partial/\partial\mu^2$ to this equation:

$$\frac{\partial}{\partial\mu^2}f(\rho) = \frac{\partial}{\partial\rho}f(\rho)\frac{\partial\rho}{\partial\mu^2} = \frac{\partial f(\rho)}{\partial\rho}\left(-\frac{s}{\mu^4}\right) = -\frac{\partial f(\rho)}{\partial\rho}\frac{\rho}{\mu^2} \tag{A.50}$$

Using the fact that:

$$\frac{\partial}{\partial a}\int_a^b dx\, f(x) = -f(a) \tag{A.51}$$

we write:

$$-\frac{\rho}{\mu^2}\frac{\partial f(\rho)}{\partial\rho} = \frac{\alpha}{2\pi}\frac{\ln\rho\, f(\rho)}{\mu^2} \tag{A.52}$$

defining $X = \ln\rho$ and applying

$$\rho\frac{\partial f}{\partial\rho} = \rho\frac{\partial f}{\partial\ln\rho}\frac{\partial\ln\rho}{\partial\rho} = \frac{\partial f}{\partial\ln\rho} \tag{A.53}$$

its possible to simplify:

$$-\frac{\partial f}{\partial X} = \frac{\alpha}{2\pi}Xf$$

101

$$\begin{aligned}
\frac{\partial f}{f} &= -\frac{\alpha}{2\pi} X \partial X \\
\ln f &= -\frac{\alpha}{4\pi} X^2 + C \\
f &= C \times e^{-\frac{\alpha}{2\pi} \ln^2 s/\mu^2}
\end{aligned} \qquad (A.54)$$

The constant C can be calculated by setting $s \to \mu^2$, reproducing the Born case were $f = 1$. The integral $\int_{\mu^2}^{s} dk_\perp / k_\perp \to 0$ this implies that $C = 1$.

This leads to the known exponentiation result:

$$f = e^{-\frac{\alpha}{2\pi} \ln^2 \frac{s}{\mu^2}} \qquad (A.55)$$

A.2 Electron Positron Annihilation

A more interesting process is the electron positron annihilation into a μ^- and a μ^+. Radiative corrections to this process yield DL contributions in the following kinematical regions:

- Hard kinematics, corresponding to a large center of mass scattering angles ($\theta = \theta_{p_1 p_1'} \approx 1$).

- Forward kinematics, when the outgoing μ^- goes in the same direction of the incoming electron ($\theta \ll 1$). This terminology was introduced in [15]. It is the forward kinematics with respect to the charge flow.

- Backward kinematics, when the outgoing μ^- goes in the opposite direction of the incoming electron ($\theta \approx \pi$).

The last two kinematical regions are of the Regge-type and will be the subject of the next sections.

A.2.1 Born approximation

In the Born approximation this process is shown in fig. A.2. Where e^+ has initial momentum
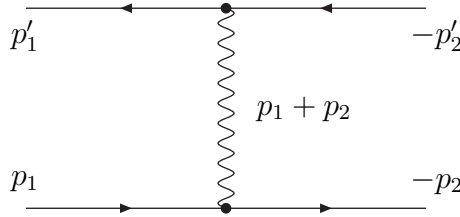

Figure A.2: $e^+ e^-$ annihilation.

p_1 and e^- p_2. The born scattering amplitude can be written as:

$$M_B = \frac{(-i)^2(-i)(-i)e^2 \bar{v}_{p_2} \gamma_\mu u_{p_1} \bar{u}_{p_1'} \gamma^\mu v_{p_2'}}{(p_1 + p_2)^2 + i\varepsilon} \tag{A.56}$$

We can define the different kinematical regions by appropriate conditions on the Mandelstam variables s, t and u. We define the forward kinematical regime as:

$$s \sim -u \gg -t \ . \tag{A.57}$$

We call it the t -kinematics. The other Regge kinematics the backward kinematics obeys the following conditions:

$$s \sim -t \gg -u \ . \tag{A.58}$$

We call it the u -kinematics. Since the calculations for this two different kinematical regions are very similar only the forward case will be illustrated. So in this regime we consider:

$$p'_1 \approx p_1$$
$$p'_2 \approx p_2 \qquad (A.59)$$

We are working in a very high energy collision where the center of mass energy is much greater than the masses of the particles involved. They can be neglected compared with s $(s \gg m_e)$.

$$s = (p_1 + p_2)^2 = p_1^2 + p_2^2 + 2p_1p_2 = m_1^2 + m_2^2 + 2p_1p_2 \approx 2p_1p_2. \qquad (A.60)$$

With this in mind and using some Dirac algebra the scattering amplitude can be simplify:

$$
\begin{aligned}
M_B &= \frac{4\pi\alpha TR[(-\hat{p}_2)\gamma_\mu\hat{p}_1\gamma_\mu]}{s + i\varepsilon} \\
&= -\frac{4\pi\alpha TR[\hat{p}_2(2p_1^\mu - \hat{p}_1\gamma_\mu)\gamma_\mu]}{s + i\varepsilon} \\
&= -\frac{4\pi\alpha TR[\hat{p}_2(-2\hat{p}_1)]}{s + i\varepsilon} \\
&= \frac{8\pi\alpha(4p_2p_1)}{s + i\varepsilon} \\
&= \frac{16\pi\alpha s}{s + i\varepsilon} \qquad (A.61)
\end{aligned}
$$

A.2.2 One-loop

The next step is to include one loop corrections in DLA to this process. For one loop corrections we have 5 diagrams that give DL contributions. Two vertex graphs, two crossed and a lather.

$$\mathcal{M}_{1-loop} = \mathcal{M}_{Ladder} + 2\mathcal{M}_{Vertex} + 2\mathcal{M}_{Cross} \qquad (A.62)$$

They will be calculated separately in the next sections.

Ladder graph

The ladder graph is plotted in figure A.2.2. To calculate this graph a specific momentum assignment is necessary to extract the main DL contributions. The k is assign to the virtual electron and not, as usually, to the photons.

$$\mathcal{M}_{Ladder} = (-i)(-i)^4(-i)^4 \frac{e^4}{(2\pi)^4} \int d^4k \frac{\bar{u}_{p_1}\gamma_\mu(\hat{k}+m)\gamma_\nu u_{(-p_2)}\bar{u}_{(-p_2)}\gamma_\nu(\hat{k}+m)\gamma_\mu u_{p_1}}{[(p_1-k)^2+i\varepsilon][(p_2+k)^2+i\varepsilon][k^2-m+i\varepsilon]^2} \quad (A.63)$$
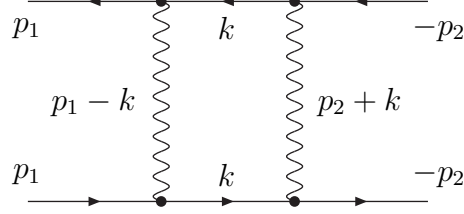
Figure A.3: 1-loop ladder graph

Exact calculations of this graph show that the main contributions are double logs. To reproduce this result using DLA we need a $k_\perp^2$ in the numerator in order to get double log result. So, all mass, α and β terms present in the numerator can be neglected because they will lead to smaller contributions. This allows the numerator to be simplified to:

$$N = \bar{u}_{p_1}\gamma_\mu \hat{k}_\perp \gamma_\nu u_{(-p_2)}\bar{u}_{(-p_2)}\gamma_\nu \hat{k}_\perp \gamma_\mu u_{p_1} \tag{A.64}$$

It is now very easy to calculate the trace of this numerator:

$$\begin{aligned}
TR[N] &= TR[\gamma_\mu \hat{k}_\perp \gamma_\nu (-\hat{p}_2)\gamma_\nu \hat{k}_\perp \gamma_\mu \hat{p}_1] \\
\\
&= TR[\gamma_\mu \hat{k}_\perp (-2(-\hat{p}_2))\hat{k}_\perp \gamma_\mu \hat{p}_1] \\
\\
&= 2TR[\gamma_\mu(-2(-k.p_2) + (-\hat{p}_2)\hat{k}_\perp)\hat{k}_\perp \gamma_\mu \hat{p}_1] \tag{A.65}
\end{aligned}$$

Since $k_\perp$ and p_2 are orthogonal and $\hat{k}_\perp.\hat{k}_\perp = k_\perp^2$ we can write this numerator as

$$TR[N] = 2k_\perp^2 TR[\gamma_\mu(-\hat{p}_2)\gamma_\mu \hat{p}_1] \tag{A.66}$$

For the denominator we can use the same procedure used in the previous section.

$$D = \frac{1}{[(p_1 - k)^2 + i\varepsilon][(p_2 + k)^2 + i\varepsilon][k^2 - m + i\varepsilon]^2} \tag{A.67}$$

After integration we get

$$\begin{aligned}
D &= \frac{1}{[s\beta - \frac{k_\perp^2}{1-\beta}][-\frac{k_\perp^2}{1-\beta}]^2 s(1-\beta)} \\
\\
&= \frac{1}{[s\beta(1-\beta) - k_\perp^2]\frac{(k_\perp^2)^2}{1-\beta}s}, \tag{A.68}
\end{aligned}$$

using the fact that $\beta \ll 1$ we can neglect β compared with 1. To have DL we need that $s\beta > k_\perp^2$. So the simplified denominator is

$$D \approx \frac{1}{s^2\beta[k_\perp^2]^2} \tag{A.69}$$

Putting it all together:

$$\begin{aligned}
\mathcal{M}_{Ladder} &= (-i)\frac{e^2}{(2\pi)^4}(2\pi i)\frac{s\pi}{2}\int dk_\perp^2 d\beta \frac{2k_\perp^2}{s\beta[k_\perp^2]^2} \times e^2 \frac{TR[\gamma_\mu(-\hat{p}_2)\gamma_\mu\hat{p}_1]}{s} \\
&= \frac{\alpha}{4\pi}\ln^2\frac{s}{\mu^2} \times M_B \tag{A.70}
\end{aligned}$$

Vertex graph

In figure A.4 the one loop vertex graphs are represented. For diagram a) one obtains:
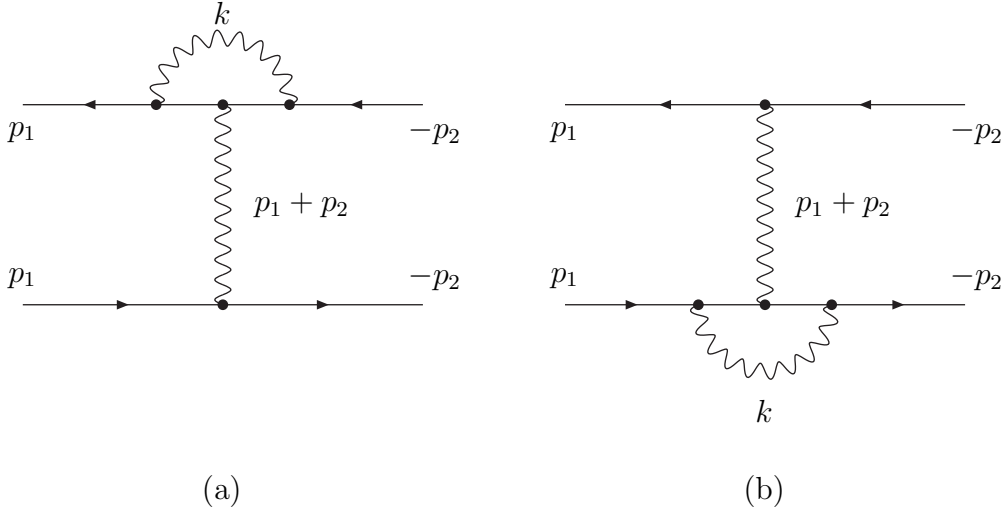

(a)   (b)

Figure A.4: 1-loop vertex graphs

$$\mathcal{M}_{vertex} = (-i)(-i)^4(-i)^4\frac{e^4}{(2\pi)^4}\int d^4k \frac{\bar{u}(-p_2)\gamma_\mu u(p_1)\bar{u}(p_1)\gamma_\nu(\hat{p}_1 - \hat{k} + m)\gamma_\mu(-\hat{p}_2 - \hat{k} + m)\gamma_\nu u(-p_2)}{[(p_1 + p_2)^2 + i\varepsilon][k^2 + i\varepsilon][(p_1 - k)^2 - m + i\varepsilon][(-p_2 - k)^2 - m + i\varepsilon]} \tag{A.71}$$

Using the same procedures we can simplify the numerator to:

$$N = (-i)(-4e^2 p_1 p_2).e^2\bar{u}(-p_2)\gamma_\mu u(p_1)\bar{u}(p_1)\gamma_\mu u(-p_2) \tag{A.72}$$

106

So the full expression can be written as

$$
\begin{aligned}
\mathcal{M}_{vertex} &= \underbrace{\frac{e^2 \bar{u}(-p_2)\gamma_\mu u(p_1)\bar{u}(p_1)\gamma_\mu u(-p_2)}{s + i\varepsilon}}_{M_B} \times \int d^4 k \frac{(-i) - 2e^2 s}{[k^2 + i\varepsilon][(p_1 - k)^2 - m + i\varepsilon][(p_2 + k)^2 - m + i\varepsilon]} \\
&= M_B \times \frac{(-i) - 2e^2 s}{[s\alpha\beta - k_\perp^2 + i\varepsilon][-s\beta + i\varepsilon][s\alpha + i\varepsilon]} \\
&= -\frac{\alpha}{4\pi} \ln^2 \frac{s}{\mu^2} \times M_B
\end{aligned}
\tag{A.73}
$$

Similar calculations can be done to the diagram b) leading to the same result.

Cross graphs

The cross graphs are represented in figure A.5. The diagram a) can be expressed as:
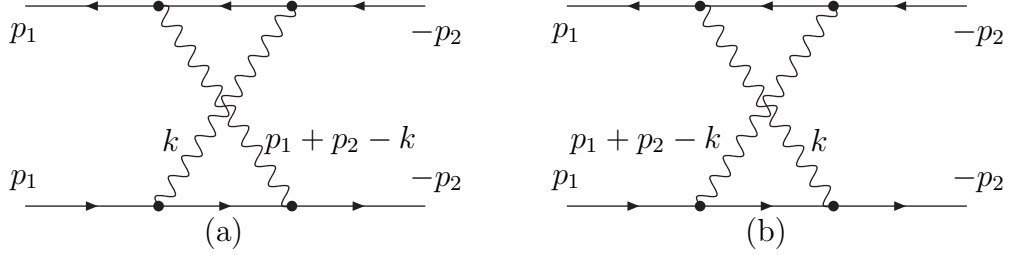

Figure A.5: 1-loop cross graphs

$$
\mathcal{M}_{cross} = (-i)(-i)^4(-i)^4 \frac{e^4}{(2\pi)^4}
\tag{A.74}
$$

$$
\int d^4 k \frac{\bar{u}(-p_2)\gamma_\mu(\hat{p}_1 - \hat{k} + m)\gamma_\nu u(p_1)\bar{u}(p_1)\gamma_\mu(-\hat{p}_2 + \hat{k} + m)\gamma_\nu u(-p_2)}{[(p_1 + p_2 - k)^2 + i\varepsilon][k^2 + i\varepsilon][(p_1 - k)^2 - m + i\varepsilon][(-p_2 + k)^2 - m + i\varepsilon]}
$$

Using DLA technique we arrive at:

$$
\mathcal{M}_{cross} = \frac{\alpha}{4\pi} \ln^2 \frac{s}{\mu^2} \times M_B
\tag{A.75}
$$

As in the previous case similar calculations can be preformed for diagram b) leading to the same result.

1-loop corrections

We are now in a position to include all 1-loop corrections to the born approximation. So the full 1-loop amplitude can be written as:

$$\mathcal{M}^{(1)} = M_B(1 + A - 2A + 2A) = M_B(1 + A), \tag{A.76}$$

where

$$A = \frac{\alpha}{4\pi} ln^2 \frac{s}{\mu^2}. \tag{A.77}$$

In the backward process the results would be somewhat different:

$$\mathcal{M}^{(1)}_{Back} = M_B(1 - A - 2A - 2A) = M_B(1 - 5A). \tag{A.78}$$

This forward/backward asymmetry is a characteristic of this process at high energies. In new accelerators this asymmetry shown in DLA calculations is expected to be observed.

A.2.3 Two-loops

The next step would be to calculate the two-loop contributions. This is a more complex job, but the main idea is the same. In the next section an illustration of the calculations of the most complex diagram, the ladder graph, will be performed.
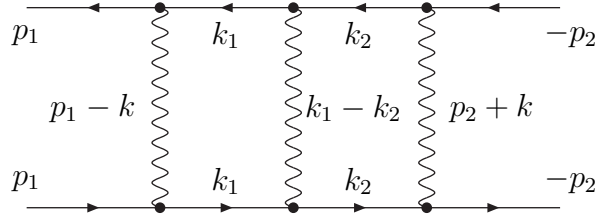
Ladder graph

Figure A.6: 1-loop ladder graph

$$
\begin{aligned}
\mathcal{M} &= (-i)(-i)^6(-i)^7 e^6 \int \frac{d^4 k_1 d^4 k_2}{(2\pi)^4 (2\pi)^4} \\
&\quad \frac{\bar{u}_{p_1}\gamma_\lambda(\hat{k}_1 + m)\gamma_\mu(\hat{k}_2 + m)\gamma_\nu u_{(-p_2)}\bar{u}_{(-p_2)}\gamma_\nu(\hat{k}_2 + m)\gamma_\mu(\hat{k}_1 + m)\gamma_\lambda u_{p_1}}{[(p_1 - k_1)^2 + i\varepsilon][(k_1 - k_2)^2 + i\varepsilon][(p_2 + k_2)^2 + i\varepsilon][k_1^2 - m + i\varepsilon]^2[k_2^2 - m + i\varepsilon]^2} \\
&= -\frac{\alpha^3}{4\pi^5} \int d^4 k_1 d^4 k_2 ... \tag{A.79}
\end{aligned}
$$

As was done before we insert Sudakov parametrization. In order to have DL we need to cancel $k_{1\perp}^2$ and $k_{2\perp}^2$ that will arise in the denominator. So all terms proportional to mass, $\beta_{1,2}$ or $\alpha_{1,2}$ can be neglected in the numerator. Using this knowledge we can simplify the numerator in the following manner:

$$N = \gamma_\lambda \hat{k}_{1\perp} \gamma_\mu \hat{k}_{2\perp} \gamma_\nu (-\hat{p}_2) \gamma_\nu \hat{k}_{2\perp} \gamma_\mu \hat{k}_{1\perp} \gamma_\lambda \hat{p}_1 \tag{A.80}$$

Using the same technique as we used for the one-loop case we can simplify this numerator in the following way:

$$N = 4k_{2\perp}^2 k_{1\perp}^2 TR[\gamma_\lambda (-\hat{p}_2) \gamma_\lambda \hat{p}_1] \tag{A.81}$$

The denominator can be divided in the following terms:

$$D = \frac{1}{\underbrace{[(p_1 - k_1)^2 + i\varepsilon]}_{(1)} \underbrace{[k_1^2 - m + i\varepsilon]^2}_{(2)} \underbrace{[k_2^2 - m + i\varepsilon]^2}_{(3)} \underbrace{[(p_2 + k_2)^2 + i\varepsilon]}_{(4)} \underbrace{[(k_1 - k_2)^2 + i\varepsilon]}_{(5)}} \tag{A.82}$$

Lets start by analyzing the new denominator term (5):

$$
\begin{aligned}
(k_1 - k_2)^2 &= k_1^2 + k_2 - 2k_1 k_2 \\
&= s\alpha_1\beta_1 - k_{1\perp}^2 + s\alpha_2\beta_2 - k_{2\perp}^2 - 2((\alpha_1 p_2 + \beta_1 p_1)(\alpha_2 p_2 + \beta_2 p_1) + k_{1\perp} k_{2\perp}) \\
&= -(k_{1\perp} - k_{2\perp})^2 + s(\alpha_1\beta_1 + \alpha_2\beta_2) - s(\alpha_1\beta_2 + \alpha_2\beta_1) \\
&= -(k_{1\perp} - k_{2\perp})^2 + s(\alpha_1 - \alpha_2)(\beta_1 - \beta_2)
\end{aligned}
\tag{A.83}
$$

It is known that $(k_{1\perp} - k_{2\perp})^2 = k_{1\perp}^2 + k_{2\perp}^2 - 2k_{1\perp}k_{2\perp}\cos(\varphi_1 + \varphi_2)$ and that:

$$\int_{-\pi}^{\pi} \frac{dx}{A + B\cos\varphi} = \frac{2\pi}{\sqrt{A^2 - B^2}} \tag{A.84}$$

Providing that $|A| > |B|$. Since we are in the DL limit we have that $|A| >> |B|$ so we can simplify this to:

$$\frac{2\pi}{\sqrt{A^2 - B^2}} \approx \frac{2\pi}{A} \tag{A.85}$$

With this knowledge we can write the denominator as:

$$
\begin{aligned}
D &= \frac{1}{[-s\alpha_1 + s\alpha_1\beta_1 - k_{1\perp}^2 + i\varepsilon][s\alpha_1\beta_1 - k_{1\perp}^2 + i\varepsilon]^2[s\alpha_2\beta_2 - k_{2\perp}^2 + i\varepsilon]^2} \times \\
&\quad \frac{1}{[s\beta_2 + s\alpha_2\beta_2 - k_{2\perp}^2 + i\varepsilon][-(k_{1\perp} - k_{2\perp})^2 + s(\alpha_1 - \alpha_2)(\beta_1 - \beta_2)]}
\end{aligned}
\tag{A.86}
$$

109

We can proceed by integrating over α_1 and α_2. To do this we can use the residues theorem. For α_1 we get:

		α_1	$Sig(\Im(\alpha_1))$
(1)		$\alpha_1 = \dfrac{-k_{1\perp}^2 + i\varepsilon}{s(1-\beta_1)}$	$1 - \beta_1$
(2)		$\alpha_1 = \dfrac{k_{1\perp}^2 - i\varepsilon}{s\beta_1}$	$-\beta_1$
(5)		$\alpha_1 = \dfrac{k_{1\perp}^2 + k_{2\perp}^2 - i\varepsilon}{s(\beta_1 - \beta_2)}$	$-\beta_1 + \beta_2$

(A.87)

For α_2:

		α_2	$Sig(\Im(\alpha_2))$
(3)		$\alpha_2 = \dfrac{k_{2\perp}^2 - i\varepsilon}{s\beta_2}$	$-\beta_2$
(4)		$\alpha_2 = \dfrac{k_{2\perp}^2 - s\beta_2 - i\varepsilon}{s\beta_2}$	$-\beta_2$
(5)		$\alpha_2 = \alpha 1 + \dfrac{k_{1\perp}^2 + k_{2\perp}^2 - i\varepsilon}{s(\beta_1 - \beta_2)}$	$\beta_1 - \beta_2$

(A.88)

Its easy to see that the only non zero situation is when $0 < \beta_1 < 1$ and $0 < \beta_2 < 1$. We still need to impose that $\beta_1 >> \beta_2$, since this is the only region where the integration over α_2 would be non zero.

In DL approximation the inequalities are very strong so we can neglect terms proportional to β_2 compared with β_1.

So for the integration we take the pole on (1) for α_1 and (5) for α_2. The propagators will now become:

$$(1) \quad \alpha_1 = \frac{-k_{1\perp}^2}{s}$$

110

(2) $\left(\dfrac{-s\beta_1 k_{1\perp}^2}{s} - k_{1\perp}^2\right)^2 = \left((1-\beta_1)k_{1\perp}^2\right)^2 \approx \left(-k_{1\perp}^2\right)^2$

(5) $\alpha_2 = \dfrac{-k_{1\perp}^2}{s} - \dfrac{k_{1\perp}^2 + k_{2\perp}^2}{s\beta_1} \approx -\dfrac{k_{1\perp}^2 + k_{2\perp}^2}{s\beta_1}$

(3) $\left(-\dfrac{s(k_{1\perp}^2 + k_{2\perp}^2)\beta_2}{s\beta_1} - k_{2\perp}^2\right)^2 \approx \left(-\dfrac{k_{1\perp}^2\beta_2 + k_{2\perp}^2\beta_1}{\beta_1}\right)^2 = \left(-k_{2\perp}^2 - \dfrac{\beta_2}{\beta_1}k_{1\perp}^2\right)^2$

(4) $s\beta_2 - \dfrac{s(k_{1\perp}^2 + k_{2\perp}^2)\beta_2}{s\beta_1} - k_{2\perp}^2 = s\beta_2 - k_{2\perp}^2 - \dfrac{\beta_2}{\beta_1}k_{1\perp}^2$ $\hspace{2cm}$ (A.89)

After taking the residues we get for the denominator:

$$(-2\pi i)^2 \int \frac{d\beta_{1,2}dk_{1,2\perp}^2}{s(\beta_1 - 1)\left(-s(\beta_1 - \beta_2)\right)\left(-k_{1\perp}^2\right)^2 \left(-k_{2\perp}^2 - \frac{\beta_2}{\beta_1}k_{1\perp}^2\right)^2 \left(s\beta_2 - k_{2\perp}^2 - \frac{\beta_2}{\beta_1}k_{1\perp}^2\right)} \hspace{1cm} (A.90)$$

where the first $s(\beta_1 - 1)$ in the denominator arises from the residue of (1) and the term $-s(\beta_1 - \beta_2)$ comes from the residue of (5). To get DL contributions we need to impose:

$$k_{2\perp}^2 \gg \frac{\beta_2}{\beta_1}k_{1\perp}^2 \hspace{3cm} (A.91)$$

$$\beta_2 \gg k_{2\perp}^2/s \hspace{3cm} (A.92)$$

So the full expression can be written as:

$$\mathcal{M}_{Lather}^{(2)} = (-)\frac{\alpha^2}{\pi^4}(2\pi i)^2 \frac{4\pi\alpha TR[\gamma_\lambda(-\hat{p}_2)\gamma_\lambda\hat{p}_1]}{s} \int \frac{d\beta_{1,2}dk_{1,2\perp}^2 k_{2\perp}^2 k_{1\perp}^2}{\beta_1\left(k_{1\perp}^2\right)^2\left(k_{2\perp}^2\right)^2\beta_2} \hspace{1cm} (A.93)$$

The solution of the integral is:

$$\int_{\mu^2}^{s} dk_{1\perp}^2 \int_{k_{1\perp}^2/s}^{1} dk_{2\perp}^2 \int_{k_{2\perp}^2/s}^{1} d\beta_2 \int_{\beta_2}^{1} d\beta_1 \frac{1}{k_{1\perp}^2 k_{2\perp}^2 \beta_1 \beta_2} = -\frac{1}{24}ln^4(s/\mu^2) \hspace{1cm} (A.94)$$

The final result is:

$$\mathcal{M}_{Lather}^{(2)} = -\frac{\alpha^2}{6\pi^2}ln^4(s/\mu^2) \times M_B \hspace{2cm} (A.95)$$

111

A.2.4 IREE

As we saw in the previous section its not necessary to calculate the direct graph-by-graph summation in all orders to produce the full DLA corrections to this process. A simpler method known as infra-red evolution equation (IREE), can be used. Its possible to obtain the DLA amplitude as a solution of an integral equation. The diagram can be represented by figure A.7. So following the same procedure as was done above from this diagram we can write:
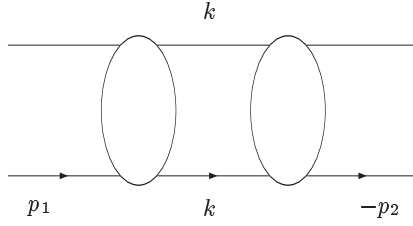

Figure A.7: Softest fermion contribution.

$$M = \frac{s}{2}\pi \int \frac{d\alpha d\beta dk_\perp^2}{(2\pi)^4} \frac{\bar{u}_{-p_2}\gamma_\mu u_k \bar{u}_k \gamma_\nu u_{p_1} \bar{u}_{p_1}\gamma_\nu u_k \bar{u}_k \gamma_\mu u_{-p_2}}{[(p_1-k)^2+i\varepsilon][(p_2+k)^2+i\varepsilon][k^2-m+i\varepsilon]^2} M\left(\frac{(p_1-k)^2}{k_\perp^2}\right) M\left(\frac{(p_2+k)^2}{k_\perp^2}\right)$$
(A.96)

The numerator can be simplified:

$$Tr(\hat{p}_2\gamma_\mu\hat{k}\gamma_\nu\hat{p}_1\gamma_\nu\hat{k}\gamma_\mu) =$$
$$4\,Tr(\hat{p}_2\hat{k}\hat{p}_1\hat{k}) =$$
$$8\,Tr(2p_2k.2p_1k - 2p_1p_1k^2) =$$
$$8\,(s\alpha s\beta - (s\alpha\beta - k_\perp^2)s) =$$
$$8\,k_\perp^2 s$$
(A.97)

Working on the denominator:

$$[(p_1-k)^2+i\varepsilon][(p_2+k)^2+i\varepsilon][k^2-m+i\varepsilon]^2 = \qquad (A.98)$$
$$[-s\alpha+s\alpha\beta-k_\perp^2-m^2+i\varepsilon][s\beta+s\alpha\beta-k_\perp^2-m^2+i\varepsilon][s\alpha\beta-k_\perp^2-m^2+i\varepsilon]^2$$

The full expression can be written as:

$$M = \frac{s}{2}\pi \int \frac{d\alpha d\beta dk_\perp^2}{(2\pi)^4} \times$$

$$\frac{8k_\perp^2 sM\left(\frac{-s\alpha+k_\perp^2-m^2}{k_\perp^2}\right) M\left(\frac{s\beta+k_\perp^2-m^2}{k_\perp^2}\right)}{[-s\alpha+s\alpha\beta-k_\perp^2-m^2+i\varepsilon][s\beta+s\alpha\beta-k_\perp^2-m^2+i\varepsilon][s\alpha\beta-k_\perp^2-m^2+i\varepsilon]^2}$$
(A.99)

112

To get DL its necessary to be in the region:

$$s\alpha, s\beta \gg k_\perp^2 \gg m^2 \tag{A.100}$$

Neglecting all non DL contributions and extracting the born amplitude its possible to write:

$$M = \frac{s^2}{(2\pi)^4} M_B \int \frac{d\alpha d\beta dk_\perp^2 (-2k_\perp^2) M\left(\frac{-s\alpha}{k_\perp^2}\right) M\left(\frac{s\beta}{k_\perp^2}\right)}{[-s\alpha + s\alpha\beta - k_\perp^2 + i\varepsilon][s\beta + s\alpha\beta - k_\perp^2 + i\varepsilon][s\alpha\beta - k_\perp^2 + i\varepsilon]^2} \tag{A.101}$$

Applying the Mellin Transform to M:

$$M\left(\frac{s}{\mu^2}\right) = \int_{-i\infty}^{i\infty} \frac{dw}{2\pi i} \left(\frac{s}{\mu^2}\right)^w f(w) \tag{A.102}$$

where $f(w)$ must go to 0 when $w \to \infty$. This transformation will introduce the following changes on the full expression:

$$
\begin{aligned}
M &= \frac{s^2}{(2\pi)^4} M_B \int \frac{dw_1}{2\pi i} \frac{dw_2}{2\pi i} f(w_1) f(w_2) \times \\
&\underbrace{\int \frac{d\alpha d\beta dk_\perp^2 (-2k_\perp^2) \left(\frac{-s\alpha}{k_\perp^2}\right)^{w_1} \left(\frac{s\beta}{k_\perp^2}\right)^{w_2}}{[-s\alpha + s\alpha\beta - k_\perp^2 + i\varepsilon][s\beta + s\alpha\beta - k_\perp^2 + i\varepsilon][s\alpha\beta - k_\perp^2 + i\varepsilon]^2}}_{J(w_1, w_2)}
\end{aligned} \tag{A.103}
$$

Since $-s\alpha$ represents the energy it has to be positive witch implies that α is negative. Its useful to replace $\alpha \to -\alpha$ and consider α as positive.

$$
\begin{aligned}
M &= \frac{s^2}{(2\pi)^4} M_B \int \frac{dw_1}{2\pi i} \frac{dw_2}{2\pi i} f(w_1) f(w_2) \times \\
&\int \frac{-d\alpha d\beta dk_\perp^2 (-2k_\perp^2) \left(\frac{s\alpha}{k_\perp^2}\right)^{w_1} \left(\frac{s\beta}{k_\perp^2}\right)^{w_2}}{[s\alpha - s\alpha\beta - k_\perp^2 + i\varepsilon][s\beta - s\alpha\beta - k_\perp^2 + i\varepsilon][-s\alpha\beta - k_\perp^2 + i\varepsilon]^2}
\end{aligned} \tag{A.104}
$$

Integrating over α taking the residues on $-s\alpha\beta - k_\perp^2 + i\varepsilon \to s\alpha = \frac{k_\perp^2}{\beta}$ leads to:

$$
\begin{aligned}
J(w_1, w_2) &= -\int \frac{d\beta dk_\perp^2}{s k_\perp^2 s\beta} \left(\frac{s\beta}{k_\perp^2}\right)^{w_2} \beta^{-w_1} \\
&-\frac{1}{s} \int_{\mu^2}^s \frac{dk_\perp^2}{k_\perp^2} \int_{k_\perp^2}^s \frac{d\beta s}{s\beta} \left(\frac{s\beta}{k_\perp^2}\right)^{w_2} \beta^{-w_1} \\
&-\frac{1}{s} \int_{\mu^2}^s \frac{dk_\perp^2}{k_\perp^2} \left(\frac{s}{k_\perp^2}\right)^{w_2} \int_{k_\perp^2/s}^1 d\beta \beta^{w_2-w_1-1}
\end{aligned} \tag{A.105}
$$

113

Integrating over β:

$$
\begin{aligned}
J(w_1, w_2) &= -\frac{1}{s(w_2 - w_1)} \int_{\mu^2}^s \frac{dk_\perp^2}{k_\perp^2} \left(\frac{s}{k_\perp^2}\right)^{w_2} \left[1 - \left(\frac{s}{k_\perp^2}\right)^{-w_2 + w_1}\right] \\
&= -\frac{1}{s(w_2 - w_1)} \int_{\mu^2}^s \frac{dk_\perp^2}{k_\perp^2} \left(\left(\frac{s}{k_\perp^2}\right)^{w_2} - \left(\frac{s}{k_\perp^2}\right)^{w_1}\right)
\end{aligned}
\tag{A.106}
$$

To simplify the calculation its easy to start by integrating one of the w and afterwards the integrations over $k_\perp^2$:

$$
-\int_{\mu^2}^s \frac{dk_\perp^2}{k_\perp^2} \left(\frac{k_\perp^2}{s}\right)^{-w} = \frac{1}{w}\left(1 - \left(\frac{s}{\mu^2}\right)^w\right)
\tag{A.107}
$$

and the final result will be:

$$
\frac{1}{8\pi^2} \int \frac{dw}{2\pi i} \left(\frac{s}{\mu^2}\right)^w f^2(w).
\tag{A.108}
$$

A.3   Mellin transform and the asymptotic form of Sommerfeld-Watson transform

The Mellin transform, named after the Finnish mathematician Hjalmar Mellin, is an integral transform that may be regarded as the multiplicative version of the two-sided Laplace transform. This integral transform is closely connected to the theory of Dirichlet series, and is often used in number theory and the theory of asymptotic expansions; it is closely related to the Laplace transform and the Fourier transform, and the theory of the gamma function and allied special functions. The popularity of this transform stems from two important properties. It allows the reduction of certain functional equations to algebraic ones, and it provides a direct mapping between asymptotic expansions of a function near zero or infinity and the set of singularities of the transform in the complex plane.

The Mellin transform of a function f is

$$
\{\mathcal{M}f\}(s) = \varphi(s) = \int_0^\infty x^s f(x) \frac{dx}{x}.
\tag{A.109}
$$

The inverse transform is

$$
\{\mathcal{M}^{-1}\varphi\}(x) = f(x) = \frac{1}{2\pi i} \int_{c-i\infty}^{c+i\infty} x^{-s}\varphi(s)\,ds.
\tag{A.110}
$$

The notation implies this is a line integral taken over a vertical line in the complex plane. For more details and proprieties see [77] and [78].

114

In our work the Mellin transform is especially useful when the function that we are working with depends on the variables through their logarithms, as is the case of the amplitudes we are calculating. But instead of using this transformation, to respect the signatures of $A^{(\pm)}$, it is more convenient to use the asymptotic form of the Sommerfeld - Watson (SW) transform:

$$A^{(\pm)}(\rho) = \int_{-\imath\infty}^{\imath\infty} \frac{d\omega}{2\pi\imath} \left(\frac{s}{\mu^2}\right)^{\omega} \xi^{(\pm)}(\omega) F^{(\pm)}(\omega), \tag{A.111}$$

where

$$\xi^{(\pm)} = -\frac{e^{-\imath\pi\omega} \pm 1}{2} \tag{A.112}$$

is the signature factor, for which this transform differs from that of Mellin. The inverse transform to Eq. (A.111) is

$$F^{(\pm)}(\omega) = \frac{2}{\sin(\pi\omega)} \int_0^{\infty} d\rho \exp(-\omega\rho) \Im_s A^{(\pm)}(\rho). \tag{A.113}$$

The Sommerfeld-Watson transform was introduced in the Regge poles approach.

Bibliography

[1] J. Abdallah et al. Search for a fourth generation b′- quark at LEP-II at $\sqrt{s} = 196 - 209$ GeV. *Eur. Phys. J.*, C50:507–518, 2007.

[2] Anthony Allen Affolder et al. Search for a fourth-generation quark more massive than the Z0 boson in $p\bar{p}$ collisions at $\sqrt{s} = 1.8$ TeV. *Phys. Rev. Lett.*, 84:835–840, 2000.

[3] T. Aaltonen et al. Search for New Particles Leading to $Z+$ jets Final States in $p\bar{p}$ Collisions at $\sqrt{s} = 1.96$- TeV. *Phys. Rev.*, D76:072006, 2007.

[4] S. Abachi et al. Top quark search with the DØ 1992 - 1993 data sample. *Phys. Rev.*, D52:4877–4919, 1995.

[5] F. Abe et al. Search for long-lived parents of Z^0 bosons in $p\bar{p}$ collisions at $\sqrt{s} = 1.8$ TeV. *Phys. Rev.*, D58:051102, 1998.

[6] Paul H. Frampton, P. Q. Hung, and Marc Sher. Quarks and leptons beyond the third generation. *Phys. Rept.*, 330:263, 2000.

[7] A. Djouadi, J. Ng, and T. G. Rizzo. New particles and interactions. 1995.

[8] Wei-Shu Hou and Robin G. Stuart. On discovering the next charge -1/3 quark through its flavor changing neutral current decays. *Phys. Rev. Lett.*, 62:617, 1989.

[9] Wei-Shu Hou and Robin G. Stuart. Flavor changing neutral currents involving heavy fermions: a general survey. *Nucl. Phys.*, B320:277, 1989.

[10] Wei-Shu Hou and Robin G. Stuart. Semileptonic flavor changing neutral current decays of the fourth generation b-prime quark. *Nucl. Phys.*, B349:91–108, 1991.

[11] Wei-Shu Hou and Robin G. Stuart. Higgs boson production from decays of the fourth generation b-prime quark. *Phys. Rev.*, D43:3669–3682, 1991.

[12] B. Haeri, A. Soni, and G. Eilam. Production of the standard higgs via decays of the b-prime quark. *Phys. Rev. Lett.*, 62:719–721, 1989.

[13] Tomer Yanir. Phenomenological constraints on extended quark sectors. *JHEP*, 06:044, 2002.

[14] V. V. Sudakov. Vertex parts at very high-energies in quantum electrodynamics. *Sov. Phys. JETP*, 3:65–71, 1956.

[15] V. G. Gorshkov, V. N. Gribov, L. N. Lipatov, and G. V. Frolov. Doubly logarithmic asymptotic behavior in quantum electrodynamics. *Sov. J. Nucl. Phys.*, 6:95, 1968.

[16] R. Kirschner and L. n. Lipatov. Double Logarithmic Asymptotics and Regge Singularities of Quark Amplitudes with Flavor Exchange. *Nucl. Phys.*, B213:122–148, 1983.

[17] E. A. Kuraev and Victor S. Fadin. On Radiative Corrections to e+ e- Single Photon Annihilation at High-Energy. *Sov. J. Nucl. Phys.*, 41:466–472, 1985.

[18] B. I. Ermolaev and Victor S. Fadin. Log - Log Asymptotic Form of Exclusive Cross-Sections in Quantum Chromodynamics. *JETP Lett.*, 33:269–272, 1981.

[19] Victor S. Fadin, L. N. Lipatov, Alan D. Martin, and M. Melles. Resummation of double logarithms in electroweak high energy processes. *Phys. Rev.*, D61:094002, 2000.

[20] B. I. Ermolaev, M. Greco, and S. I. Troyan. On the forward-backward charge asymmetry in e+ e- annihilation into hadrons at high energies. *Phys. Rev.*, D67:014017, 2003.

[21] L. N. Lipatov. Bremsstrahlung in backward e+ e- scattering as a multiregge process. *Yad. Fiz.*, 14:160–177, 1971.

[22] B. I. Ermolaev and L. N. Lipatov. Multi-Regge amplitudes for bremsstrahlung in e+ e- backward scattering. *Sov. J. Nucl. Phys.*, 47:841–848, 1988.

[23] B. I. Ermolaev and L. N. Lipatov. Gluon bremsstrahlung in quark - anti-quark backward scattering at high-energies. *Sov. J. Nucl. Phys.*, 48:715–720, 1988.

[24] B. I. Ermolaev, L. N. Lipatov, and Victor S. Fadin. On bremsstrahlung factorization in qcd. *Yad. Fiz.*, 45:817–823, 1987.

[25] E. Laenen, J. Smith, and W. L. van Neerven. Top quark production cross-section. *Phys. Lett.*, B321:254–258, 1994.

[26] Gerard 't Hooft and M. J. G. Veltman. Regularization and Renormalization of Gauge Fields. *Nucl. Phys.*, B44:189–213, 1972.

[27] James J. Carazzone, Enrico C. Poggio, and Helen R. Quinn. A Calculation of Asymptotic Behavior of Form-Factors in Nonabelian Gauge Theories. *Phys. Rev.*, D11:2286–2297, 1975.

[28] John M. Cornwall and George Tiktopoulos. On-Shell Asymptotics of Nonabelian Gauge Theories. *Phys. Rev. Lett.*, 35:338, 1975.

[29] V. V. Belokurov and N. I. Usyukina. On exponentiation of the singlet quark form-factor in the leading logarithm approximation. *Phys. Lett.*, B94:251–253, 1980.

[30] E. A. Kuraev and Victor S. Fadin. Double Logarithmical Asymptotic of Fermion Inelastic Form- Factor in Nonabelian Gauge Theory. *Yad. Fiz.*, 27:1107–1111, 1978.

[31] G. Passarino and M. J. G. Veltman. One Loop Corrections for e+ e- Annihilation Into mu+ mu- in the Weinberg Model. *Nucl. Phys.*, B160:151, 1979.

[32] M. Greco, G. Pancheri-Srivastava, and Y. Srivastava. Radiative Corrections to e+ e- → mu+ mu- Around the Z0. *Nucl. Phys.*, B171:118, 1980.

[33] P. Hansen. Measurements of heavy flavor forward backward asymmetries at LEP-1. Prepared for International Europhysics Conference on High- Energy Physics (HEP 2001), Budapest, Hungary, 12-18 Jul 2001.

[34] V. G. Gorshkov, V. N. Gribov, L. N. Lipatov, and G. V. Frolov. Backward electron - positron scattering at high- energies. *Sov. J. Nucl. Phys.*, 6:262, 1968.

[35] W. M. Yao et al. Review of particle physics. *J. Phys.*, G33:1–1232, 2006.

[36] D. Decamp et al. Determination of the Number of Light Neutrino Species. *Phys. Lett.*, B231:519, 1989.

[37] P. A. Aarnio et al. Measurement of the Mass and Width of the Z0 Particle from Multi - Hadronic Final States Produced in e+ e- Annihilations. *Phys. Lett.*, B231:539, 1989.

[38] B. Adeva et al. A Determination of the Properties of the Neutral Intermediate Vector Boson Z0. *Phys. Lett.*, B231:509, 1989.

[39] M. Z. Akrawy et al. Measurement of the Z0 Mass and Width with the OPAL Detector at LEP. *Phys. Lett.*, B231:530, 1989.

[40] K. Hagiwara et al. Review of particle physics. *Phys. Rev.*, D66:010001, 2002.

[41] V. A. Novikov, L. B. Okun, Alexandre N. Rozanov, and M. I. Vysotsky. Extra generations and discrepancies of electroweak precision data. *Phys. Lett.*, B529:111–116, 2002.

[42] Hong-Jian He, Nir Polonsky, and Shu-fang Su. Extra families, Higgs spectrum and oblique corrections. *Phys. Rev.*, D64:053004, 2001.

[43] Abdesslam Arhrib and Wei-Shu Hou. Window on Higgs boson: Fourth generation b' decays revisited. *Phys. Rev.*, D64:073016, 2001.

[44] S. M. Oliveira and R. Santos. Bounds on the mass of the b' quark, revisited. *Phys. Rev.*, D68:093012, 2003.

[45] U. Cotti, J. L. Diaz-Cruz, R. Gaitan, H. Gonzales, and A. Hernandez-Galeana. New Higgs signals induced by mirror fermion mixing effects. *Phys. Rev.*, D66:015004, 2002.

[46] George Triantaphyllou. Mirror fermions and the hierarchy problem. 1999.

[47] Marko B. Popovic. Third generation seesaw mixing with new vector-like weak- doublet quarks. *Phys. Rev.*, D64:035001, 2001.

[48] J. A. Aguilar-Saavedra. Effects of mixing with quark singlets. *Phys. Rev.*, D67:035003, 2003.

[49] Witold Skiba and David Tucker-Smith. Using jet mass to discover vector quarks at the LHC. *Phys. Rev.*, D75:115010, 2007.

[50] Anupama Atre, Marcela Carena, Tao Han, and Jose Santiago. Heavy Quarks Above the Top at the Tevatron. 2008.

[51] Torbjorn Sjostrand et al. High-energy-physics event generation with PYTHIA 6.1. *Comput. Phys. Commun.*, 135:238–259, 2001.

[52] J. Jersak, E. Laermann, and P. M. Zerwas. Electroweak Production of Heavy Quarks in e+ e- Annihilation. *Phys. Rev.*, D25:1218, 1982.

[53] W. Bernreuther et al. Top quark physics: Theoretical aspects. Prepared for Workshops on Future e+ e- Colliders, Hamburg, Germany, Sep 2-3, 1991 and Saariselka, Finland, Sep 9-14, 1991.

[54] Paul H. Frampton and Pham Quang Hung. Long-lived quarks? *Phys. Rev.*, D58:057704, 1998.

[55] P. Q. Hung and Marc Sher. Experimental constraints on fourth generation quark masses. *Phys. Rev.*, D77:037302, 2008.

[56] Thomas Hahn. Generating Feynman diagrams and amplitudes with FeynArts 3. *Comput. Phys. Commun.*, 140:418–431, 2001.

[57] J. Kublbeck, M. Bohm, and Ansgar Denner. FEYN ARTS: computer algebraic generation of Feynman graphs and amplitudes. *Comput. Phys. Commun.*, 60:165–180, 1990.

[58] R. Mertig, M. Bohm, and Ansgar Denner. FEYN CALC: Computer algebraic calculation of Feynman amplitudes. *Comput. Phys. Commun.*, 64:345–359, 1991.

[59] G. J. van Oldenborgh and J. A. M. Vermaseren. New Algorithms for One Loop Integrals. *Z. Phys.*, C46:425–438, 1990.

[60] G. J. van Oldenborgh. FF: A Package to evaluate one loop Feynman diagrams. *Comput. Phys. Commun.*, 66:1–15, 1991.

[61] T. Hahn and M. Perez-Victoria. Automatized one-loop calculations in four and D dimensions. *Comput. Phys. Commun.*, 118:153–165, 1999.

[62] B. Mele, S. Petrarca, and A. Soddu. A new evaluation of the t –¿ c H decay width in the standard model. *Phys. Lett.*, B435:401–406, 1998.

[63] G. Eilam, J. L. Hewett, and A. Soni. Rare decays of the top quark in the standard and two Higgs doublet models. *Phys. Rev.*, D44:1473–1484, 1991.

[64] V. N. Gribov. Bremsstrahlung of hadrons at high energies. *Sov. J. Nucl. Phys.*, 5:280, 1967.

[65] P. Ciafaloni and D. Comelli. Electroweak Sudakov form factors and nonfactorizable soft QED effects at NLC energies. *Phys. Lett.*, B476:49–57, 2000.

[66] Michael Melles. Mass gap effects and higher order electroweak Sudakov logarithms. *Phys. Lett.*, B495:81–86, 2000.

[67] Ansgar Denner, M. Melles, and S. Pozzorini. Two-loop electroweak angular-dependent logarithms at high energies. *Nucl. Phys.*, B662:299–333, 2003.

[68] Johann H. Kuhn, A. A. Penin, and Vladimir A. Smirnov. Subleading Sudakov logarithms in electroweak processes. *Nucl. Phys. Proc. Suppl.*, 89:94–99, 2000.

[69] S. Moch. Sudakov logarithms in four-fermion electroweak processes at high energy. *Nucl. Phys. Proc. Suppl.*, 116:23–27, 2003.

[70] A. Barroso, B. I. Ermolaev, M. Greco, S. M. Oliveira, and S. I. Troyan. Electroweak 2 –¿ 2 amplitudes for electron positron annihilation at TeV energies. *Phys. Rev.*, D69:034012, 2004.

[71] V. G. Gorshkov, L. N. Lipatov, and M. M. Nesterov. On j-plane singularities of e-minus muon-minus scattering amplitudes. *Yad. Fiz.*, 9:1221–1231, 1969.

[72] M. Chaichian and B. Ermolaev. Factorization theorem for photons and gluons in hard processes. *Nucl. Phys.*, B451:194–206, 1995.

[73] John M. Cornwall and George Tiktopoulos. Infrared Behavior of Nonabelian Gauge Theories. *Phys. Rev.*, D13:3370, 1976.

[74] J. Frenkel and J. C. Taylor. Exponentiation of Leading Infrared Divergences in Massless Yang-Mills Theories. *Nucl. Phys.*, B116:185, 1976.

[75] V. V. Belokurov and N. I. Usyukina. Double logarithmic asymptotic behavior of vertex functions in quantum chromodynamics. I. *Theor. Math. Phys.*, 44:657–663, 1981.

[76] V. V. Belokurov and N. I. Usyukina. Double logarithmic asymptotic behavior of vertex functions in quantum chromodynamics. II. Eighth order of perturbation theory. *Theor. Math. Phys.*, 45:957–962, 1980.

[77] Wojciech Szpankowski. *Average Case Analysis of Algorithms on Sequences*, chapter 9. John Wiley & Sons, New York, 2001.

[78] Wikipedia. Mellin transform — wikipedia, the free encyclopedia, 2008. [Online; accessed 4-July-2008].